ABSTRACT

SUPRAMOLECULAR DEVICES AS SELECTIVE RECEPTORS

By

Sahar Roshandel

August 2015

We have found that calixarenes are good receptors of choline (trimethylammonium group) and they have strong affinity to form host-guest complexes with a variety of molecules carrying this moiety. Furthermore, the ability of lower rim carboxylic acid calix[n]arenes and upper rim phosphonic acid functionalized calix[4]arene to transport choline-conjugated drugs through a liquid membrane was discovered. The results demonstrate that these systems are highly efficient toward transporting choline-conjugated targets, as well as neurotransmitters that possess ionizable amine termini. The breadth of compounds that are transported is significant, facing limitations only when the payloads become extremely lipophilic. These developments reveal new approaches towards attempting synthetic receptor mediated selective small molecule transport in vesicular and cellular systems.

SUPRAMOLECULAR DEVICES AS SELECTIVE RECEPTORS

A THESIS

Presented to the Department of Chemistry and Biochemistry

California State University, Long Beach

In Partial Fulfillment

of the Requirements for the Degree

Master of Science in Chemistry

Committee Members:

Michael P. Schramm, Ph.D. (chair)
Paul T. Buonora, Ph.D.
Eric R. Marinez, Ph.D.

College Designee:

Christopher Brazier, Ph.D.

By Sahar Roshandel

B.Sc., 2011, Isfahan University of Technology, Isfahan, Iran

August 2015

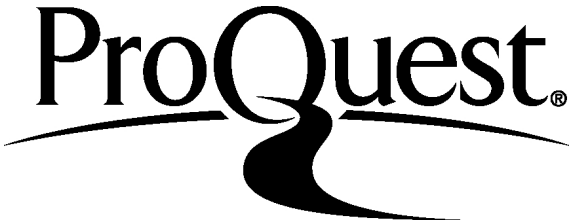

ACKNOWLEDGMENTS

I wish to express my sincere thanks to people who have always supported me druing my time at CSULB to complete my M.Sc. degree. Special thanks to my lovely friends: Sarah, Sophia, Malinda, Sewwandi, JoAnna, and Cheryl. You made the last three years such a memorable time for me, and your support was what sustained me thus far. Also, I would like to take this opportunity to express gratitude to all of the chemistry department staff: Irma, Mirna, Cynthia, and Ray. I sincerely appreciate all your kindness.

I would like to thank Dr. Adhikari and the faculty of the CSULB Department of Chemistry and Biochemistry, especially Drs. Bu, Buonora, Derakhshan, Marinez, Nakayama, Schramm, and Sorin. Thank you for your dedication and generosity with your time in helping, advising and guiding me during my time at CSULB.

Finally, this thesis is dedicated to my family, Manouchehr Roshandel, Houriyeh Bagherzadeh, and Babak Roshandel who have supported me tremendously throughout my education. I am very blessed to have such a supportive family who incite me to strive toward my goals. Thank you!

TABLE OF CONTENTS

Page

APPENDICES Page

LIST OF TABLES

TABLE Page

LIST OF FIGURES

FIGURE Page

FIGURE Page

LIST OF SCHEMES

SCHEME Page

CHAPTER 1

AN OVERVIEW OF SUPRAMOLECULAR DEVICES

1.1. Calixarenes

Calixarenes are one major class of supramolecular cyclooligomers. They are prepared from the condensation of *p*-substituted phenols with formaldehyde under a variety of different conditions.[1] Scheme 1 illustrates a synthetic approach of calixarenes under basic condition. The word "calixarene"–derived from a Greek word *calix crater,* meaning a large vase–was first used by Gutsche because of the vase-shaped conformation.[1] Due to the presence of a small cavity, the calixarenes are able to act as host molecules and hold smaller molecules or ions inside.

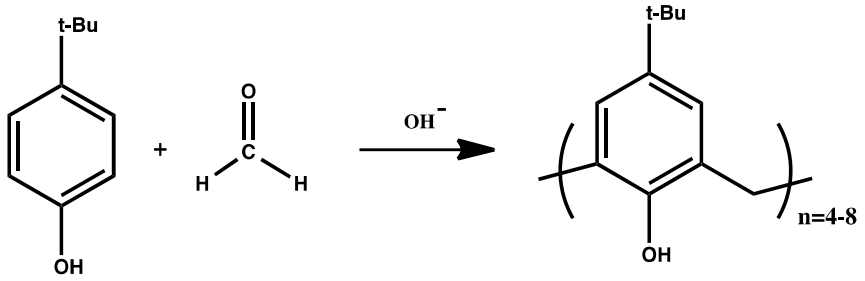

Calix[n]arene

SCHEME 1. Formation of calix[n]arenes from condensation of *p*-substituted phenols with formaldehyde. Number in square bracket denotes the number of phenolic units.

The Ar-CH_2-Ar bonds in the structure of calixarenes enable conformational interconversions. There are two possible pathways for such interconversions: 1) through upper rim where para substituents can swing through the annulus, and 2) through lower rim where hydroxyl groups can swing through the annulus.

These interconversions lead to four diastereoisomers known as the cone, partial cone, 1,2-alternate and 1,3-alternate conformers as shown in Figure 1. Among these, the cone conformer is the most stable conformer due to the intramolecular hydrogen bonds between hydroxyl groups at the lower rim of the molecule.

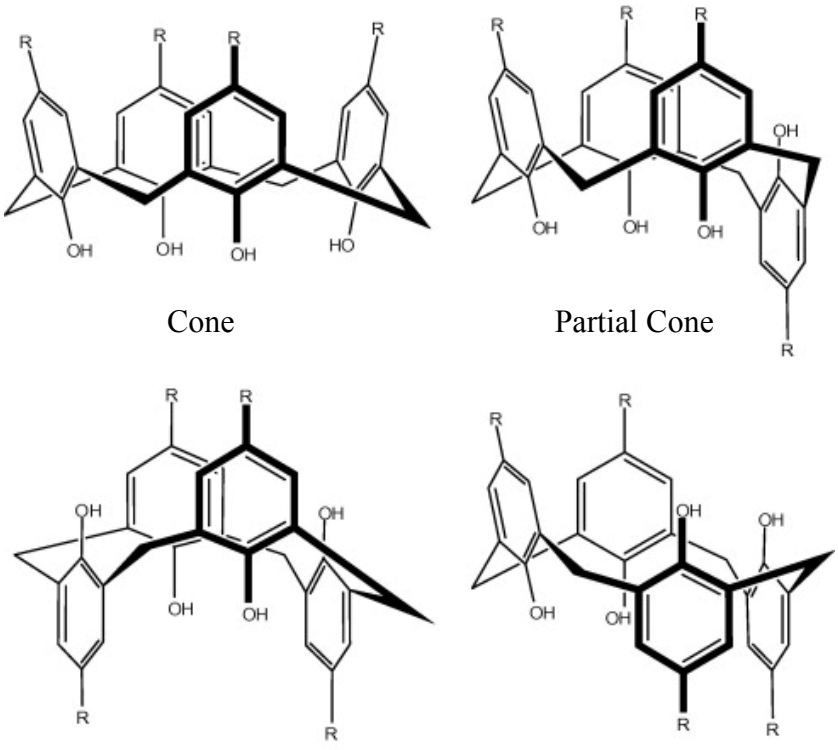

FIGURE 1. Various conformations of calix[4]arene.

The four possible conformations of calix[4]arene can be identified through the ^{1}H and ^{13}C NMR patterns of the bridging methylene group. Although partial cone and 1,2-alternate conformations show a similar pattern for the bridging methylene group, the two conformation can be identified from the aromatic pattern of the spectrum (Figure 2).[2]

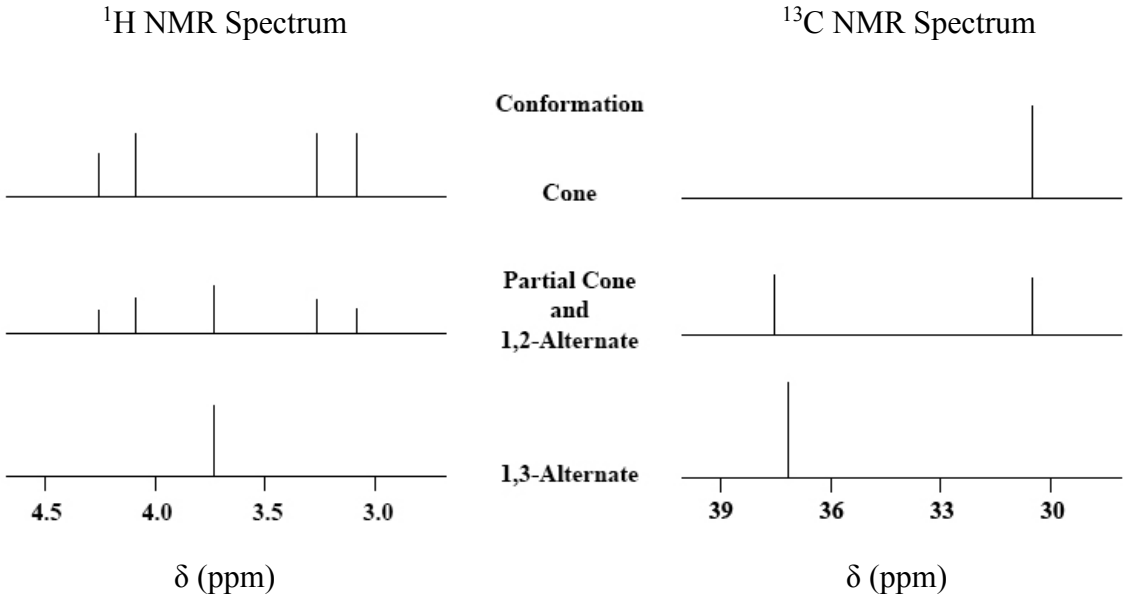

FIGURE 2. Patterns of the signals of the bridging methyl group in calix[4]arene.

Resorcinarenes are a second major class of cyclooligomers that are formed from the condensation of resorcinols with aldehydes as shown in Scheme 2. Unlike the orientation of OH groups in calixarenes that are directed toward the interior of the macrocyclic ring, the orientation of OH groups in resorcinarenes are directed away from the annulus. The resulting arrangement of more rigid and preorganized OH groups enables resorcinarenes to be used as frameworks to elaborate more complex structures.

As such, they are widely used as the basic structures to synthesize capsules that are used in host-guest chemistry.[3,4]

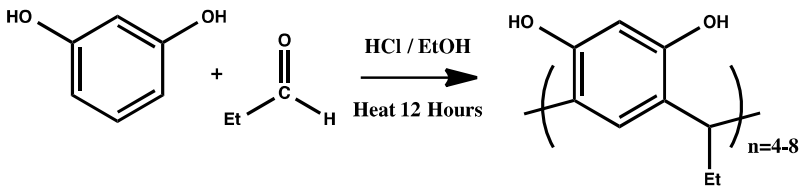

Resorcin[n]arene

SCHEME 2. Formation of resorcin[n]arenes from condensation of resorcinols with aldehydes. Number in square bracket denotes the number of repeating aromatic units.

1.2. Host-Guest Chemistry

Host-guest chemistry refers to non-covalent bonding interactions between two or more molecules. Hydrogen bonding, π-π interactions, metal coordination, and/or electrostatic interactions are examples of possible interactions to hold molecules close to each other. In the host-guest supramolecular complexes, the molecules with concave surfaces behave as receptors of the guest molecules.

Encapsulation refers to one type of host-guest interactions in which the host molecule completely surrounds the guest molecule. Since the formations of capsules are due to weak intermolecular interactions such as hydrogen bonding, their formation and dissociation are reversible and depends on factors such as temperature, type of solvent and pH.

In host–guest chemistry, guest molecules are affected by the steric conditions of the host molecules; therefore, concentration of guest molecules are temporarily increased, which can accelerate rates of reaction. In 1993, J. Rebek described the first catalytic effect of the molecular capsules. Rebek with Mendoza et al.[5] synthesized a semispherical structure that undergoes reversible dimerization to form a closed-shell cavity. The structure held together by eight hydrogen bonds is shown in Figure 3.

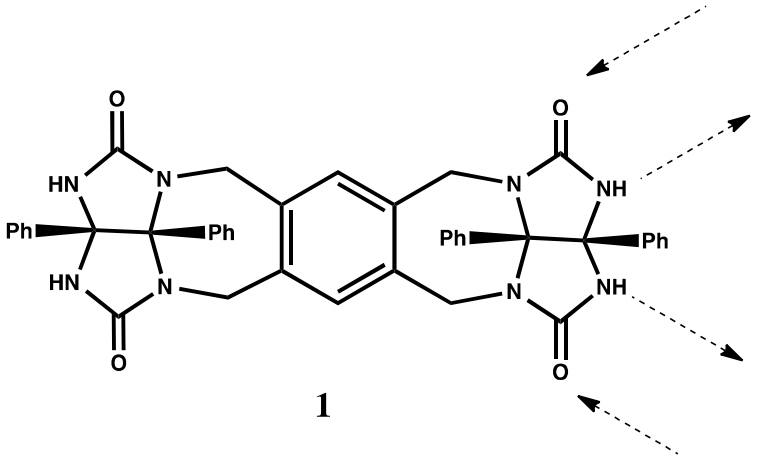

1

FIGURE 3. Structure of a self-complementary module capable of forming a dimeric capsule through hydrogen bonding.

Assembly of two of the self-complementary molecules through hydrogen bonding can form a capsule with a small internal cavity. A tennis ball is a good macroscopic analogy of how two self-complementary compartments can form a capsule with ability of encapsulating a small guest molecule (Figure 4).[5]

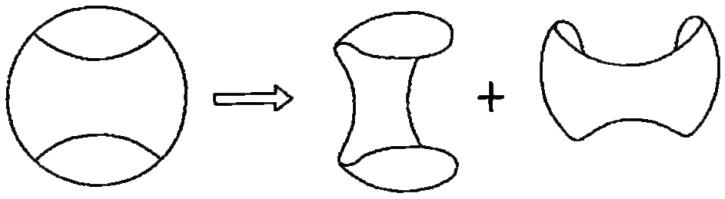

FIGURE 4. Tennis ball assembly from two self-complementary compartments.

An attempt to increase the internal volume of the capsules was carried out by the same group in 1994. They synthesized a chemical structure called "soft ball" with a similar array of hydrogen bonds as of **1** that enables the formation of a self-assembled capsule. When compound **2** is compared to **1** in size, the larger size of **2** compartments leads to a larger interior cavity to accommodate and transport complementary size and shape guest molecules (Figure 5).[6] It was demonstrated that a homo-dimerization of two **2** molecules gives a semispherical closed-shell capsule with the internal volume of 400 Å. This self-assembly capsule is capable of encapsulation of smaller molecules of complementary size and shape.

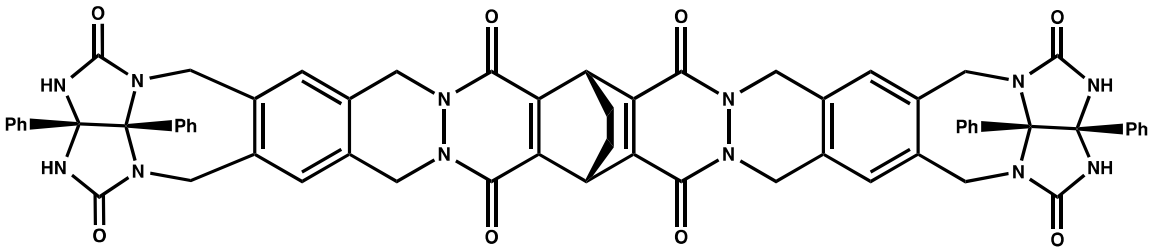

2

FIGURE 5. The structure of a large self-complementary module capable of forming a dimeric capsule through hydrogen bonding.

Another approach to synthesize capsules was carried out by chemical modification of resorcinarenes. Such cage-like capsules can mechanically surround and isolate smaller guest molecules in a reaction; therefore, they can temporarily divide the reaction environment into two domains: 1) on domain where reagents that are in a solution can react normally, and 2) off domain where reagents are encapsulated and are not active.

The internal cavity of resorcinarene-based capsules is large enough to enable them to encapsulate large guest molecules or two or three small molecules of complementary size and shape. In 1998, Heinz et al. synthesized a resorcinarene based cylindrical capsule that was held together with eight hydrogen bonds (Scheme 3).[7] The dimerization of **3·3** takes place in the rim-to-rim manner to give the large *cylindrical* capsule with the internal volume of 420 $Å^3$.

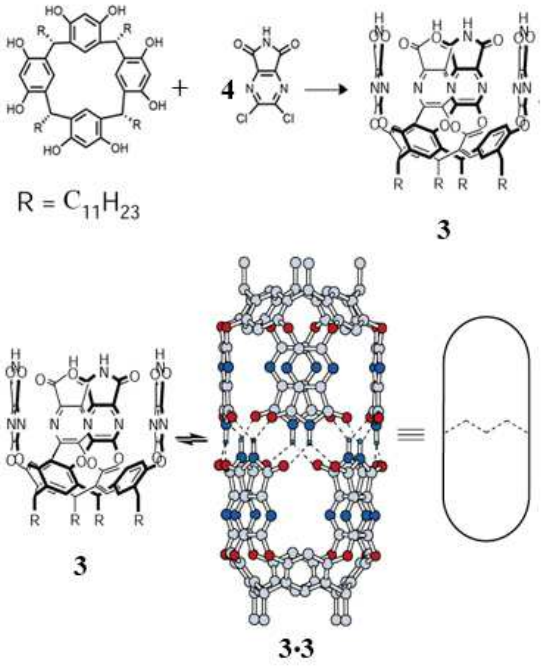

SCHEME 3. Two resorcinarene based cavitands **3** self assembled through hydrogen bonding into a cylindrical capsule **3·3**.

In 2004, Scarso et al. studied reversible encapsulation of a series of normal alkane guests in **3·3** cylindrical capsule by NMR methods.[8] They demonstrated that for hydrocarbons smaller than n-hexane, two guests can easily enter the host, and they move freely within; however, for longer alkanes such as n-decane, the aromatic walls of the host will twist to provide more space to accommodate a single guest. Longer alkanes–up to n-tetradecane–can be accommodated in such capsules only if the alkanes adopt a helical conformation to fit in the cavity.

The finite length and internal volume of capsules hardens and sometimes limits encapsulation of longer guest molecules such as long alkyl substituted molecules; therefore, in 2006 Ajami et al. attempted to elongate cylindrical capsules to study host-guest chemistry of longer guest molecules.[9] They discovered that glycolurils (**4a**, **4b**) could insert themselves between the two halves of the capsule **3·3** to give a new version of cylindrical capsules **5**. Addition of spacer elements expanded the internal volume of capsule **3·3** by ~200 $Å^3$ and increased the length by ~7 Å with. The **4a** and **4b** molecules that were used as spacer elements are capable of hydrogen bonding to hold the cylindrical structure (Figure 6).[9] The expanded capsule **5** posses appropriate size and length to accommodate normal alkanes up to $C_{21}H_{44}$.

Subsequently, further studies proved that normal alkanes that are longer than C_{20} can also be encapsulated within more extended capsules. Based on NMR studies they confirmed that excess addition of glycolurils would lead to addition of an extra belt of glycolurils to accommodate longer guest molecules. The formation of extended capsules happens when, and only when, suitable guests are present in the noncompeting solvent system. Therefore, depending on the size of the guest molecules, more glycoluril belts

can accommodate to encapsulate the guest molecule, for instance hyperextended capsules contain three or four glycoluril belts to accommodate long normal alkanes (Figure 7).[10–12]

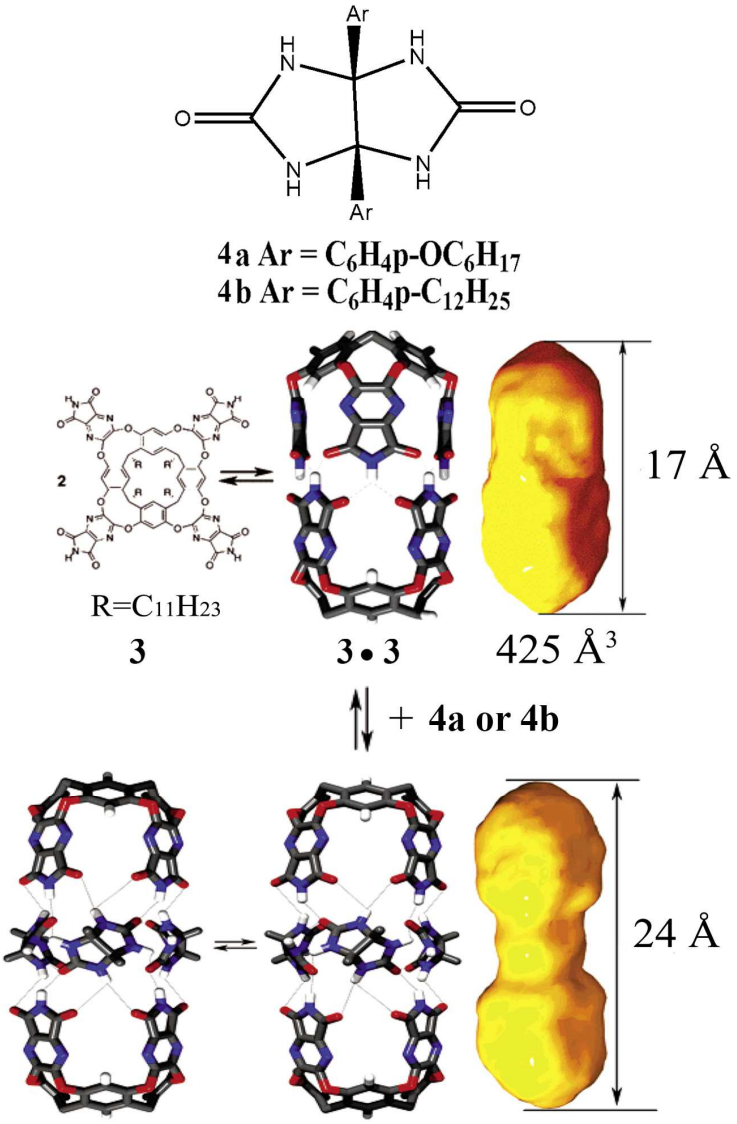

FIGURE 6. (Top) Structure of spacer elements (Middle) Structure of the dimeric 3•3 capsule (Bottom) Structure of the expanded capsule with added spacers.

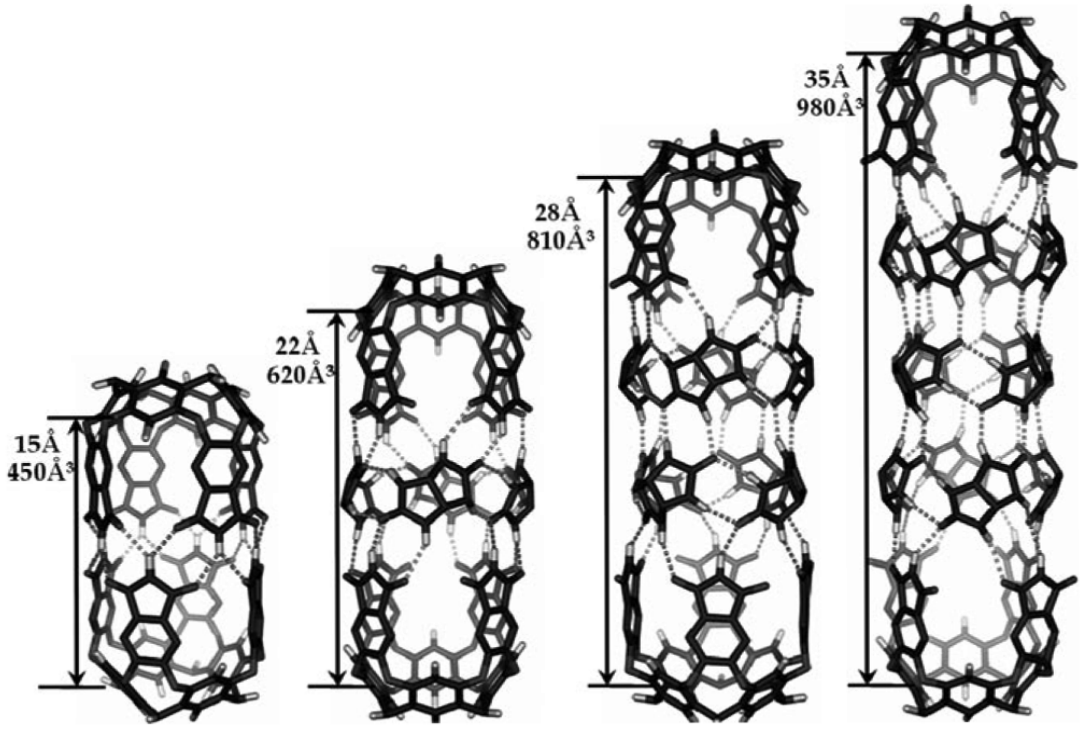

FIGURE 7. A comparison of dimensions and inner space of extended capsules with the original capsule.

Formation of capsules exploits intermolecular forces such as hydrogen bonds, aromatic π-stacking and polar interactions. These forces can bring molecules together into complexes that can temporarily bond groups of two or more molecules to form supramolecular structures. Molecular recognition and encapsulation rely upon the size and shape of the complementary guest molecules, as well as the chemical functionalities of host and guest molecules. The greatest challenge in this field is the characterization of aggregate structures. While NMR spectroscopy provide indirect evidence for formation of discrete aggregation, X-ray crystallography can be insurmountably difficult since these molecules do not crystalize.

1.3. Drug Delivery

The efficacy of drug-transport systems depends on various factors such as solubility, biocompatibility and the release of the encapsulated drug at the pharmacological sites of action. In the last two decades, many drug-transport systems have been developed that revolutionizes the way many drugs are transported and delivered.[13] Among which, the strategies that rely on the synthesis of drug–polymer conjugates or embedding drugs in polymer, vesicle, or micelle carriers have shown promising results in transporting drugs in the body.[14] However, these systems were not successful in transporting drugs in several applications, mostly in transporting drugs to the brain. The unsuccessful transport of drugs is due to blood-brain barrier, which is a highly hydrophobic barrier that separates the brain tissue from the blood circulation. The selectivity of the barrier prevents penetration of harmful substance into the central nervous system; however, lipophilic substances can easily penetrate into this hydrophobic environment.[15] In 2007, William M. Pardridge reported that basically 100% of large-molecule drugs and >98% of small-molecule drugs cannot be transported across the blood-brain barrier.16 This has raised concerns about finding effective drug carriers that can transport neurological drugs across the blood-brain barrier.

Later that same year, Schramm et al. reported that resorcin[4]arene derivatives adopt a cavity conformation in aqueous micellar environments.[17] By that time resorcinarene were proven to be a good framework to elaborate more complex cavitands.[3,4] Additionally, their efficiency in serving as a host for complementary guest molecules,[4] as a reaction accelerator [18,19] and as a catalyst [20] had been proven by numerous publications. Therefore, the ability of adopting a cavity conformation in an

aqueous micellar environment could make resorcinarenes to be a suitable prototype to serve as a drug carrier.

Recently, Adhikari et al. have reported that resorcinarene cavitands have a strong binding affinity toward the complementary guest molecules such as choline that restrains the efficient release of guest molecules.[21] Instead, they studied the ability of calixarene species with ionizable groups in extraction of the complementary guest molecules from aqueous layer into organic layer. The results were promising enough to encourage us to study the ultimate transport of drug conjugates via different calixarene derivatives.

1.4. This Work

The use of calixarene and resorcinarene cavitands presents a novel approach to transport drugs compared to common approaches of drug delivery. Tools such as covalent attachment of a drug to a delivery vehicle or emulsification in lipid micelles have already been employed successfully.[13] Herein we aim to develop a synthetic host-guest system that functions in biological environments with the following principles in mind: 1) the receptor should localizes in the hydrophobic interior of the cell membrane, 2) the receptor should be benign to the cell and not cause leakage in or out of the cell, 3) the systems should be able to selectively transport a wide variety of drug payloads that are easily appended with a receptor complementary handle, and 4) the receptor should transport more than one equivalent of payload. This ambitious list of principles is already at work for valinomycin and nonactin, which inspired us to explore the strengths and weaknesses of the different types of calixarenes as receptors of ammonium ion.[22,23] We are positive that calixarenes could serve as an effective receptors of guest molecules that possess ammonium ion and we are hopeful that this property can ultimately increase

the efficiency of transporting drug-choline conjugated through a calixarene-mediated liquid membrane.

CHAPTER 2

EXPANDING THE INNER VOLUME OF CAPSULES

2.1. Introduction

Condensation of resorcinol with aldehydes under acidic conditions leads to cyclic tetramers, which are known as resorcinarenes. Thermodynamically, resorcin[4]arene is the more favored product of this condensation and have been widely used as highly specific ligand in analytical chemistry,[24,25] sensor techniques [26,27] and medical diagnostics [28,29]. Additionally, due to the rigid orientation of the hydroxyl groups in resorcinarenes, there is an enormous interest in using them as frameworks for elaborating complex structures. As discussed in the first chapter, resorcinarenes can be used as building blocks of many capsules that can encapsulate complementary guest molecules. Over years, many attempts have been made to increase the internal volume of resorcinol capsule to turn them into a suitable host for more bulky molecules or two or more smaller molecules.

Utilizing resorcin[5]arene as building blocks of capsule instead of resorcin[4]arene would drastically increase the internal volume of cavitands and capsules. However, isolating resorcin[5]arene is very difficult since it is a kinetic product of the condensation of resorcinol and aldehydes. Herein, we are trying to examine the idea of making resorcin[5]arene by using rigid penta aldehydes calix[5]arene as a template (Scheme 4). However, calix[4]arene was used as a model compound due to it's cone

conformation, ease of synthesis, and lower cost. If the condensation of tetra aldehyde calix[4]arene with resorcinol yields resorcin[4]arene stacked on calix[4]arene, we can apply the same reaction sequence on the penta aldehyde calix[5]arene.

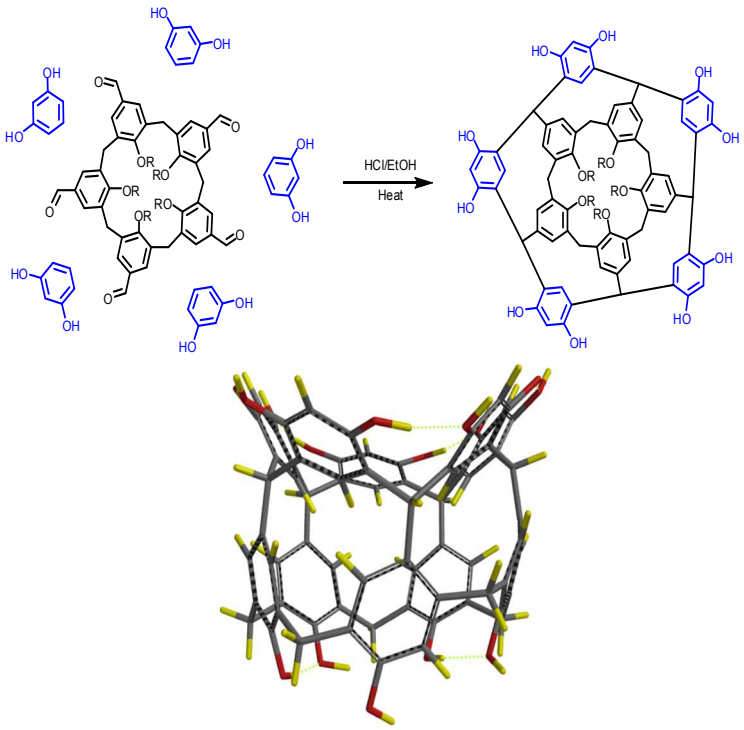

SCHEME 4. Proposed synthetic scheme of resorcin[5]arene stacked on calix[5]arene.

2.2. Results and Discussion

The first attempt to prepare a tetra aldehyde calix[4]arene started with removal of the tert-butyl groups from the upper rim of commercially available para-tert-butyl-calix[4]arene under ambient conditions. By treating the commercially available *p*-tert-

butyl-calix[4]arene with aluminum chloride and phenol in dry toluene as shown in Scheme 5, compound **6** was achieved in 80% yield.[30]

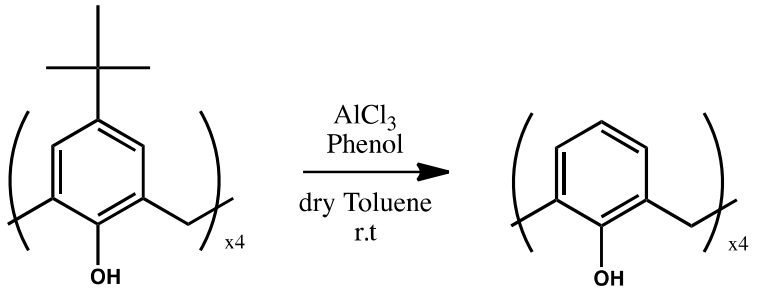

6

80%

SCHEME 5. Synthetic scheme of compound 6.

Next, **6** was treated with dodecyl iodide in presence of sodium hydride in dimethylformamide to obtain alkyl chains on the lower rim of the calix[4]arene **7** in 91% yield (Scheme 6).[31]

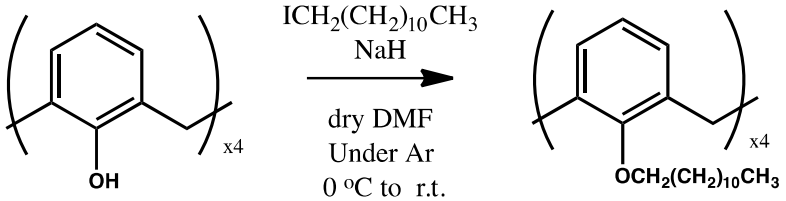

6 **7**

91%

SCHEME 6. Synthetic scheme of compound 7.

Then, tetrakis(dodecyloxy)calix[4]arene **7** reacted with dichloromethyl methyl ether in presence of titanium tetrachloride to form the desired tetra-aldehyde template **8** in 35% yield (Scheme 7).[32]

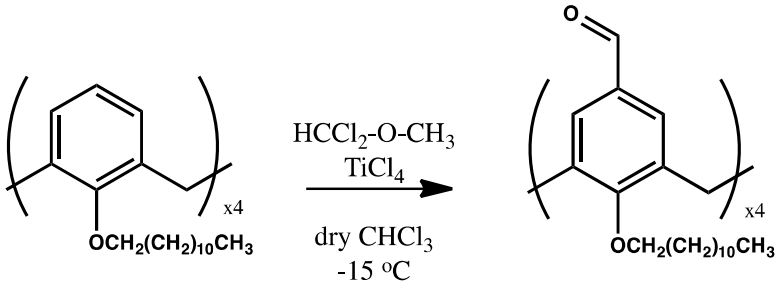

7 **8**

35%

SCHEME 7. Synthetic scheme of compound 8.

Finally, condensation of **8** with resorcinol was carried out under acidic conditions to obtain the desired product **9** (Scheme 8). However, the reaction yielded a highly insoluble precipitate that was not soluble with common solvent systems. Due to the solubility problems, we were not able to characterize the precipitate of this reaction. Many solvent combinations were tried to no avail.

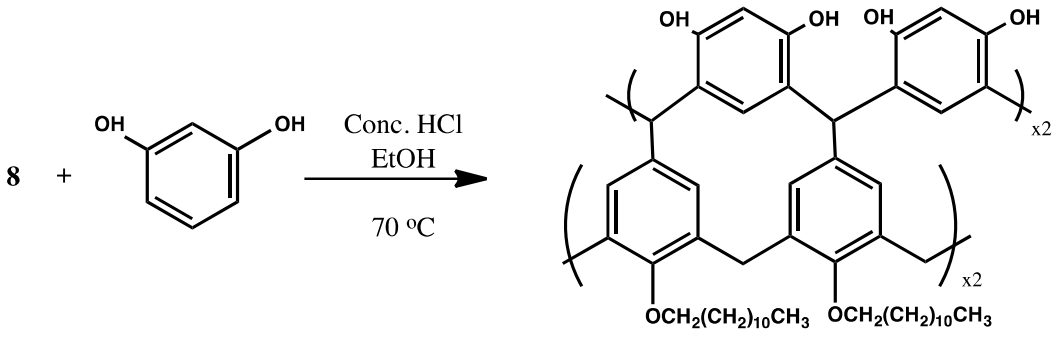

9

SCHEME 8. Synthetic attempt to produce compound 9.

In order to solve the solubility problem, we decided to synthesis a calixarene that posses more polar substitutes in the lower rim. Therefore, **6** was treated with [2- [2- (2-methoxy ethoxy) ethoxy] ethoxy] *p*-toluene sulfonate to obtain **10** in 57% yield (Scheme 9).[33]

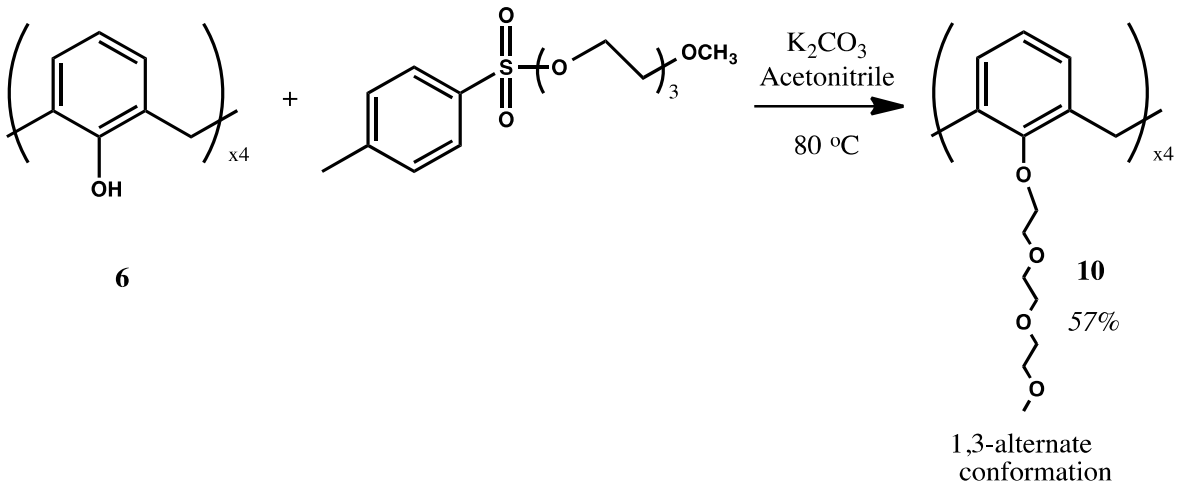

SCHEME 9. Synthetic scheme of compound 10 in 1,3-alternate conformation.

The crude ^{1}H NMR spectra of **10** illustrated that the obtained product is not in the desired conformation (cone conformation), which makes it impossible to obtain the desired tetra-aldehyde template. Subsequently, we attempted to carry out the same reaction using NaH instead of K_2CO_3, hoping that the smaller size of sodium would help the calixarene to stay in cone conformation. However, the latter reaction also gave **10** in 1,3-alternate conformation with the same yield as the former reaction.

Moreover, we examined if the conformation of **10** would change in formylation step; therefore, **10** was treated with dichloromethyl methyl ether in the presence of

titanium tetrachloride to obtain **11** (78% crude yield). The crude ^{1}H NMR spectrum of **11** illustrated that it is also in the 1,3-alternate conformation (Scheme 10).

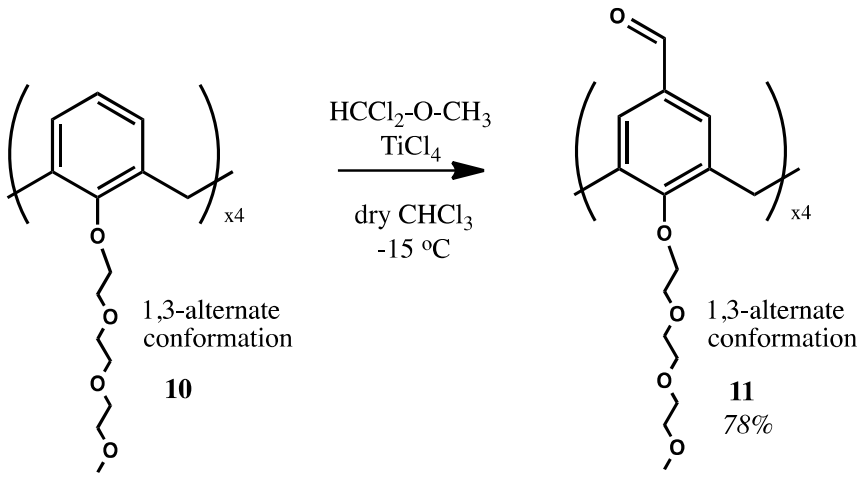

SCHEME 10. Synthetic scheme of compound 11 in 1,3-alternate conformation.

Since the conformation remained the same under different reaction conditions, we conclude that the 1,3-alternate conformation forms due to the electronic repulsion and/or steric hindrance of the four polyether substituents. Therefore, to decrease the possible repulsion and/or steric hindrance, substitutes with a shorter length should be used at the lower rim. Additionally, having asymmetrical substituents on a complex will decrease the symmetry of it, which will increase the solubility of the complex. Consequently, we decided to synthesize dibenzyloxy-bis (2-methoxyethoxy) calix[4]arene that posses substituents with less steric hindrance and has a lower symmetry than **10**.

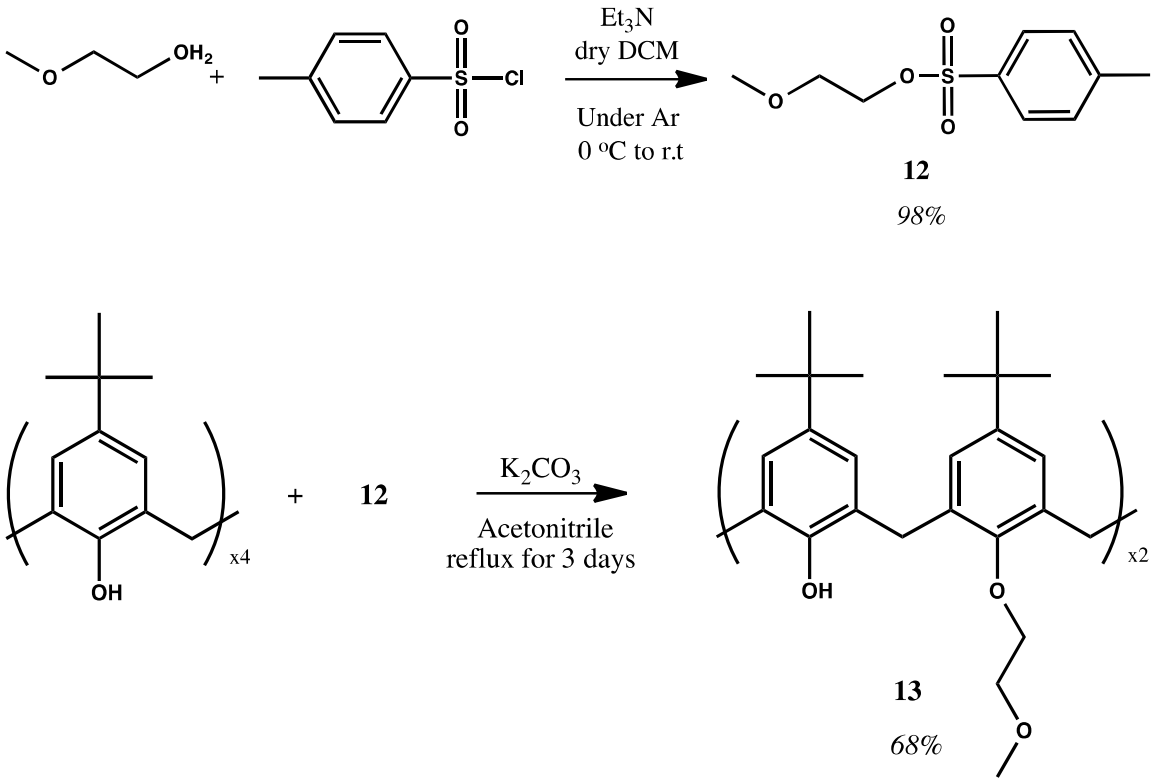

SCHEME 11. Synthetic scheme of compound 12 and 13.

First, 2-methoxy ethanol was reacted with *p*-toluenesulfonyl chloride in presence of triethylamine to produce 2-methoxyethyl tosylate **12** in 98% yield as shown in Figure 17. Then, commercially available p-tert-butyl-calix[4]arene was treated with two equivalents of 2-methoxyethyl tosylate **12** in the presence of potassium carbonate in acetonitrile to afford **13** in yield 68% (Scheme 11).[33]

Reaction of **13** with 2 equivalents of benzyl bromide in the presence of potassium carbonate produced **14** in 67% yield (Scheme 12). Subsequently, **14** was treated with aluminum chloride and phenol in dry toluene to remove the tert-butyl groups from the upper rim of **14** but after several attempts the reaction was not successful. We suspect that the presence of benzyl substitutes is interfering with the reaction.

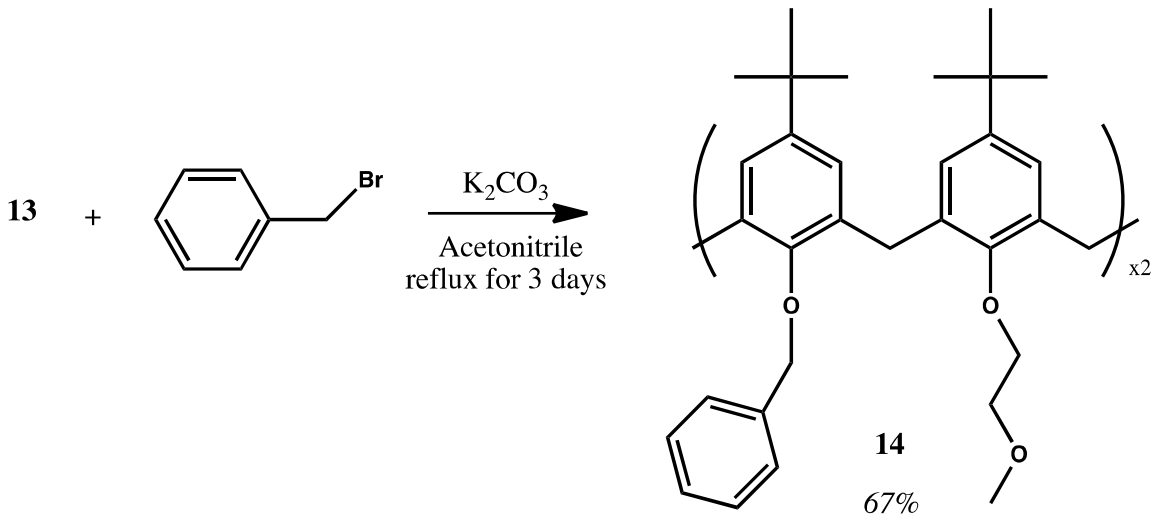

SCHEME 12. Synthetic scheme of compound 14 in cone conformation.

Consequently, another attempt was made to synthesize dibenzyloxy-bis (2-methoxyethoxy) calix[4]arene, where de-tert-butylation reaction was carried out initially. Compound **6** was reacted with two equivalents of benzyl bromide in presence of potassium carbonate in dry acetone under reflux conditions to produce **15** in 82% yield.[34] Lastly, compound **15** was reacted with two equivalents of **12** to produce **16** in 73% yield (Scheme 13).[33] The H^1NMR spectra of **15** and **16** prove that both compounds are in cone conformation; however, we are unable to say whether the lower rim substitutes are added in alternative positions or adjacent positions. To confirm the structure, x-ray crystallography can be conducted.

Finally, the formylation reaction of **16** was carried out; however, after several attempts, the desired product was not isolated, which may be due to the reason that the benzyloxy substitutes also under goes formylation.

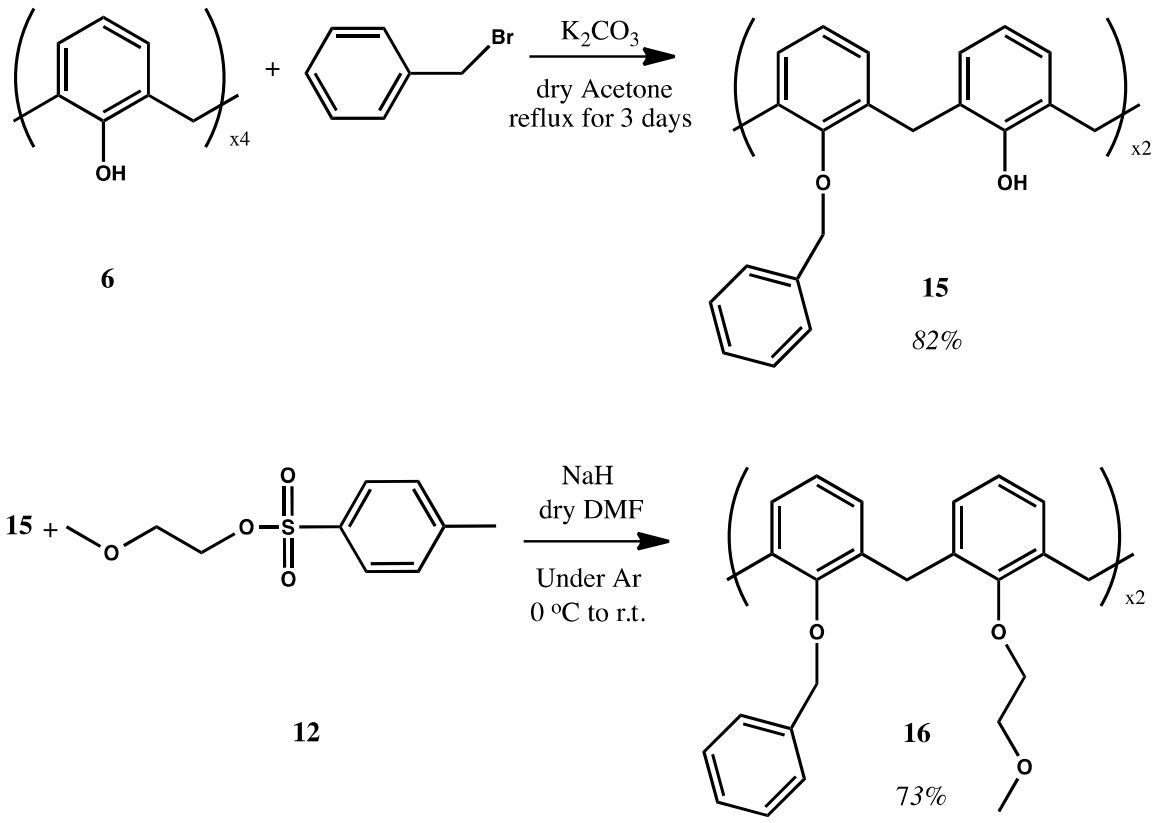

SCHEME 13. Synthetic schemes of compound 15 and 16 in cone conformation.

To eliminate the interruption of benzyloxy groups in the formylation step, we decided to introduce a normal alkyl chain instead of the benzyloxy substitutes. While the new compound would not tend to undergo side reactions in the formylation step, the normal alkyl chains will lead to an asymmetrical structure that increases the solubility. Thus, compound **6** was reacted with two equivalences of 1-iodooctyl in presence of potassium carbonate under reflux condition to produce **17** in 96% yield.[34] Subsequently, the product **17** was treated with two equivalences of **12** in presence of NaH to afford **18** in 48% yield (Scheme 14).[33]

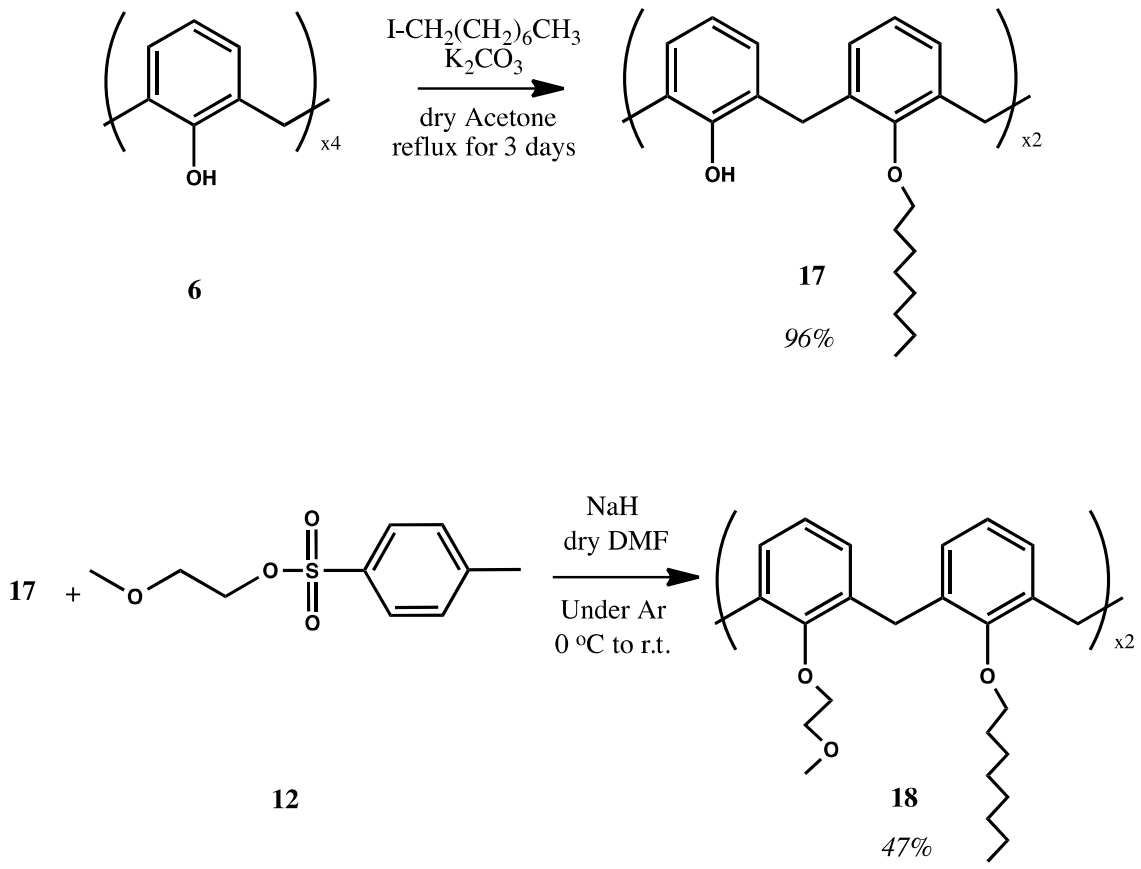

SCHEME 14. Synthetic schemes of compounds 17 and 18 in cone conformations.

Subsequently, we carried out the formylation reaction. Compound **18** was treated with hexamethylenetetramine in trifluoroacetic acid in dry chloroform to achieve compound **19** in cone conformation and 35% yield (Scheme 15).[35] The final step, which is condensation of compound **19** with resorcinol, was carried out in presence of excess amount of concentrated hydrochloric acid in ethanol to achieve the desire product **20** (Scheme 15).

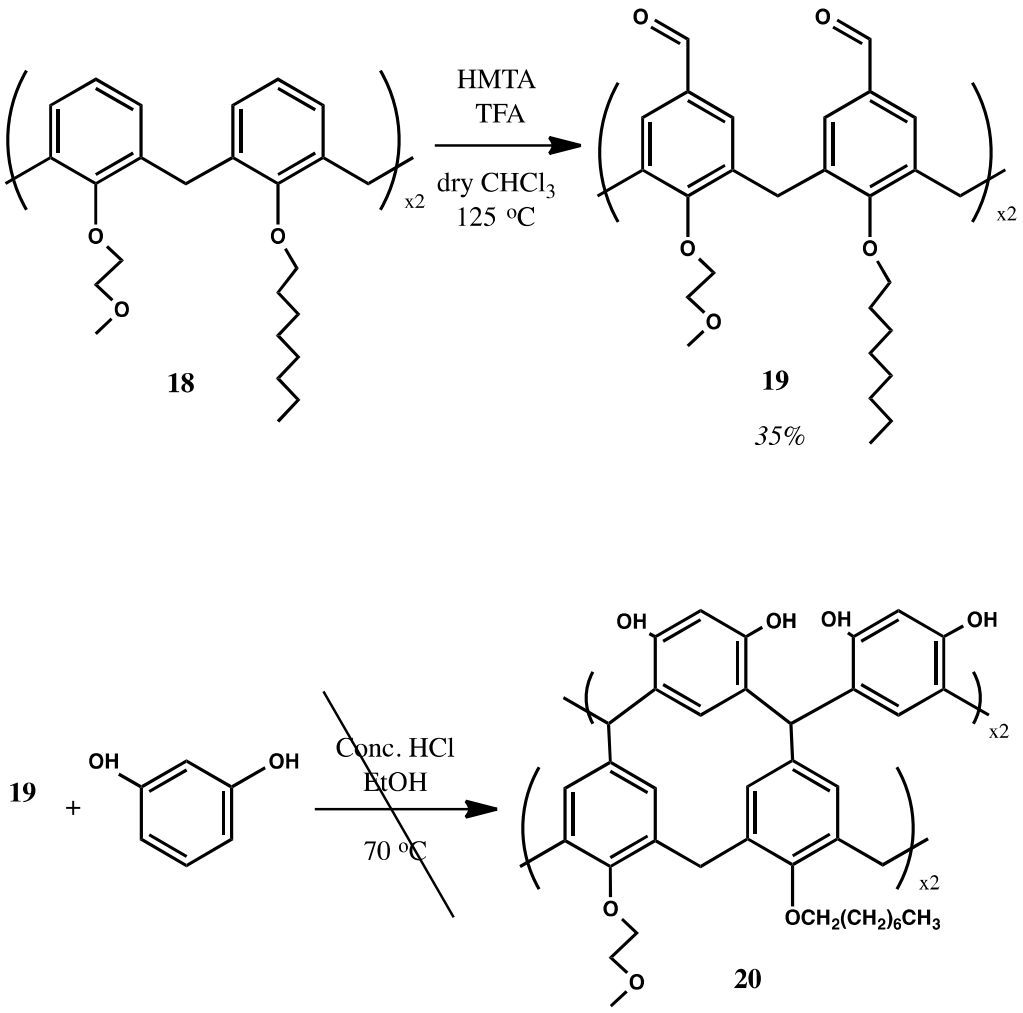

SCHEME 15. Synthetic scheme of compound 19 and molecular structure of desired final product 20.

Several attempts were made to solubilize the residue of the final step, which is condensation of resorcinol with tetra-aldehyde calix[4]arene; however, the residue was insoluble is all common solvents systems. The solubility problem hindered the characterization of the collected residue.

2.3. Conclusion

The objective of this project was to synthesize larger resorcinarenes as thermodynamic products. Our strategy to accomplish such products was to synthesize a template (calix[5]arene tetra-aldehyde) that can undergo condensation reaction with resorcinol to afford a stacked assembly of resorcin[5]arene on calix[5]arene. We were hoping that resorcin[5]arene can be synthesized as a thermodynamic product by using a rigid template. Since calix[5]arene adopts various conformations, as a model compound, calix[4]arene was used because its cone conformation facilitates the synthesis.

Numerous attempts were made to synthesize a highly soluble tetra-aldehyde calix[4]arene that possesses a rigid cone conformation, such as the introduction of: lower rim substitutes with different polarities to solve the solubility problem, lower rim substitutes that are different in lengths to reduce the potential steric hindrance, and mixed lower rim substitutes to increase the solubility, etc. However, the product of the final reaction–condensation of resorcinol with tetra-aldehyde calix[4]arene–was a highly insoluble residue which hindered the characterization of the obtained residue. So due to our model compound's lack of characterization, we did not further pursue calix[5]arenes as a template.

The highly insoluble residue from the final step–condensation of resorcinol with tetra-aldehyde calix[4]arene–might be due to: 1) poor solubility of the desired target molecule, 2) potential side reactions that can occur such as condensation of a resorcinol with two calix[4]arene tetra-aldehyde molecules that yield highly insoluble final products, or 3) a combination of both possibilities listed above.

To decrease the probability of occurrence of the side reactions, the condensation reaction should be controlled in a way that four equivalents of resorcinols are exposed to only one equivalent of calix[4]arene tetra-aldehyde. Slow addition of an acid activated calixarene to a high concentration of resorcinols, for example, might decrease the probability of occurrence of the side reactions.

CHAPTER 3

TRANSPORT STUDIES OF CHOLINE-CONJUGATED DRUGS

3.1. Introduction

In the last two decades, many drug delivery systems have been developed and some have received clinical approval but challenges for an effective drug transport still remain.[13,14,16] Our contribution in this field stems from the history of supramolecular host-guest chemistry particularly related to the role of calixarene cavitands as host molecules.

It has been reported that resorcinarenes can function in aqueous lipid systems as host [17] for a complementary guest molecule and they can function as a platform for switching.[36] Furthermore, it has been proven that resorcinarenes can distribute themselves evenly in lipid bilayer systems.[37] Although these properties enable resorcinarenes to be a good candidate for drug delivery in lipophilic conditions, due to the strong binding affinity of such molecules to the complementary guest molecules, extraction and ultimate transport of target molecules is not successful.[21]

A preliminary study done by our group demonstrates that calixarene species with ionizable groups are capable of binding with a choline group–quaternary ammonium salt–. The ^{1}H NMR spectrum of a mixture of calix[4]are phosphonic acid (host) and FITC-choline (guest) proves the binding of host and guest molecules (Figure 8). The dashed rectangular in Figure 8 shows the corresponding peak of quaternary ammonium

group. The up field shift in the spectrum denotes that the host molecule is bound with the guest molecule. Furthermore, the same study proves that calixarenes with ionizable groups are able to extract a hydrophilic molecule with a choline handle from hydrophilic environment into lipophilic environments. [21]

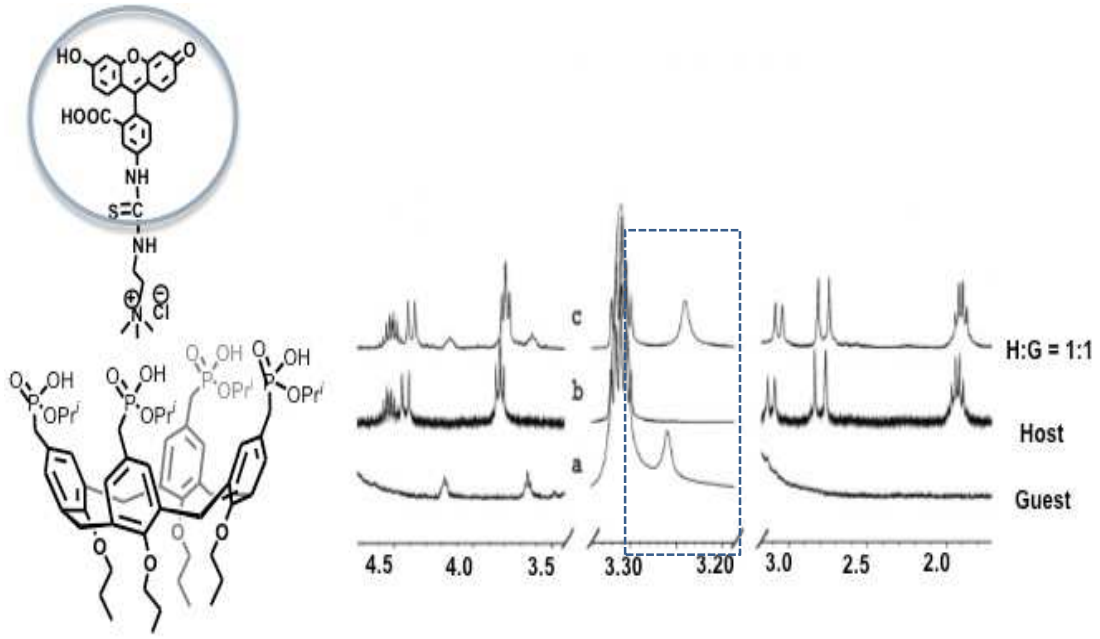

FIGURE 8. 300 MHz ^{1}H NMR of calix[4]arene phosphonic acid and FITC choline in MeOH-d4

Our approach for drug delivery relies on the interaction of series of calixarene-based supramolecular hosts molecules with variety of drug-choline conjugates.[38] Initially a series of drug-choline conjugates were prepared that afforded us wide-ranging chemical properties. Afterward, the host-guest interactions between choline group and the receptors encouraged us to explore the ability of the calixarene-based supramolecular

hosts to transport drug-choline conjugates and neurotransmitters through a lipophilic membrane.

To achieve an effective transport, the receptor molecule (host) should be able to: 1) bind with the hydrophilic guest molecule, 2) extract the guest molecule into a lipophilic environment, and 3) release the guest molecule into a hydrophilic environment. We are hopeful that this approach will ultimately solve some drug-transport problems across highly lipophilic membranes. This work has been built on a variety of prior reports with trimethylammonium guests.[39–44]

3.2. Experimental Conditions

In order to explore the potential of different calixarene derivatives in transport of choline-conjugated drugs through a lipophilic membrane, three-phase U-tube transport experiments were conducted by using an U-shaped glass tube as shown in Figure 9.

The organic phase consisted of 10 mL solution of 0.5 mM calixarene-based receptors in dichloromethane (DCM) or chloroform. The source phase consisted of 4 mL aqueous solution of a substrate in either MilliQ water or HEPES buffer (4-(2-hydroxyethyl)-1-piperazineethanesulfonic acid). The receiving phase was either pure milliQ water, 0.1 M HCl or HEPES buffer (4-(2-hydroxyethyl)-1-piperazineethanesulfonic acid). The U-tube's upper ends were sealed and the experiments were started by stirring the organic phase with magnetic stirring bar at stirring speed of 400 rpm.

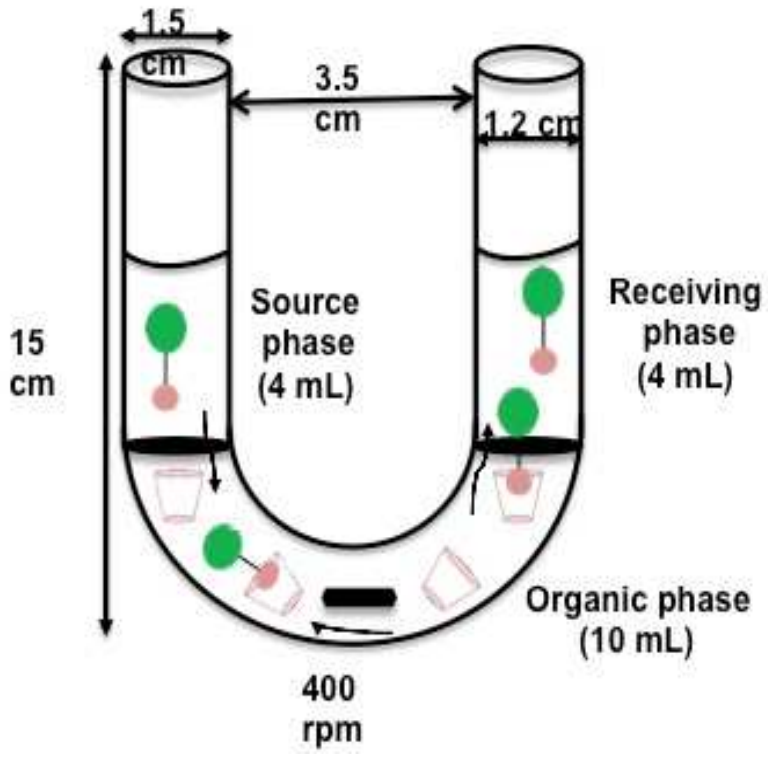

FIGURE 9. U-tube apparatus showing dimensions and experimental conditions.

After 72 hours of stirring, an aliquot from both source and receiving phases were collected and analyzed with UV-vis spectrophotometer after adequate dilution against a standard serial dilution curve. Then transport flux of each set was calculated. Two sets of experiments were conducted and the data presented are the average values. Control experiments were performed using pure DCM as the organic phase.

3.3. Transport Flux Calculation

Transport flux of series of Choline-conjugated drugs were calculated using the following formula [45]

$$\text{Transport Flux} = \frac{\text{Moles Transported}}{\text{Area} * \text{Time}}$$

where in this project time was kept constant (72 hours) and area is calculated based on the average radius of U-tubes that were used

$$\text{Area} = \pi r^2 = 1.130\ \text{cm}^2\ (r = 0.6\ \text{cm})$$

In order to determine the moles transported during the time = 72 hours, the following formula is used

$$\text{Moles Transported} = \frac{(\text{Abs} - b) * d}{a} * \text{Volume of receiving phase (L)}$$

where *a* is the slope of the calibration curve, *b* is the intercept of the calibration curve, *d* is the dilution factor and *Abs* is the absorbance of the receiving phase.

3.4. Results and Discussions

In this project, our choice of calixarene-based supramolecular hosts are upper-rim tetraphosphonic acid calix[4]arene **21** [46], a homologous series of lower rim carboxylic acid calix[4] **22** [47], calix[5] **23** [48] and calix[6] **25** [21]– arenes and upper-rim tetrasulphonic acid calix[4]arene **25** [49] (Figure 10).

Presence of an ionizable moiety on the structure of host molecules is essential to achieve a desired hydrophilicity, without compromising their lipophilicity. This

collection of ionizable receptors afforded us an easy access to a good range of pKa values. Furthermore, we wished to test the effect of size and preorganization-flexibility of the cavitands on the transport rate; therefore, different cavitand size were utilized in this projects. With calix[6]arene we have varied the preorganization-flexibility, since calix[4] and calix[5]arenes are less likely to interconvert into up-down isomers. [1]

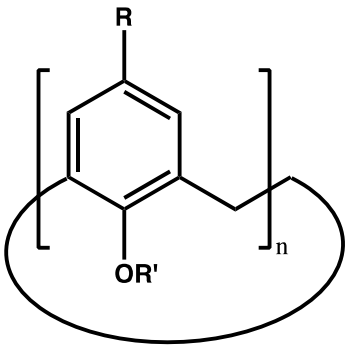

21 R = $CH_2P(O)(OH)(OPri)$, R' = nPr, n = 4
22 R = t-butyl, R' = CH_2COOH, n = 4
23 R = t-butyl, R' = CH_2COOH, n = 5
24 R = t-butyl, R' = CH_2COOH, n = 6
25 R= SO_3H, R' = H, n = 4

FIGURE 10. Molecular structures of calixarene-based receptors.

The guest-choline conjugates were synthesized following either path one or path two depending on the presence of either carboxylic or phenolic functional groups, as shown below (Scheme 16).

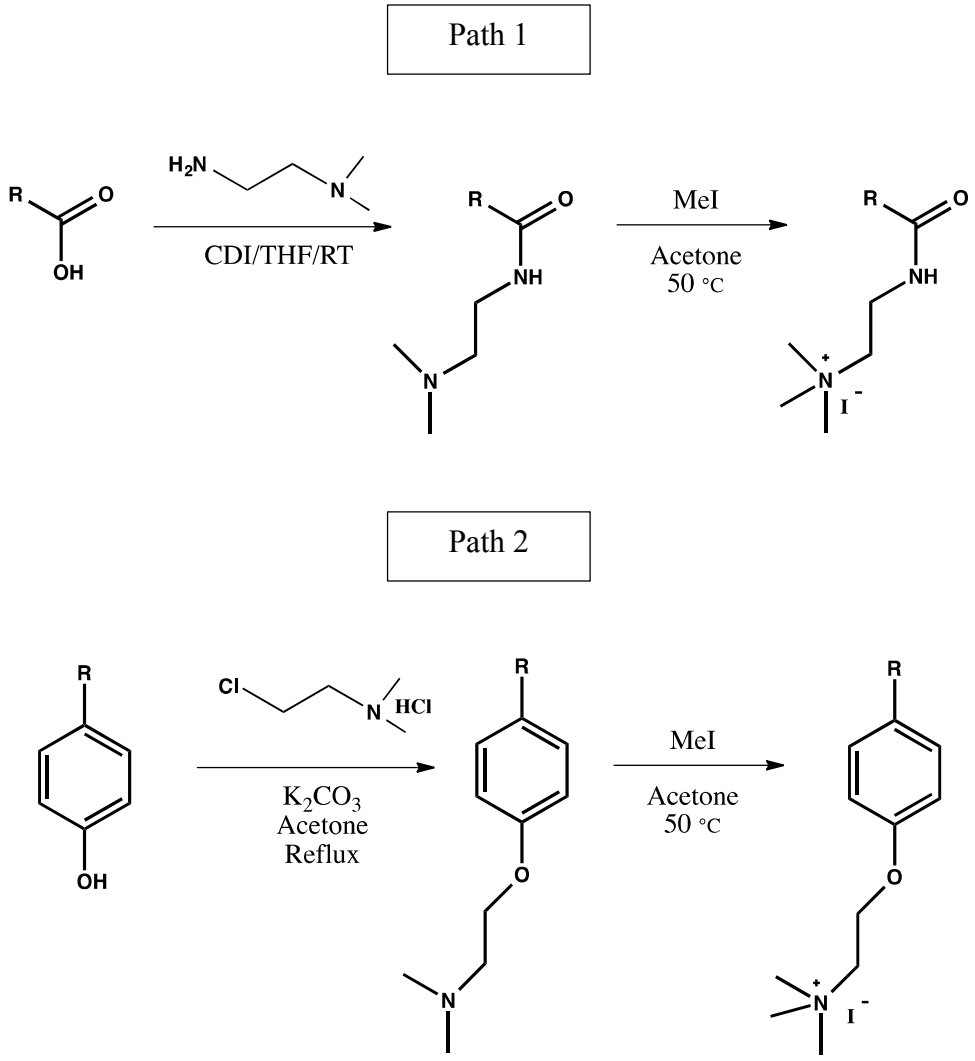

SCHEME 16. Synthesis of drug-choline conjugates.

From analytical point of view, our initial choices of guests were choline conjugated fluorescein isothiocyanate (FITC-choline)[50] **26** and choline conjugated nitrobenzoxadiazole (NBD-choline)[51] **27** (Figure 11). These molecules are fluorescence active and allow us to study the transport ability of the host based on fluorescence measurement.

The three-phase experiments were used to evaluate the transport of **26** and **27** mediated by **22**, **23**, and **24**. Table 1 summarizes the transport flux of these series of experiments.[21] When the transport fluxes are compared to the control experiments, the results indicates that the presence of the choline handle accelerated the transport of payloads, regardless of the pH of the receiving phase. Therefore, it can be concluded that the choline handle could indeed be used to transport payload through a lipophilic liquid membrane.

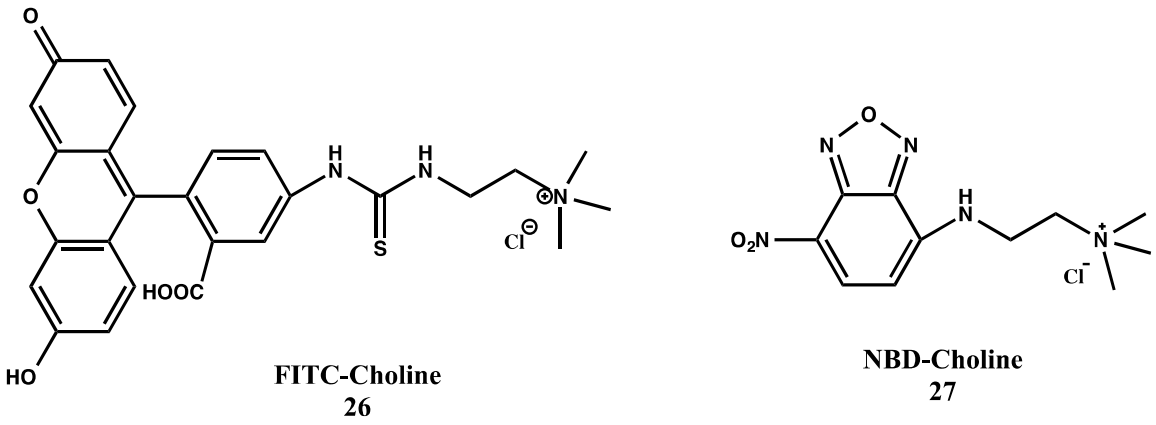

FIGURE 11. Structures of the fluorescence active FITC-Choline 26 (left) and NBD-Choline 27 (right).

The transport efficiency of calixarene carboxylic acids **22**, **23**, and **24** towards FITC-choline **26** differed significantly as the internal volume of the calixarenes changed. The results demonstrate that the calix[4]arene carboxylic acid **22** has some advantages for transport.

TABLE 1. Transport Flux for 26 and 27 Mediated by 22, 23, and 24

Host	Guest	Transport Flux ($\mu molcm^{-2}min^{-1}$)	Control ($\mu molcm^{-2}min^{-1}$)	Receiving phase
22[a]	**26**	1.6×10^{-5}	0	MQ Water
	26	1.2×10^{-5}	0	0.1 M HCl
	27	3.9×10^{-5}	1.3×10^{-5}	MQ Water
	27	9.4×10^{-5}	1.3×10^{-5}	0.1 M HCl
23 [b]	**26**	$(8.86 \pm 4.43)\times10^{-6}$	0	MQ Water
	26	$(6.95 \pm 0.70)\times10^{-6}$	0	0.1 M HCl
	27	$(9.07 \pm 2.92)\times10^{-7}$	1.3×10^{-5}	MQ Water
	27	$(5.50 \pm 1.32)\times10^{-5}$	1.3×10^{-5}	0.1 M HCl
24 [a]	**26**	0	0	MQ Water
	26	1.9×10^{-6}	0	0.1 M HCl
	27	3.1×10^{-6}	1.3×10^{-5}	MQ Water
	27	2.6×10^{-4}	1.3×10^{-5}	0.1 M HCl

[a] Calixarene-based receptors (500 μM) in CH_2Cl_2; guests were dissolved in water, stirred for 96 h at 400 rpm. [b] Calix[5] CH_2COOH 23 receptor (500 μM) in DCM; guests were dissolved in water, stirred for 72 h at 400 rpm.

When calix[5]arene carboxylic acid **23** was evaluated under neutral conditions, the transport flux decreased significantly. Ultimately, when calix[6]arene carboxylic acids **24** was evaluated, no transport was observed. Acidification of the receiving phase also resulted in a decreasing trend in transport flux as the internal cavity increased.

Similarly, when NBD-choline **27** was studied using calixarene carboxylic acids in neutral condition, a decreasing trend was observed as the size of the cavitands increased. Notably, when calix[6]arene hexacarboxylic acid **24** was evaluated, only extraction took place, which resulted in lower value for transport flux than control. Interestingly, when the receiving phase was acidified, the transport flux increased 2.5, 61 and 84 fold when **22**, **23**, and **24** were used respectively, which indicates that for optimized transport of this combination of host and guest, a large pH gradient is required.

When FITC-choline **26** was used as the guest, the acidification of receiving phase did not change the transport flux significantly; however, when NBD-choline **27** was used as the guest, an efficient transport was not possible until after acidification of the receiving phase. This indicates that the presence of an ionizable moiety in guest molecules play a key role in an efficient transport. Since NBD-choline **27** lacks an ionizable moiety, a large pH gradient is require to protonate the corresponding acetate anion on host molecules **22**-**24** to enable the guest release at receiving phase interface, whereas the existence of an ionizable moiety in FITC-choline **26** enables an efficient transport independent of the pH.

The transport results of FITC-choline **26** and NBD-choline **27** were promising enough that motivated us to study the transport flux of some drug and drug-like-choline conjugates. Thus, we explored the three-phase transport of BOC protected tryptophan-choline **28** (Figure 12) facilitated by four different receptors **21**, **22**, **23**, and **24** under different receiving phase conditions (neutral and acidic).

The three-phase transport flux of tryptophan-choline **28** indicates when phosphonic acid **21** was utilized as a receptor in neutral conditions, the transport flux of **28** increased by 4.5 fold compared to the control experiments (Table 2). Receptors **22**-**25** were not as efficient as **21** in delivering the guest into the receiving phase–, but the results show that they are excellent extractors.

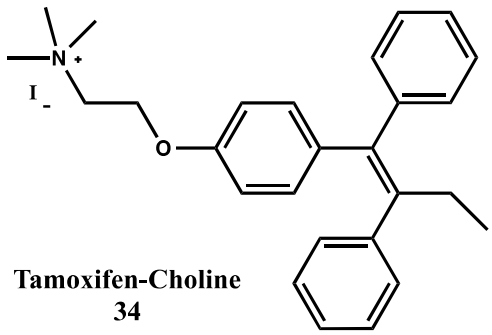

Tamoxifen-Choline
34

FIGURE 12. Structure of BOC protected tryptophan-choline 28.

TABLE 2. Three-Phase Transport of Tryptophan-Choline 28 with Various Receptors [a]

Receptor (0.5 mM)	Transport Flux ($\mu molcm^{-2}min^{-1}$)	Enhancement [b]	Receiving phase
21	$(5.76 \pm 0.09)\times10^{-5}$	4.5	MQ Water
	$(1.13 \pm 0.02)\times10^{-4}$	6.3	0.1 M HCl
22	$(1.18 \pm 0.00)\times10^{-5}$	0.9	MQ Water
	$(1.66 \pm 0.07)\times10^{-4}$	9.2	0.1 M HCl
23	$(3.03 \pm 0.00)\times10^{-6}$	0.2	MQ Water
	$(1.71 \pm 0.18)\times10^{-4}$	9.6	0.1 M HCl
24	0	0	MQ Water
	$(1.18 \pm 0.07)\times10^{-4}$	6.6	0.1 M HCl
Control (no host)	1.27×10^{-5}	-	MQ Water
	1.79×10^{-5}	-	0.1 M HCl

[a] 0.5 mM receptor in 10 mL DCM, 0.5 mM substrate was charged in the source phase in 4 mL of MQ water, and a receiving phase of 4 mL water or 0.1 M HCl was added. After 72 hours of stirring with shaking speed of 400 rpm, an aliquot form the receiving phase was removed and analyzed by UV/Vis measurement at the corresponding absorbance maximum against a calibration curve, reported as duplicate runs with ± maximum deviation form the mean. [b] Enhancement: flux/flux of corresponding control.

The results indicate that acidification of receiving phase increases the transport rate remarkably. While host **21** shows the same efficiency as the neutral receiving phase, host **22** and **23** become exceptional transporters with transport enhancement of >9 fold.

When host **24** was utilized as the receptor, with neutral receiving phase, no transport was observed but acidification of the receiving phase led to 6.6 fold enhancement in transport of the guest molecule. It is possible that the enhancement in transport is a result of preorganization effect because **24** is more likely to interconvert into up-down isomers and acidification of receiving phase helps it to hold a better organized conformation.

Based on the transport flux results of FITC-choline **26**, NBD-choline **27**, and Tryptophan-choline **28**, receptors **21** and **22** (Figure 13) are the most efficient receptors in delivering the conjugates moiety into receiving phase. Thereafter, receptor **21** and **22** were selected for further studies.

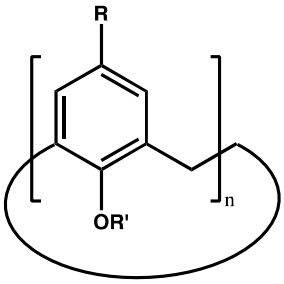

21 R = $CH_2P(O)(OH)(OPri)$, R' = nPr, n = 4
22 R = t-butyl, R' = CH_2COOH, n = 4

FIGURE 13. Molecular structure of calix[4]arene phosphonic acid 21 and calix[4]arene carboxylic acid 22.

Next, the transport flux of two drug-choline conjugates: acetaminophen-choline **29** and ibuprofen-choline **30** were explored (Figure 14). These two molecules were studied because of their slightly different solubility properties, although their structures are very similar. Acetaminophen-choline **29** is more hydrophilic, while ibuprofen-choline is more lipophilic **30**, and this enables us to study the effect of guest molecules'

solubility properties on the transport rate of drug-choline conjugates through a lipophilic membrane.

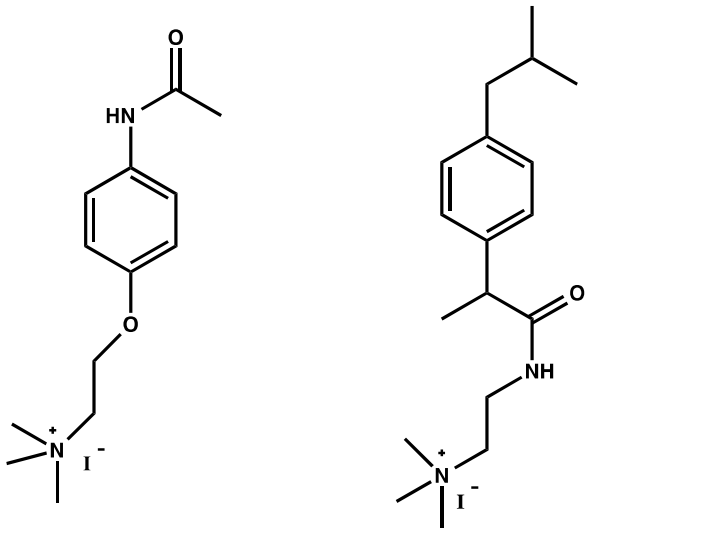

Acetaminophen-Choline
29

Ibuprofen-Choline
30

FIGURE 14. Molecular structures of acetaminophen-choline 29 (left) and ibuprofen-choline 30 (right).

The three-phase transport of both acetaminophen-choline **29** and ibuprofen-choline **30** indicates that the transport fluxes of **29** and **30** are enhanced in presence of either **21** or **22**. However, due to dissimilarities in the structure of the guest molecules–**30** is more hydrophobic than **29**–different efficiencies in transport are achieved. While receptor **22** appears as a better transporter of the less lipophilic guest under acidic conditions, receptor **21** shows significant enhancement in transporting slightly more lipophilic guest at lower pH. Table 3 summarizes the three-phase transport fluxes of **29** and **30**.

TABLE 3. Three-Phase Transport of Acetaminophen-Choline 29 and Ibuprofen-Choline 30 with 21 and 22 Receptors [a]

Receptor (0.5 mM)	Guest (0.5 mM)	Transport Flux ($\mu molcm^{-2}min^{-1}$)	Enhancement [b]	Receiving phase
21	**29**	$(5.42 \pm 0.09)\times10^{-6}$	2.9	MQ Water
		$(1.60 \pm 0.12)\times10^{-6}$	0.8	0.1 M HCl
22	**29**	$(4.25 \pm 0.36)\times10^{-6}$	2.2	MQ Water
		$(1.17 \pm 0.15)\times10^{-5}$	6.0	0.1 M HCl
Control (no host)	**29**	1.89×10^{-6}	-	MQ Water
		1.96×10^{-6}	-	0.1 M HCl
21	**30**	0	0	MQ Water
		$(1.32 \pm 0.10)\times10^{-4}$	5.6	0.1 M HCl
22	**30**	0	0	MQ Water
		$(7.08 \pm 0.20)\times10^{-5}$	3.0	0.1 M HCl
Control (no host)	**30**	2.37×10^{-5}	-	MQ Water
		2.37×10^{-5}	-	0.1 M HCl

[a] 0.5 mM receptor in 10 mL DCM, 0.5 mM substrate was charged in the source phase in 4 mL of MQ water, and a receiving phase of 4 mL water or 0.1 M HCl was added. After 72 hours of stirring with shaking speed of 400 rpm, an aliquot form the receiving phase was removed and analyzed by UV/Vis measurement at the corresponding absorbance maximum against a calibration curve, reported as duplicate runs with ± maximum deviation form the mean. [b] Enhancement: flux/flux of corresponding control.

Based on the transport results of FITC-choline **26**, NBD-choline **27**, Tryptophan-choline **28**, acetaminophen-choline **29**, and ibuprofen-choline **30**, host **21** is more promising in transporting hydrophilic drugs through lipophilic membrane when the receiving phase is neutral, while host **22** shows the most significant enhancement in transporting more lipophilic guests under acidic conditions.

The subsequent choices of guest are two neurotransmitters (dopamine **31** and serotonin **32)** that possess alkyl ammonium termini (Figure 15). Numerous studies report that the ammonium groups can be bound with calixarenes through cation-π interactions,

specially with derivatives of calix[5]arene.[52–55] Therefore, in these set of transport experiments, receptor **23** was also employed as a receptor along with receptors **21** and **22**.

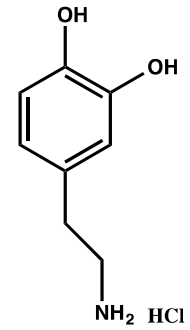

Dopamine HCl
31

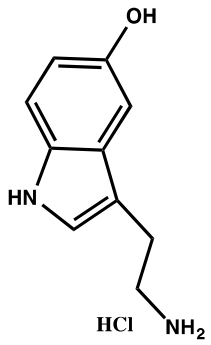

Serotonin HCl
32

FIGURE 15. Molecular structure of Dopamine·HCl 31 and Serotonin·HCl 32.

When the three-phase transport of dopamine **31** was studied utilizing calixarene receptors, significant enhancements were observed. Under neutral conditions, the presence of calix[4]arene phosphonic acid **21** as a receptor enhanced the transport flux by 22 fold (Table 4). Acidification of receiving phase led to a 13.1 fold enhancement in transport flux, which is considerably high. Such enhancement in transport rate illustrates that acidification of receiving phase facilities the release of guest molecule by protonating the host molecule at the receiving phase.

Calix[4]arene carboxylic acid **22** enhanced the transport flux by 1.9 and 2 fold under neutral and acidic conditions respectively. However, when calix[5]arene carboxylic acid **23** was utilized as receptor, a 9 fold enhancement in transport rate was achieved under neutral conditions. This is consistent with the literature that indicate calix[5]arenes are better binders of calix[4]arenes.

TABLE 4. Three-Phase Transport of Dopamine·HCl 31 and Serotonin·HCl 32 with 21, 22 and 23 Receptors [a]

Receptor (0.5 mM)	Guest (5 mM)	Transport Flux ($\mu molcm^{-2}min^{-1}$)	Enhancement [b], [c]	Receiving phase
21	**31**	$(1.18 \pm 0.02)\times10^{-4}$	22.1	MQ Water
		$(6.38 \pm 0.41)\times10^{-5}$	13.1	0.1 M HCl
22	**31**	$(9.91 \pm 1.12)\times10^{-6}$	1.9	MQ Water
		$(9.75 \pm 0.25)\times10^{-6}$	2.0	0.1 M HCl
23	**31**	$(4.48 \pm 0.33)\times10^{-5}$	9.0	MQ Water
		$(1.34 \pm 0.27)\times10^{-5}$	2.9	0.1 M HCl
Control (no host)	**31**	5.34×10^{-6}	-	MQ Water
		4.87×10^{-6}	-	0.1 M HCl
21	**32**	$(7.73 \pm 0.10)\times10^{-5}$	13.6	MQ Water
		$(5.03 \pm 0.84)\times10^{-5}$	8.9	0.1 M HCl
22	**32**	$(1.83 \pm 0.23)\times10^{-5}$	3.2	MQ Water
		$(5.67 \pm 0.43)\times10^{-6}$	1.0	0.1 M HCl
23	**32**	$(2.59 \pm 0.02)\times10^{-5}$	4.6	MQ Water
		$(5.22 \pm 0.40)\times10^{-5}$	9.2	0.1 M HCl
Control (no host)	**32**	0	-	MQ Water
		0	-	0.1 M HCl

[a] 0.5 mM receptor in 10 mL DCM, 0.5 mM substrate was charged in the source phase in 4 mL of MQ water, and a receiving phase of 4 mL water or 0.1 M HCl was added. After 72 hours of stirring with shaking speed of 400 rpm, an aliquot form the receiving phase was removed and analyzed by UV/Vis measurement at the corresponding absorbance maximum against a calibration curve, reported as duplicate runs with ± maximum deviation form the mean. [b] Dopamine enhancement: flux/flux of corresponding control. [c] Serotonin enhancement could not be determined due to lack of transport in the control experiments; herein is the relative transport compared to all hosts (21-23).

When serotonin **32** was subjected to the three-phase transport, no transport was observed without receptors. Once again, receptor calix[4]arene phosphonic acid **21** turns out to be the most efficient transporter. Between calix[4]arene carboxylic acid **22** and calix[5]arene carboxylic acid **23**, the latter is a better transporter, specifically under acidic conditions. Overall, receptor calix[4]arene phosphonic acid **21** displays higher efficiency

in transporting alkyl ammonium compounds through a lipophilic membrane under both neutral and acidic conditions.

The next set of experiments was conducted to get a better understanding of the necessity of choline handles and receptors for an efficient drug transport through a lipophilic membrane. Bentiromide-choline **33** was chosen due to its large polar structure (Figure 16) to see if the presence of choline handle can enhance the transport efficiency of more bulky compounds. Receptors calix[4]arene phosphonic acid **21** and calix[4]arene carboxylic acid **22** were used to study the three-phase transport of bentiromide and bentiromide-choline under neutral and acidic conditions.

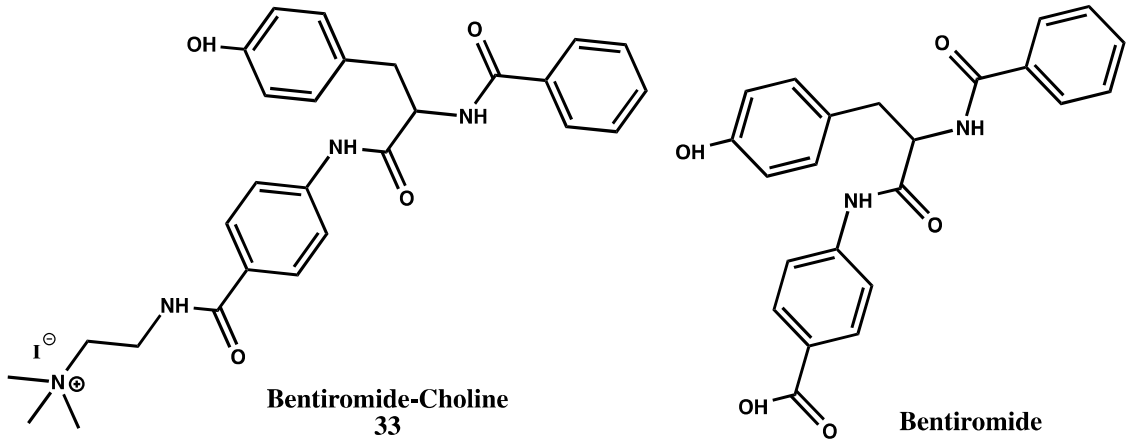

FIGURE 16. Molecular structure of bentiromide-choline 33 (left) and bentiromide (right).

Bentiromide shows some solubility problems in water and when it was exposed to the three-phase transport experiment, significant amount of precipitate formed at the source-organic interface. However, introduction of the choline handle made the

compound highly soluble, which can be clearly concluded when the control transport rates of the two compounds are compared (Table 5).

Under acidic condition, the control transport flux of bentiromide is nearly 6 times higher than that of bentiromide-choline **33**, which most likely is due to the mechanical transport of the precipitate across the organic membrane. Moreover, in three-phase transport of bentiromide, when calix[4]arene phosphonic acid **21** was utilized as the receptor, considerably low enhancement in transport flux (1.4 fold) was achieved; however, a 7-fold enhancement of transport flux of bentiromide-choline **33** was achieved in the presence of **21**.

TABLE 5. Three-Phase Transport of Bentiromide and Bentiromide-Choline 33 with 21 and 22 Receptors [a]

Receptor (0.5 mM)	Guest (0.5 mM)	Transport Flux ($\mu molcm^{-2}min^{-1}$)	Enhancement [b]	Receiving phase
21	**33**	$(2.27 \pm 0.53)\times10^{-5}$	7.0	MQ Water
		$(2.16 \pm 0.32)\times10^{-5}$	4.0	0.1 M HCl
22	**33**	$(3.06 \pm 0.80)\times10^{-5}$	5.7	MQ Water
Control (no host)	**33**	3.23×10^{-6}	-	MQ Water
		5.36×10^{-6}	-	0.1 M HCl
21 [c]	Bentiromide	$(4.70 \pm 0.81)\times10^{-5}$	1.4[c]	MQ Water
Control [c]	Bentiromide	$(3.22 \pm 0.64)\times10^{-5}$	-	MQ Water

[a] 0.5 mM receptor in 10 mL DCM, 0.5 mM substrate was charged in the source phase in 4 mL of MQ water, and a receiving phase of 4 mL water or 0.1 M HCl was added. After 72 hours of stirring with shaking speed of 400 rpm, an aliquot form the receiving phase was removed and analyzed by UV/Vis measurement at the corresponding absorbance maximum against a calibration curve, reported as duplicate runs with ± maximum deviation form the mean. [b] Dopamine enhancement: flux/flux of corresponding control. [c] At the source-organic interface, a thin layer of precipitate formed and we measured a significant decrease in concentration of the source phase (up to 50%) without an equal increase in the receiving phase.

Noticeably, the presence of the trimethylammonium group increases both the water solubility of bentiromide and the transport flux rate of it in the presence of calix[4]arene phosphonic acid **21**. Therefore, we believe that introduction of a choline handle can be a good strategy to increase the water solubility of more lipophilic compounds and/or enhance their transport rate through highly lipophilic conditions.

The next choice of guest was tamoxifen-choline **34**; a highly lipophilic substrate even after introduction of choline handle (Figure 17). Unfortunately, due to the limited solubility of this compound in water (less than 0.1 mM), no transport was observed and significant partitioning into DCM took place in the absence of host. In presence of host **21**, further extraction into DCM was observed.

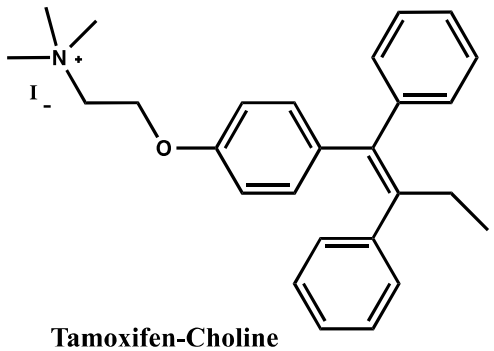

Tamoxifen-Choline
34

FIGURE 17. Molecular structure of tamoxifen-choline 34.

In an effort to transport tamoxifen-choline **34** through a bulk liquid membrane, an inverse transport experiment in which the aqueous phase contained the highly water soluble calix[4]arene tetrasulphonic acid **25** was utilized. Ethyl acetate was used as the

source and receiving phase and charged the former with tamoxifen-choline **34**. Under this extreme inversion of conditions we found that **34** has some background transport with a transport flux of 1.34×10^{-5} ($\mu molcm^{-2}min^{-1}$) but with calix[4]arene tetrasulphonic acid **25** present, the flux decreases to 6.48×10^{-6} ($\mu molcm^{-2}min^{-1}$). The decrease in transport flux in presence of host **25** indicates that the host is extracting guest into lipophilic membrane but not releasing it into the receiving phase.

Next, we changed the source and receiving phases from water to HEPES buffer (4-(2-hydroxyethyl)-1-piperazineethanesulfonic acid, pH 7.4), because the buffered systems would more closely approximate those systems in which we envision the ultimate application of the idea reported herein. The three-phase transport of dopamine **31** and serotonin **32** were studied in the presence of calix[4]arene phosphonic acid 21 (Table 6).

When **31** was subjected to the three-phase transport experiment under buffered conditions, 4.6-fold enhancement in transport flux was achieved. In contrast, in case of **32**, changing the receiving phase from MQ water to HEPES, did not increase the transport rate to a considerable extent. However, we can safely conclude that our strategy to transport drugs is more efficient under buffered condition, which would be a better mimic of the blood-brain barrier environment. Yet, the efficacy of the buffered condition in drug transport should be further studied for the other drug-choline conjugates.

TABLE 6. Three-Phase Transport of Dopamine·HCl 31 and Serotonin·HCl 32 with Receptor 21 [a]

Receptor (0.5 mM)	Guest (5 mM)	Transport Flux ($\mu molcm^{-2}min^{-1}$)	Enhancement [b]	Receiving phase
21	**31**	$(1.18 \pm 0.02)\times10^{-4}$	1	MQ Water
		$(5.41 \pm 0.41)\times10^{-4}$	4.6	HEPES Buffer
Control (no host)	**31**	5.34×10^{-6}	-	MQ Water
		0	-	HEPES Buffer
21	**32**	$(7.73 \pm 0.10)\times10^{-5}$	1	MQ Water
		$(1.09 \pm 0.51)\times10^{-4}$	1.41	HEPES Buffer
Control (no host)	**32**	0	-	MQ Water
		$(1.87 \pm 0.02)\times10^{-5}$	-	HEPES Buffer

[a] 0.5 mM receptor in 10 mL DCM, 5 mM substrate was charged in the source phase in 4 mL of HEPES buffer or MQ water, and a receiving phase of 4 mL HEPES buffer or MQ water was added. After 72 hours of stirring with shaking speed of 400 rpm, an aliquot form the receiving phase was removed and analyzed by UV/Vis measurement at the corresponding absorbance maximum against a calibration curve, reported as duplicate runs with ± maximum deviation form the mean. [b] Enhancement could not be determined due to lack of transport in some of the control experiments; herein the enhancements of buffered experiments is the relative transport compared to the corresponding fluxes in MQ water

3.5. Conclusion

Several studies have successfully utilized the U-tube apparatus to study the transport flux of hydrophilic compounds through a lipophilic membrane via host-guest interactions.[56–59] These studies indicate that an effective transport takes place when the host molecules are able to bind effectively with the guest molecules through non-covalent bonding.

In this work, we are presenting a novel approach to transport hydrophilic guest molecules that are not able to bind effectively with calixarene host molecules. Our approach for transporting such molecules is by means of introducing a receptor's complementary handle to the guest molecules, which can then effectively bind with the

calixarene hosts. Formerly, we have found that calixarene species with ionizable groups are capable of binding with a choline group; therefore, the choline group was introduced to a series of guest molecules to serve as the complementary handle.[21]

In this work, we have successfully studied the potential of a variety of calixarenes in transporting a series of choline-drug conjugates and neurotransmitters through a hydrophobic liquid membrane. The collection of the guest molecules afforded us a variety of functional groups, lipophilicities and molecular complexities. This allowed us to make an initial study of the limits of selective drug-conjugate transport. The collection of the host molecules enabled us to study the effect of different pK_a values and different sizes of host molecules on the transport rates.

There are two key factors for an effective transport of hydrophilic molecules through a lipophilic membrane: 1) The presence of a receptor's complementary handle, and 2) The presence of a host molecule of the complementary handle.

Former transport study indicates that FITC and NBD molecules cannot get transported through a lipophilic membrane, while FITC-choline and NBD-choline show significant enhancement in transport rate.[21] This confirms that the presence of a receptors complementary handle is a necessity for effective transport of highly hydrophilic compounds.

As shown in Chapter 3, the presence of the proper calixarene host in the lipophilic membrane enhances the transport rate of guest molecules up to 22-fold. Such an enhancement in transport rate is due to the ion-ion interaction of the choline group with the ionizable host molecule. It is noteworthy to mention that studies have shown that there is a cation-π interaction between the choline group and the calixarenes [53,60] ;

however, our former transport study confirms that no transport takes place when the host molecule does not possess an ionizable moiety.[21] Therefore, we can conclude that transport takes place due to the effective ion-ion interaction of the choline group with the ionizable calixarenes.

Based on the data collected in this project, calix[4]arene phosphonic acid **21** serves as the most effective transporter of more hydrophobic guest molecules in buffered, acidic, and neutral conditions. Instead, for more hydrophilic guest molecules, calix[4]arene carboxylic acid **22** serves as the most effective transporter in only acidic conditions. This might be due to the difference in the pK_a values of the host molecules. Since calix[4]arene carboxylic acid **22** has a higher pK_a value than calix[4]arene phosphonic acid **21**, acidification of the receiving phase facilitates the protonation of the acetate groups on **22**. This ultimately results in release of the guest molecule into the receiving phase.

Furthermore, the transport rates of choline-conjugated drugs in the presence of different sizes of host molecules confirms that calix[4]arenes are the best transporters, while calix[5] and calix[6]arenes are better extractors. This lack of transport does not mean that calix[5] and calix[6]arenes are poor binders of the choline handle. They can be either strong binders of the choline handle that are not willing to release the guest into the receiving phase, or they can be poor binders of the choline handle that are not able to bind at the source-organic interface. In order to explore whether they are strong or poor binders of the choline handle, one could perform a series of extraction studies utilizing different sizes of host molecules.

It has been proven that supramolecular receptors are compatible with cells, and their localization tendencies in giant unilamellar vesicles could be monitored.[37] Therefore, we hope that a drug can be appended to a calixarene-based receptor, once lodged in a cell membrane, the calixarene can serve as a selective shuttle. We believe that this strategy will provide new ideas and approaches to the drug transport problem. However, it is important to state that in this strategy, we assume that the presence of choline groups do not interfere with the drug's activity.

The preliminary transport results of this project are promising, yet the further studies could broaden our understanding of these transport systems. For instance, exploring the size limitation of the guest molecules by studying the transport flux of peptides with various lengths, and developing a new strategy to release lipophilic substrates into a hydrophilic receiving phase.

CHAPTER 4

EXPERIMENTAL

General consideration:

All the ^{1}H NMR was acquired on Bruker Fourier 300 MHz or Bruker Avance III 400 MHz spectrometers at 298 K. All the ^{13}C NMR was acquired on Bruker Apollo 400 MHz at 100 or 75 MHz at 298 K. The data collected was processed via iNMR 3.5.1 program using a Fourier transform with exponential weighting.

All the NMR solvents were purchased from Cambridge Isotope Laboratories and residual solvent peak was used as an internal standard. All ultra violet (UV) measurements were obtained using a UV-2401 PC Shimadzu spectrophotometer (Shimadzu, Japan).

All chemicals used in this project were of reagent grade or better and used without further purification unless otherwise noted. SiliaFlash® P60 ACADEMIC Silica Gel, 40-60 μm, 60A was purchased from Silicycle [Quebec City (Quebec), CA]. Mass analyses were conducted at the University of California, Riverside High Resolution Mass Spectrometry Facility, Riverside, CA, USA. All the compounds that are labeled with an asterisk were synthesized by Dr. Biren Adhikari.

Synthesis of **6** [30]

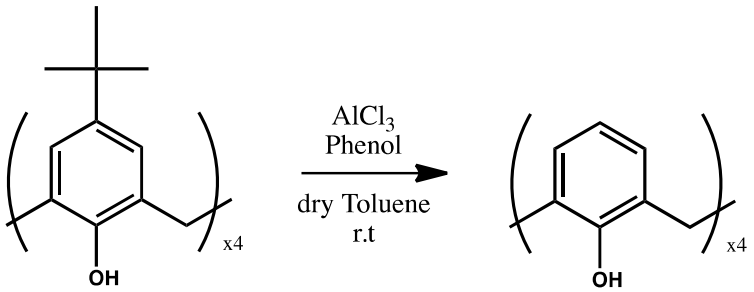

6

To a solution of commercially available *p-tert*-butylcalix[4]arene (2 g, 3.08×10^{-3} mol) in dry Toluene (14 mL), Aluminum Chloride (4.4 g, 3.3×10^{-2} mol, 10.6 eq.) and Phenol (1.4 g, 1.5×10^{-2} mol, 4.8 eq.) were added and the reaction mixture was stirred for one hour at room temperature in an inert atmosphere. The completion of the reaction was monitored by TLC (5: 1 Hex: EtOAc) until the disappearance of starting material. After 1 day of stirring, 3 mL of 1N Hydrochloric acid was added to the reaction. The Toluene layer was extracted and washed with distilled water two times. The organic layer was dried over anhydrous magnesium sulfate, and the volatiles were removed under reduced pressure. The removal of the solvent under reduced pressure yielded an orange colored residue, which was recrystallized from methanol one time to afford 1.05 g (80%) of colorless crystals. ^{1}H NMR (300 MHz, $CDCl_3$), δ 10.20 (s, 1H), 7.06 (d, 2H), 6.74 (t, 1H), 4.25 (bs, 1H), 3.56 (bs, 1H)

Synthesis of **7** [31]

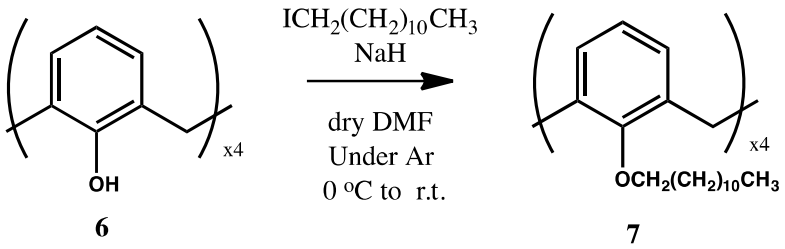

To a solution of **6** (0.5 g, 1.18×10^{-3} mol) in dry Dimethylformamide (10 mL) cooled at 0 °C, NaH (0.23 g, 9.42×10^{-3} mol, 8 eq.) was added and then the reaction was stirred for 1 hour in an inert atmosphere. After an hour, 1-Iodododecane (2.3 mL, 9.42×10^{-3} mol, 8 eq.) was added to the mixture. Subsequently the cooling bath was removed and the reaction mixture was allowed to stir overnight. The reaction monitored by TLC (6: 1 Hex: EtOAc) until the disappearance of starting material. Excess amount of NaH was decomposed with addition of 10 mL distilled water. Afterward the product extracted with Dichloromethane (2x10 mL). The organic layer was collected and washed with distilled water twice followed by drying over anhydrous magnesium sulfate. The volatiles were removed under reduced pressure. The residue of evaporation was purified by flash column chromatography on silica gel eluting with 6: 1 Hex: EtOAc solvent system to obtain 1.18 g (91%) of pure product. ^{1}H NMR (300 MHz, $CDCl_3$), δ 6.61-6.54 (m, 3H), 4.43 (d, 1H), 3.87 (t, 2H), 3.14 (d, 1H), 1.90 (p, 2H), 1.27 (bs, 18H), 0.88 (t, 3H)

Synthesis of **8** [32]

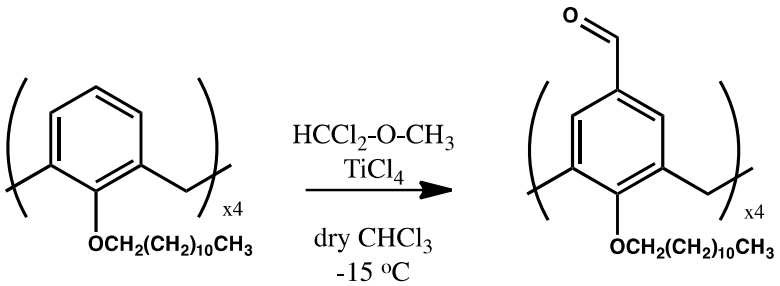

7 **8**

To a solution of α,α-dichloro- methyl methyl ether (0.28 mL, $3.19x10^{-3}$ mol, 13.5 eq.) in dry $CHCl_3$ (10 mL), $TiCl_4$ in 1M $CHCl_3$ (3.7 mL, $3.7x10^{-3}$ mol, 15.8 eq.) was added. After the resulting solution was cooled to -15 °C, a solution of tetrakis(dodecyloxy)calix[4]arene **7** (0.260 g, $2.3x10^{-4}$ mol) in dry $CHCl_3$ (10 mL) was added dropwise over 5 min. The reaction was stirred at -15 °C for 1 h, then the cooling bath was removed and the reaction mixture was allowed to stir overnight. The reaction monitored by TLC (2: 1 Hex: EtOAc) until the disappearance of starting material. The reaction was carefully quenched with 1 N HCl (10 mL), allowed to stir for 1 hour and then the product extracted with CH_2Cl_2 (2x10 mL). DCM layer was collected and washed with 1 N HCl (2x10 mL), followed by drying over anhydrous magnesium sulfate. The residue of evaporation was purified by flash column chromatography on silica gel eluting with 2: 1 Hex: EtOAc solvent system to obtain 0.1 g (36%) of pure product. ^1H NMR (300 MHz, $CDCl_3$), δ 9.58 (s, 1H), 7.15 (s, 2H), 4.49 (d, 1H), 3.95 (t, 2H), 3.34 (d, 1H), 1.88 (p, 2H), 1.26 (bs, 18H), 0.87 (t, 3H)

Synthesis of **10** [33]

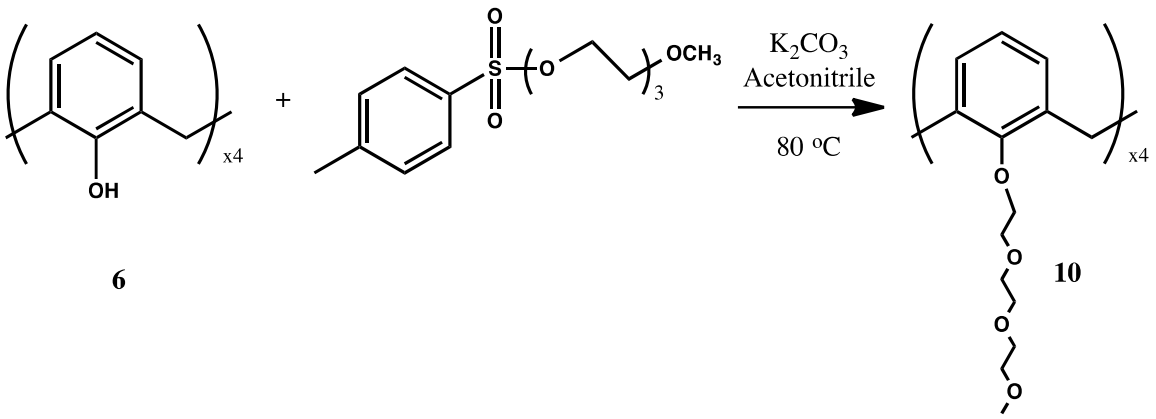

To a solution of **6** (0.230 g, $5.4x10^{-4}$ mol) in acetonitrile (5 mL), potassium carbonate (2.21 g, $1.6x10^{-2}$ mol, 29 eq.) was added. The reaction stirred for 2 hours at room temperature then [2-[2-(2-methoxy ethoxy) ethoxy] ethoxy] p-toluene sulfate (I) (1.37 mL, $4.3x10^{-3}$ mol, 8 eq.) was added. The reaction mixture was stirred under refluxing condition for 3 days. The reaction monitored by TLC (5: 1 Hex: EtOAc) until the disappearance of starting material. Afterwards volatiles were removed under reduced pressure and the residue dissolved in 8 mL dichloromethane and 4 mL 1N hydrochloric acid. The organic layer was collected and washed with distilled water two times, followed by drying over anhydrous magnesium sulfate. Volatiles were removed with rotary evaporator to afford 31 mg (57%) of the crude material. Crude ^{1}HNMR analysis indicated that **10** is in 1,3-alrtenate conformation, which is not the desired cone conformation; therefore, no further purification was performed.

Synthesis of **11** [32]

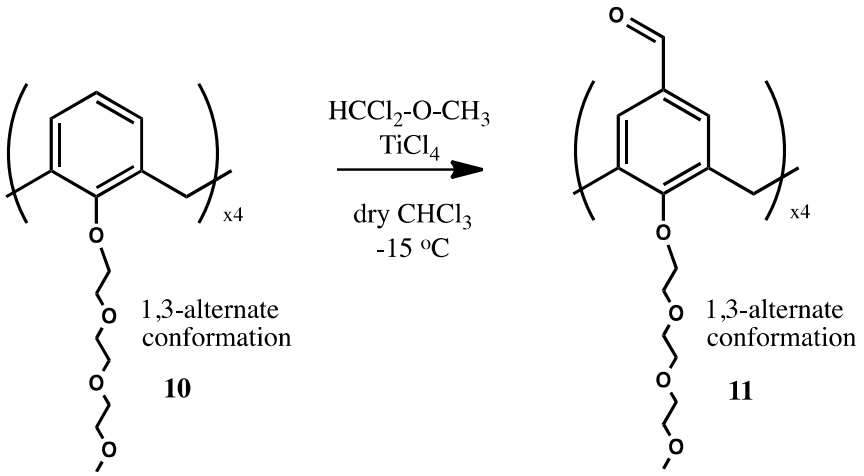

To a solution of α,α-dichloro- methyl methyl ether (84 µL, $9.3x10^{-4}$ mol, 13.5 eq.) in dry $CHCl_3$ (3 mL), $TiCl_4$ in 1M $CHCl_3$ (1.1 mL, $1.09x10^{-3}$ mol, 15.8 eq.) was added. After the resulting solution was cooled to -15 °C, a solution of **10** (70 mg, $7x10^{-5}$ mol) in dry $CHCl_3$ (1.5 mL) was added dropwise over 5 min. The reaction was stirred at -15 °C for 1 h, then the cooling bath was removed and the reaction mixture was allowed to stir overnight. The reaction monitored by TLC (2: 1 Hex: EtOAc) until the disappearance of starting material. The reaction was carefully quenched with 1 N HCl (10 mL), allowed to stir for 1 hour and then the product extracted with CH_2Cl_2 (2x10 mL). DCM layer was collected and washed with 1 N HCl (2x10 mL), followed by drying over anhydrous magnesium sulfate to afford 64 mg (78%) crude material. The crude ^{1}HNMR analysis indicated that **11** is in 1,3-alrtenate conformation, which is not our desired conformation; therefore, no further purification was performed.

Synthesis of **12**

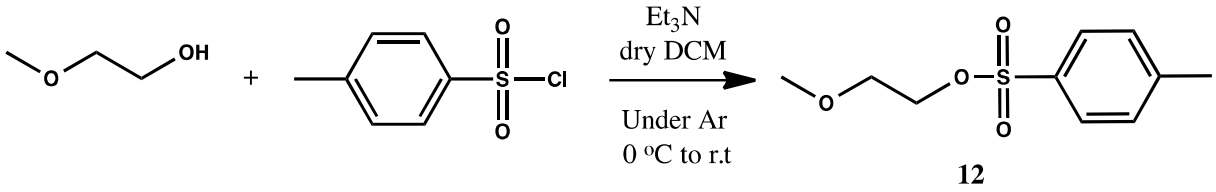

12

To a solution of 2-methoxy ethanol (5 g, $6.6x10^{-2}$ mol) in dry dichloromethane (20 mL), triethylamine (14 mL, $9.8x10^{-2}$ mol, 1.5 eq.) was added while kept in an inert atmosphere. Next, the resulting solution was cooled down in an ice bath, and after 5 min *p*-toluenesulfonyl chloride (13.72 g, $7.2x10^{-2}$ mol, 1.1 eq.) was added to the reaction mixture. The reaction stirred at 0 °C for 15 min, then the cooling bath was removed and the reaction mixture was allowed to stir overnight in an inert atmosphere at room temperature. The reaction monitored by TLC (5: 1 Hex: EtOAc) until the disappearance of starting material. Next, 10 mL distilled water was added and the product extracted with dichloromethane (2x10 mL). The organic layer was collected and washed with distilled water two times, then followed by drying over anhydrous magnesium sulfate. Subsequently, volatilize were removed under reduced pressure. The removal of volatiles under reduced pressure yielded pure product as a coreless liquid (87%) density = 1.2 $g.cm^{-3}$. ^1H NMR (300 MHz, $CDCl_3$), δ7.79 (d, 2H), 7.34 (d, 2H), 4.15 (t, 2H), 3.57 (t, 2H), 3.29 (s, 3H), 2.44 (s, 3H)

Synthesis of **13** [33]

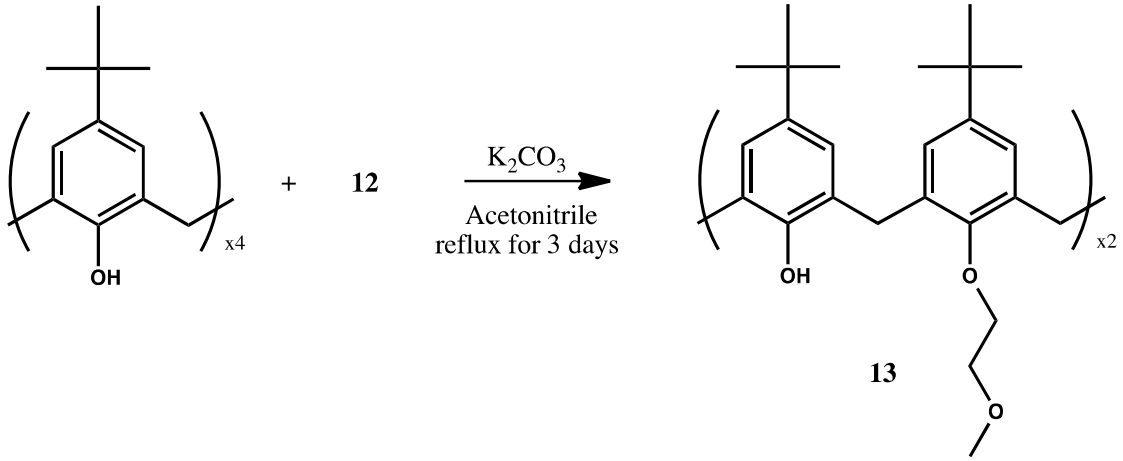

To a solution of *p-tert*-butylcalix[4]arene (0.15 g, 2.3×10^{-4} mol) in acetonitrile (9 mL), K_2CO_3 (0.926 g, 6.7×10^{-3} mol, 29 eq.) was added. The reaction stirred for 2 hours at room temperature then 2-methoxyethyl tosylate **12** (0.35 mL, 1.8×10^{-3} mol, 8 eq.) was added. The reaction mixture was stirred under refluxing condition for 3 days. The reaction monitored by TLC (5: 1 Hex: EtOAc) until the disappearance of starting material. Volatiles were removed under reduced pressure and the residue dissolved in 7 mL DCM and 5 mL 1N HCL. DCM layer was collected and washed with water two times, followed by drying over anhydrous magnesium sulfate. Removal of the solvent under reduced pressure yielded white residue, which was recrystallized from methanol one time to afford 120 mg (68%) of the pure product. ^{1}H NMR (300 MHz, $CDCl_3$), δ 7.31 (s, 2H), 7.04 (s, 4H), 6.79 (s, 4H), 4.36 (d, 4H), 4.15 (t, 4H), 3.87 (t, 4H), 3.54 (s, 6H), 3.29 (d, 4H), 1.28 (s, 18H), 0.96 (s, 18H)

Synthesis of **14** [33]

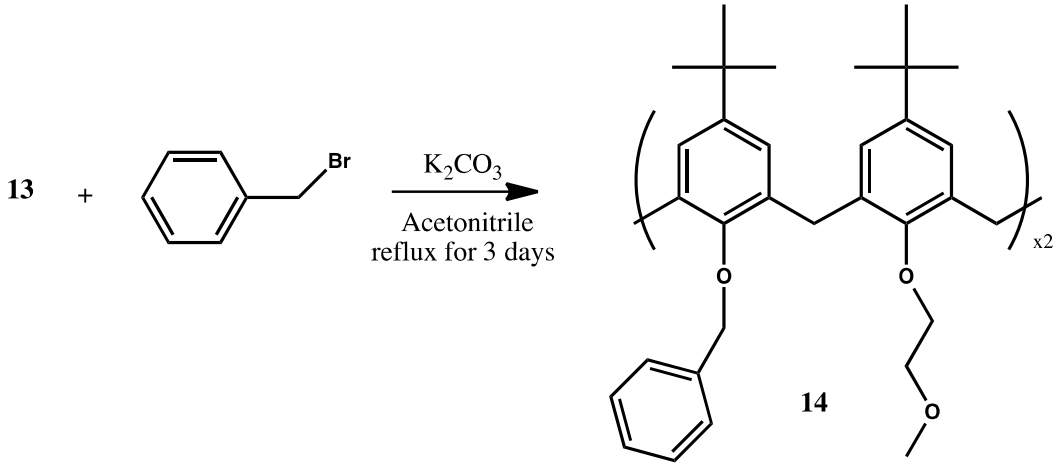

To a solution of **13** (100 mg, $1.3x10^{-4}$ mol) in acetonitrile (5 mL), K_2CO_3 (180 mg, $1.3x10^{-3}$ mol, 10 eq.) was added and the reaction mixture stirred for 1 hour. Benzyl bromide (0.16 mL, $1.3x10^{-3}$ mol, 10 eq.) was added to the reaction mixture and was stirred under refluxing condition for 3 days. The cooling bath was removed and the reaction mixture was allowed to stir overnight. The reaction monitored by TLC (5: 1 Hex: EtOAc) until the disappearance of starting material. Volatiles were removed under reduced pressure and the residue dissolved in 7 mL DCM and 5 mL 1N HCL. DCM layer was collected and washed with water two times, followed by drying over anhydrous magnesium sulfate. DCM layer was collected and washed with water, followed by drying over anhydrous magnesium sulfate. The residue of evaporation was purified by flash column chromatography on silica gel eluting with 5: 1 Hex: EtOAc solvent system to obtain 83 mg (67%) of the pure product. ^{1}H NMR (300 MHz, $CDCl_3$), δ 7.49 (d, 4H), 7.40-7.33 (m, 6H), 7.04 (s, 4H), 6.50 (s, 4H), 4.73 (s, 4H), 4.36 (d, 4H), 4.36 (d, 4H), 3.99 (t, 4H), 3.59 (t, 4H), 3.08 (d, 3H), 3.04 (s, 6H), 1.29 (s, 18H), 0.86 (s, 18H)

Synthesis of **15** [34]

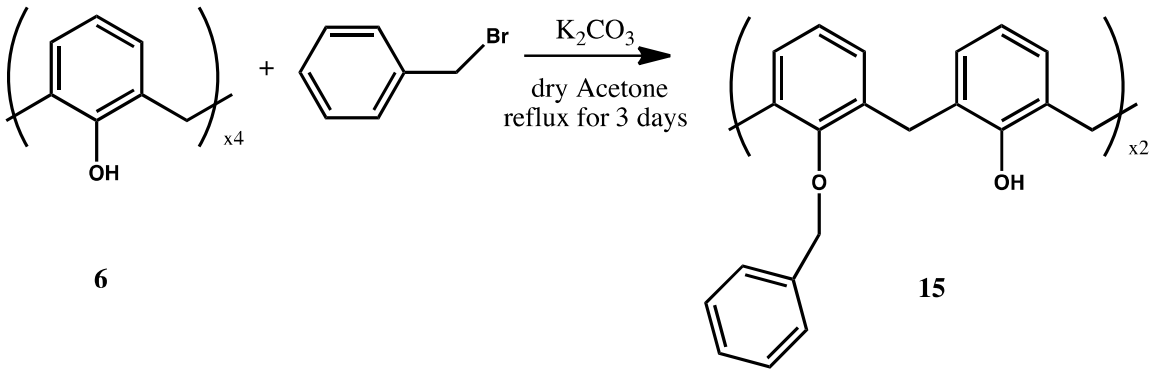

6 **15**

To a solution of calix[4]arene **6** (1.5 g, $3.5x10^{-3}$ mol) in dry acetone (9 mL), K_2CO_3 (1.07 g, $7.77x10^{-3}$ mol, 2.2 eq.) was added. The reaction stirred for 2 hours at room temperature then benzyl bromide (1.06 mL, $8.83x10^{-3}$ mol, 2.5 eq.) was added. The reaction mixture was stirred under refluxing condition for 3 days. The reaction monitored by TLC (5: 1 Hex: EtOAc) until the disappearance of starting material. Volatiles were removed under reduced pressure and the residue dissolved in 8 mL DCM and 4 mL 1N HCL. DCM layer was collected and washed with water two times, followed by drying over anhydrous magnesium sulfate. Removal of the solvent under reduced pressure yielded white residue, which was recrystallized from methanol one time to afford 1.73 g (82%) of the pure product. ^{1}H NMR (300MHz, $CDCl_3$), δ 7.82 (s, 2H), 7.67-7.63 (m, 4H), 7.38-7.34 (m, 6H), 7.04 (d, 4H), 6.89 (d, 4H), 6.75 (t, 2H), 6.65 (t, 2H), 5.06 (s, 4H), 4.31 (d, 4H), 3.34 (d, 4H).

Synthesis of **16** [33]

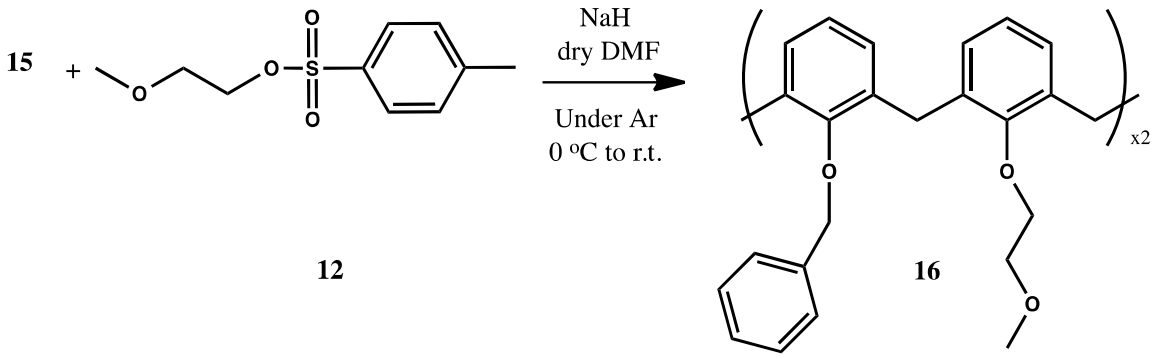

To a solution of **15** (1.7 g, 2.81×10^{-3} mol) in dry DMF (25 mL) cooled at 0 °C, NaH (0.56 g, 1.4×10^{-2} mol, 5 eq.) was added and stirred for 1 hour in an inert atmosphere. 2-methoxyethyl tosylate **12** (2.7 mL, 1.4×10^{-2} mol, 5 eq.) was added to the mixture. The cooling bath was removed and the reaction mixture was allowed to stir overnight. The reaction monitored by TLC (5: 1 Hex: EtOAc) until the disappearance of starting material. Excess NaH was decomposed with addition of 10 mL distilled water and the product extracted with CH_2Cl_2 (2x10 mL). DCM layer was collected and washed with water, followed by drying over anhydrous magnesium sulfate. The residue of evaporation was purified by flash column chromatography on silica gel eluting with 5: 1 Hex: EtOAc solvent system to obtain 1.45 g (73%) of white pure product. ^{1}H NMR (300MHz, $CDCl_3$), δ7.45 (d,4H), 7.38-7.25 (m, 6H), 6.86-6.71 (m, 6H), 6.42-6.32 (m, 6H), 4.87 (s, 4H), 4.37 (d, 4H), 4.04 (t, 4H), 3.59 (t, 4H), 3.13 (s, 6H), 3.07 (d, 4H)

Synthesis of **17** [34]

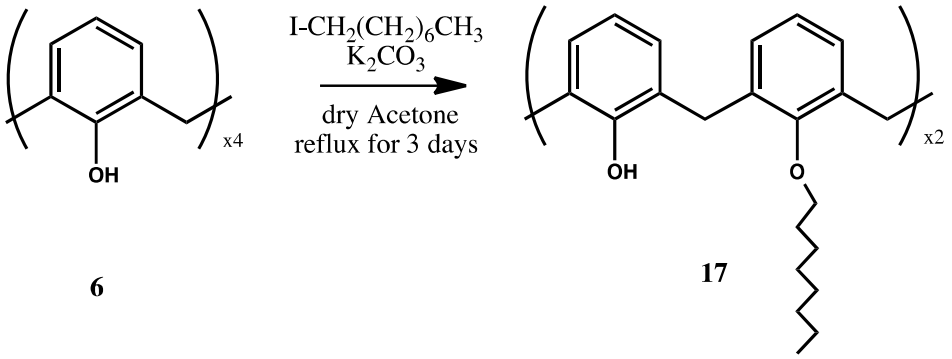

6 **17**

To a solution of calix[4]arene **6** (500 mg, 1.18×10^{-3} mol) in dry acetone (10 mL), potassium carbonate (358 mg, 2.59×10^{-3} mol, 2.2 eq.) was added. The reaction stirred for 2 hours at room temperature, and then 1-Iodooctane (0.53 mL, 2.94×10^{-3} mol, 2.5 eq.) was added. The reaction mixture was stirred under refluxing condition for 3 days. The reaction monitored by TLC (5: 1 Hex: EtOAc) until the disappearance of starting material. Volatiles were removed under reduced pressure and the residue was dissolved in 8 mL dichloromethane and 4 mL 1N hydrochloric acid. The organic layer was collected and washed with water two times, followed by drying over anhydrous magnesium sulfate. The removal of the solvent under reduced pressure yielded oily liquid, which was recrystallized from methanol one time to afford 732 mg (96%) of the pure white product. ^{1}H NMR (300MHz, $CDCl_3$), δ 8.28 (s, 2H), 7.07 (d, 4H), 6.94 (d, 4H), 6.76 (t, 2H), 6.66 (t, 2H), 4.43 (d, 4H), 4.02 (t, 4H), 3.40 (d, 4H), 2.09 (p, 4H), 1.71 (p, 4H), 1.45-1.34 (m, 20H), 0.92 (t, 6H).

Synthesis of **18** [33]

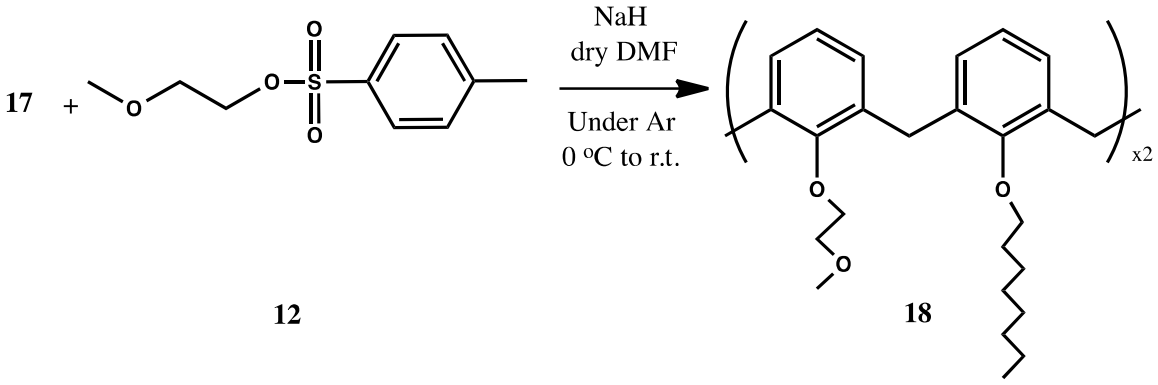

To a solution of **17** (350 mg, 5.39×10^{-4} mol) in dry dimethylformamide (8 mL) cooled at 0 °C, sodium hydride (107 mg, 2.69×10^{-3} mol, 5 eq.) was added and stirred for 1 hour in an inert atmosphere. Subsequently, 2-methoxyethyl tosylate **12** (0.52 mL, 2.69×10^{-3} mol, 5 eq.) was added to the mixture. The cooling bath was removed and the reaction mixture was allowed to stir overnight at room temperature. The reaction monitored by TLC (5: 1 Hex: EtOAc) until the disappearance of starting material. The excess amount of sodium hydride was decomposed with addition of 10 mL distilled water and the product extracted with dichloromethane (2x10 mL). The organic layer was collected and washed with water, followed by drying over anhydrous magnesium sulfate. The volatiles were removed using rotary evaporator to obtain 414 mg (47%) of the crude product. No further purification was performed on the crude product.

Synthesis of **19** [35]

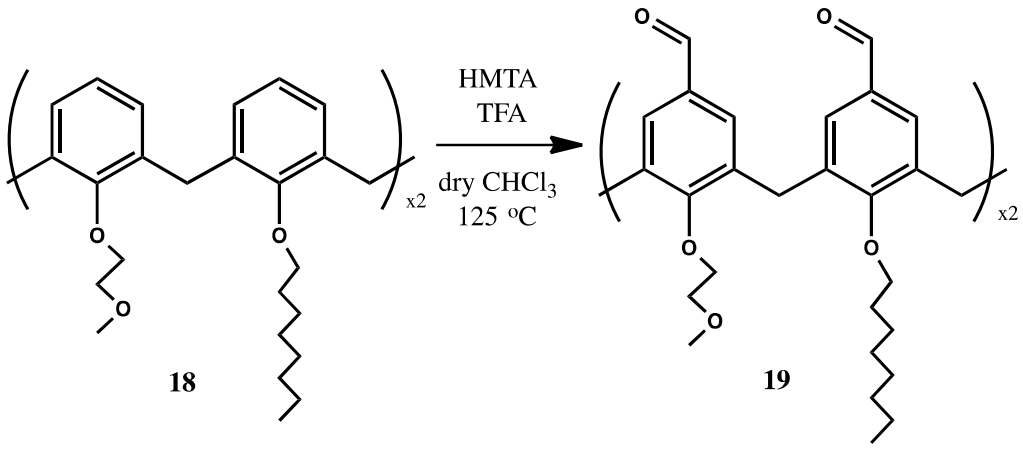

18 **19**

To a solution of **18** (60 mg, 7.84×10^{-5} mol) in TFA (1.5 mL) and dry $CHCl_3$ (0.2 mL), hexamethylenetetramine (HMTA) (329 mg, 2.35×10^{-3} mol, 30 eq.) was added and stirred for 2 days at 125 °C in a capped vial. The reaction monitored by TLC (2: 1 Hex: EtOAc) until the disappearance of starting material. 6 mL 1N HCl and 6 mL DCM was added to the reaction mixture and allowed to stir vigorously for an hour. The product was extracted with CH_2Cl_2 (2x10 mL) and washed with water, followed by drying over anhydrous magnesium sulfate. The residue of evaporation was purified by flash column chromatography on silica gel eluting first with 2: 1 Hex: EtOAc then followed by 1: 1 Hex: EtOAc solvent system to obtain 24 mg (35%) of the pure product. ^{1}H NMR (300MHz, $CDCl_3$), δ 9.65 (s, 2H), 9.53 (s, 2H), 7.25 (s, 4H), 7.08 (s, 4H), 4.54 (d, 4H), 4.18 (t, 4H), 3.98 (t, 4H), 3.79 (t, 4H), 3.37 (s, 6H), 3.35 (d, 4H), 1.89 (p, 4H), 1.38-1.29 (m, 20H), 0.89 (t, 6H).

Synthesis of **25** [49]

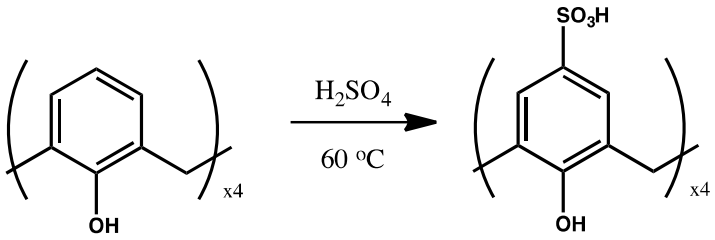

6 **25**

Calix[4]arene **6** (1 g, 2.85×10^{-3}) was mixed with concentrated sulfuric acid (8 mL) and then the reaction mixture stirred at 80 °C for 3 hours. The completion of the reaction was followed by the addition of an aliquot of the reaction mixture into water. The reaction was considered as completed when no water insoluble material was detected. Subsequently, the reaction mixture was cooling down to the room temperature, and the precipitate was recovered by filtration. Next, the precipitate was dissolved in water, and the solution was neutralized by $BaSO_4$. Precipitated $BaSO_4$ was removed by filtration, and then Na_2CO_3 was added to the filtrate until the pH of 8-9 was achieved. An insoluble material (if any) was removed by filtration. Subsequently, the solution was concentrated under reduced pressure, and then diethyl ether was added to the remaining solution to precipitate the product. The precipitate was collected by filtration, and it was dried under reduced pressure to afford 1.66 g (95%) of the pure product. ^{1}H NMR (300MHz, D_2O), δ 7.55 (s, 8H), 4.01 (s, 8H).

Synthesis of **28** *

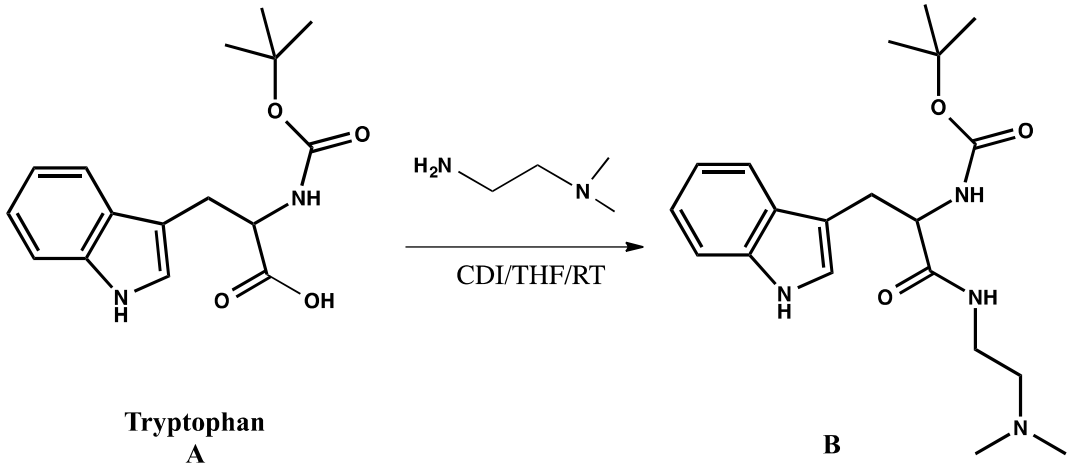

Tryptophan
A

B

Synthesis of **B** [62]

To a solution of 0.8 g (2.6 mmoles) **A** and 0.48 g (2.86 mmoles) carbonyldiimidazole (CDI) in 8 mL dry THF under N_2 atmosphere was added 322 uL (2.86 mmole, 1.1 eq) N,N,-dimethylethylenediamine. The mixture was stirred at room temperature for 24 hours and the solvent was removed by rotary evaporation. The resulted viscous residue was taken up in $CHCl_3$ (30 mL), washed in sequence with 20 mL each of 1 M HCl, 10% $NaHCO_3$, water and brine, and dried over anhydrous Na_2SO_4. Removal of the solvent by rotary evaporation followed by high vacuum drying yielded 0.84 g **B** as a sticky semi-solid (85.4% yield). ^{1}H NMR (300MHz, $CDCl_3$), δ 8.40 (bs, 1H), 7.63 (d, 1H), 7.34 (d, 1H), 7.08-7.20 (m, 2H), 7.04 (s, 1H), 6.17 (bs, 1H), 5.29 (bs, 1H), 4.39 (q, 1H), 3.26-3.33 (m, 1H), 3.09-3.19 (m, 3H), 2.12 (s, 2H), 1.98 (s, 6H), 1.42 (s, 9H). The triplets at 1.85 and 3.74 ppm are due to residual THF.

Synthesis of **28** from **B**

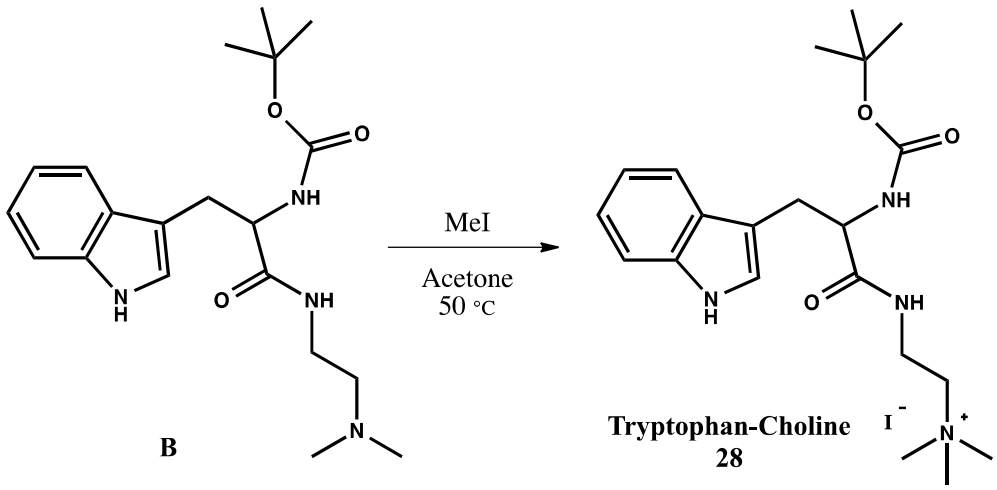

Under nitrogen atmosphere, a mixture of 0.35 g (0.93 mmoles) **B** and 0.15 mL (2.33 mmoles, 2.5 eq) methyl iodide in 5 mL acetone was mixed and the reaction mixture was stirred at 50^0C for 40 hours. Then volatiles were removed under reduced pressure. The removal of the solvent yielded an off-white spongy solid, which slowly converted to a sticky liquid. The product was taken up in chloroform (10 mL) and extracted with 5 mL distilled water two times. The combined aqueous fraction was rotary evaporated to dryness and further dried under high vacuum overnight. ^{1}H NMR (300 MHz, MeOH-d4), δ 7.58 (d, 1H), 7.37 (d, 1H), 7.17 (s, 1H), 7.02-7.14 (m, 2H), 4.24 (t, 1H), 3.36-3.53 (m, 2H), 3.00-3.07 (m, 2H), 2.95 (s, 9 H), 1.40 (s, 9H).

Synthesis of **29** *

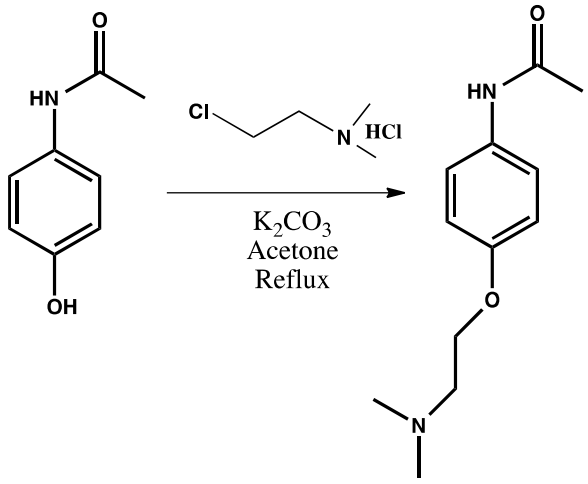

C **D**

Synthesis of **D**

Under nitrogen atmosphere, a mixture of 0.5 g (3.30 mmoles) 4-acetamidophenol **C**, 1.00 g (7.26 mmoles, 2.2 eq) anhydrous K_2CO_3 and 0.55 g (3.64 mmoles, 1.1 eq) N,N-dimethyl-2-chloroethyamine in 15 mL dry acetone was stirred at refluxing condition for 48 hrs. After cooling the reaction mixture to the room temperature, solvent was removed by rotary evaporation and the solid was partitioned between 30 mL $CHCl_3$ and 20 mL water. The separated aqueous fraction was extracted with $CHCl_3$ (2x10 mL) and the combined chloroform fraction was washed with water (2x20 mL). Drying of the organic fraction (Anhy $MgSO_4$) followed by solvent removal by rotary evaporation yielded 0.37 g **D** as a semi-solid material (50% yield). ^{1}H NMR (300 MHz, $CDCl_3$), δ 7.33-7.38 (m, 2H), 6.82-6.87 (m, 2H), 4.02 (t, 2H), 2.69 (t, 2H), 2.16 (s, 6H), 2.12 (s, 3H).

Synthesis of **29** from **D**

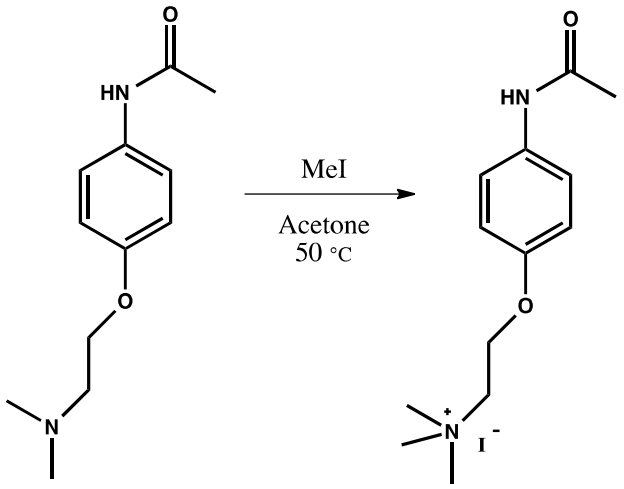

D

Acetaminophen-Choline
29

A solution of 0.36 g (1.62 mmoles) **D** and 0.3 mL (4.86 mmoles, 3 eq) methyl iodide in 7 mL acetone was prepared. The reaction mixture was stirred at 50 ℃ for 30 minutes. The desired material start precipitating after 30 minutes of stirring; however, the reaction mixture was allowed to stir overnight. Subsequently the reaction mixture was cooled down to the room temperature, and the precipitate was collected by filtration. The collected solid was washed with cold acetone two times and dried under reduced temperature. The desired product was obtained as white solid (0.28 g, 48% yield). ^{1}H NMR (300 MHz, D2O), δ 7.32 (d, 2H), 7.01 (d, 2H), 4.47-4.51 (m, 2H), 3.80 (t, 2H), 3.23 (s, 9H), 2.12 (s, 3H).

Synthesis of **30** *

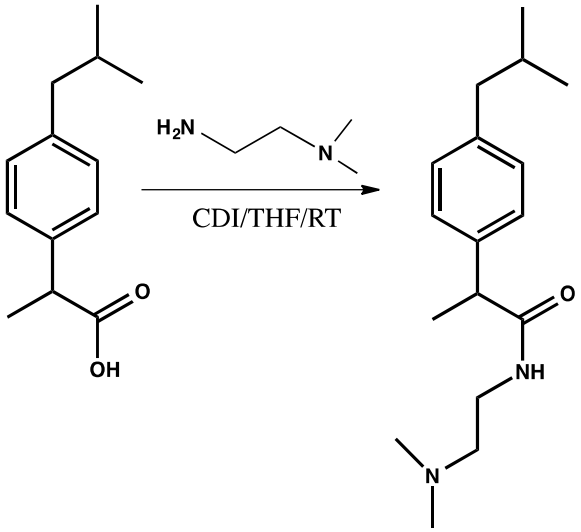

E **F**

Synthesis of **F**

To a stirred solution of 0.5 g (2.42 mmoles) ibuprofen **E** and 0.44 g (2.66 mmoles, 1.1 eq) carbonyl diimidazole in 10 mL dry THF under nitrogen atmosphere, 300 uL (2.66 mmole, 1.1 eq) N,N,-dimethylethylenediamine was added and the mixture was stirred at room temperature for 48 hrs. The solvent was removed by rotary evaporation. The resulting thick liquid was dissolved in chloroform (20 mL) and washed with water (20 mL). The aqueous fraction was extracted with chloroform (2x20 mL), and the combined organic fraction was washed with 30 mL each of 0.1 M HCl, 0.1 M NaOH and water. Drying of organic phase over anhy. $MgSO_4$ followed by solvent removal afforded 0.6 g **F** as a colorless viscous liquid (90% yield). ^{1}H NMR (300 MHz, $CDCl_3$), δ 7.20 (d, 2H), 7.90 (d, 2H), 5.95 (bs, 1H), 3.51 (q, 1H), 3.16-3.34 (m, 2H), 2.44 (d, 2H), 2.27-2.32 (m, 2H), 2.11 (s, 6H), 1.79-1.88 (m, 2H), 1.50 (d, 3H), 0.88 (d, 6H).

Synthesis of **30** from **F**

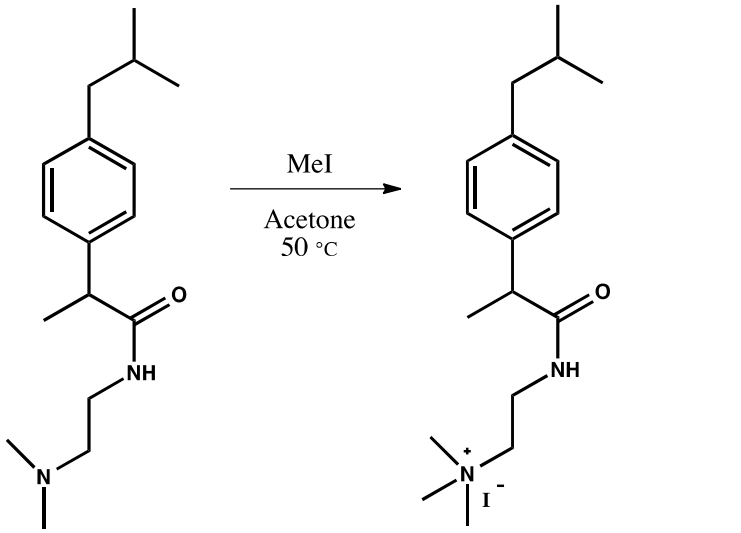

F **Ibuprofen-Choline**
30

To 0.4 g (1.45 mmoles) of compound **F** in dry acetone (7 mL), 0.27 mL (4.34 mmoles, 3 eq) methyl iodide was added. The reaction mixture was stirred at 50 ℃ for 30 minutes under nitrogen atmosphere. The desired material start precipitating after 30 minutes of stirring; however, the reaction mixture was allowed to stir overnight. Subsequently the reaction mixture was cooled down to the room temperature, and then diethyl ether was added to the reaction mixture to precipitate the product. The precipitates were collected by filtration, and then dried under reduced pressure to afford 0.43 g of the desired material as a white solid (71.7% yield). ^{1}H NMR (300 MHz, MeOH- d4), δ 7.25 (d, 2H), 7.11 (d, 2H), 3.53-3.74 (m 1H), 3.40-3.44 (m, 3H), 3.33 (s, 9H), 2.44 (d, 2H), 1.76-1.90 (m, 1H), 1.44 (d, 3H), 0.89 (d, 6H).

Synthesis of **33** [62]

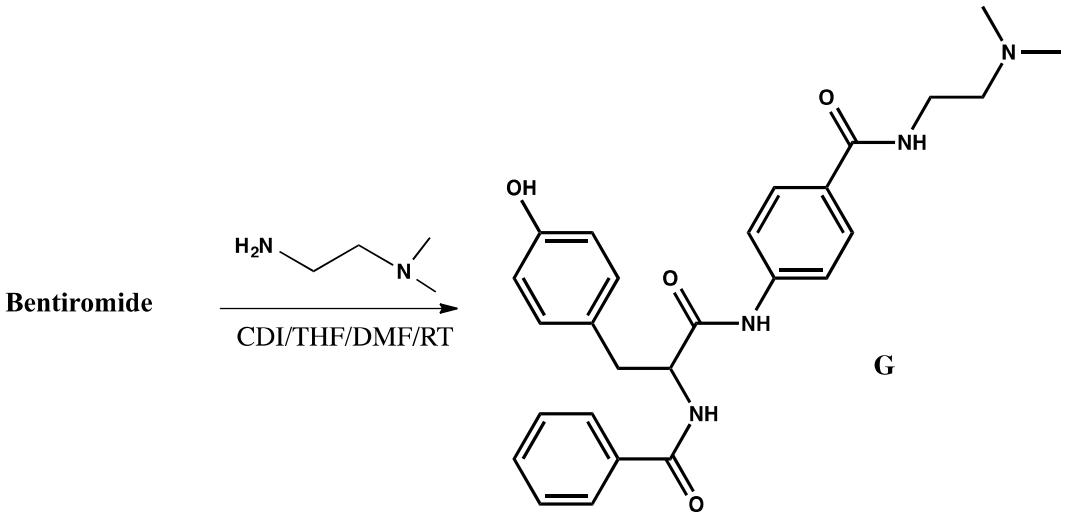

Synthesis of **G**

To a solution of bentiromide (100 mg, 2.47×10^{-4} mol) in dry tetrahydrofuran (2 mL) and dry dimethylformamide (0.1 mL), carbonyldiimidazole (120 mg, 7.41×10^{-3} mol, 3 eq.) was added. The reaction mixture was stirred at room temperature in an inert atmosphere for 2 hours. Subsequently, *N*,*N*′-Dimethylethylenediamine (30 µL, 2.72×10^{-4} mol, 1.1 eq.) was added to the reaction mixture and then the reaction was allowed to stir overnight. Afterward 5 mL of 1N hydrochloric acid was added to the reaction mixture. The product was extracted with 10 ml ethyl acetate two times, and then followed by drying over anhydrous magnesium sulfate. The volatiles were removed under reduced pressure to complete dryness. The removal of the solvent yielded 90 mg (96%) of the pure oily product **G**.

Synthesis of **33** from **G**

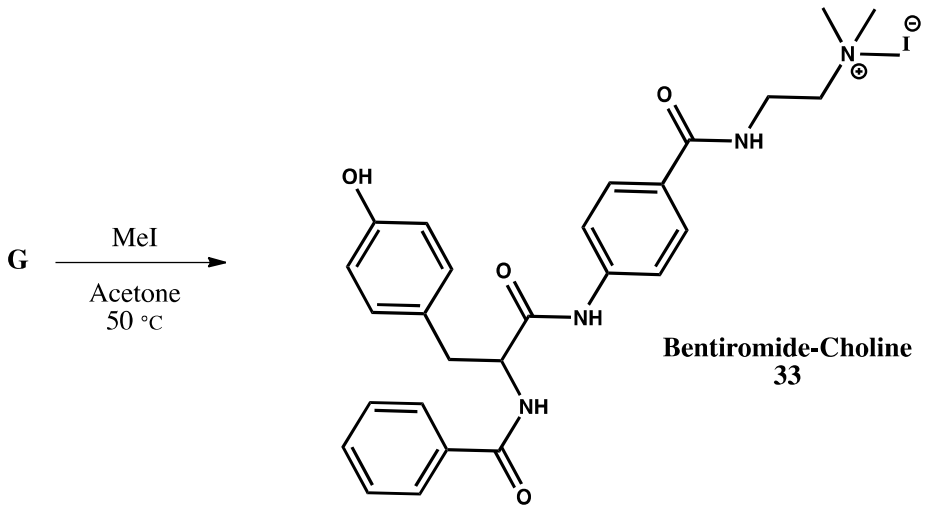

To a solution of **G** (65 mg, $1.37x10^{-4}$ mol) in methanol (0.5 mL), methyl iodide (34 μL, $5.48x10^{-4}$ mol, 4 eq.) was added and the reaction mixture was stirred at 60 °C for 3 days. The desired material start precipitating after first day of stirring; however, the reaction mixture was allowed to stir for 3 days. Subsequently the reaction mixture was added on diethyl ether to precipitate the product. The precipitate was collected by filtration, and product was dried under reduced pressure to afford 45 mg (67%) of the white pure product. ^{1}H NMR (300MHz, CD_3OD), δ 7.80 (t, 4H), 7.66 (d, 2H), 7.54 (t, 1H), 7.45 (t, 2H), 7.13 (d, 2H), 6.69 (d, 2H), 4.85 (t, 1H), 3.85 (t, 2H), 3.59 (t, 2H), 3.24 (s, 9H), 3.18 (dd, 1H), 3.07 (dd, 1H). ^{13}C NMR (100MHz, CD_3OD), δ 172.7, 170.3, 169.8, 157.4, 143.2, 135.2, 132.9, 131.4, 129.9, 129.5, 129.2, 128.8, 128.5, 120.7, 116.3, 65.9, 58.0, 54.1, 38.3, 35.2.

Synthesis of **34** *

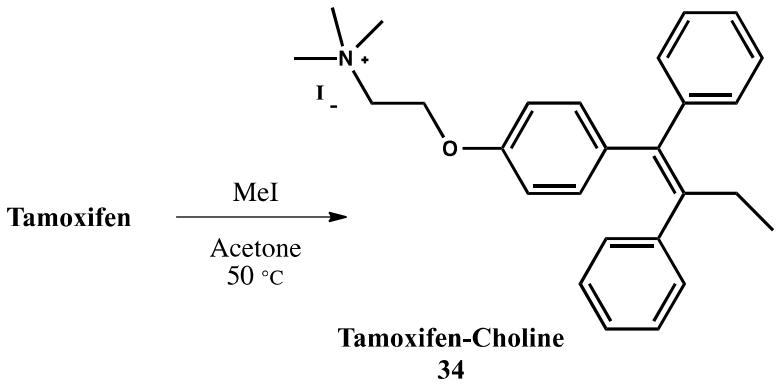

Under nitrogen atmosphere, a mixture of 0.05 g (0.135 mmoles) tamoxifen and 0.034 mL (0.54 mmoles, 4 eq) methyl iodide in 5 mL acetone was stirred at 50 ℃ for 48 hrs. A white solid was formed while cooling the reaction mixture to room temperature. Separation of the solid by filtration followed by washing with cold acetone afforded the pure product (0.06 g, 87% yield). ^{1}H NMR (400 MHz, CDCl3: MeOH-d4 = 4: 1), δ 7.04-7.32 (m, 10H), 6.76-6.79 (m, 2H), 6.50-6.54 (m 2H), 4.25-4.28 (m, 2H), 3.85 (t, 2H), 3.26 (s, 9H), 2.40 (q, 2H), 0.87 (t, 3H).

APPENDICES

APPENDIX A

TRANSPORT FLUX CALCULATIONS

Transport results of FITC-choline **26**:

Experimental conditions:

Receptor's concentration: 0.5 mM

Receptor's volume: 10 mL

Substrate's concentration: 0.5 mM

Stirring speed: 400 rpm

λmax in neutral condition: 492 nm

Stirring time: 72 Hours

λmax in acidic condition: 439 nm

Volume of source and receiving phases: 4 mL

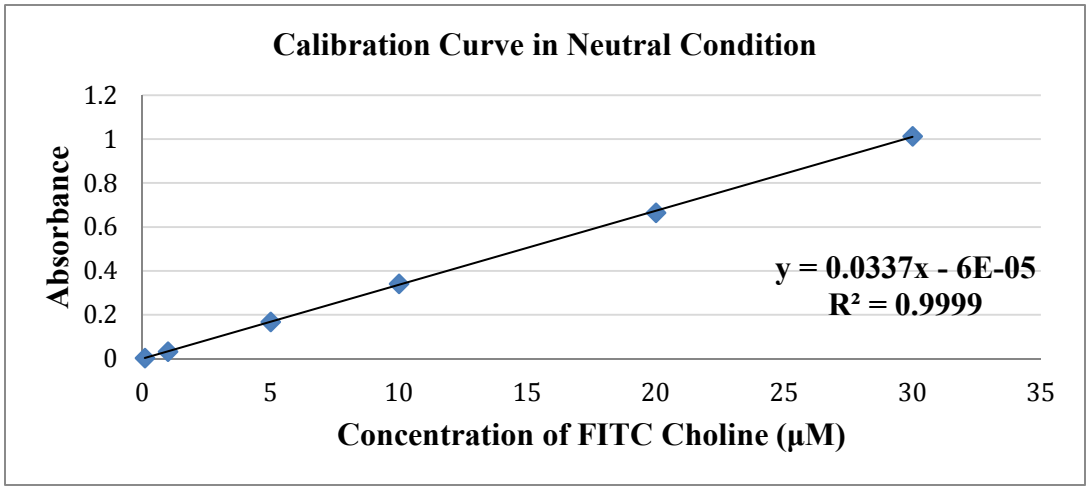

FIGURE 18. Calibration curve of FITC-choline in neutral condition.

Concentration of the substrate (µM)	UV-Vis Absorbance
30	1.013
20	0.665
10	0.342
5	0.168
1	0.033
0.1	0.003

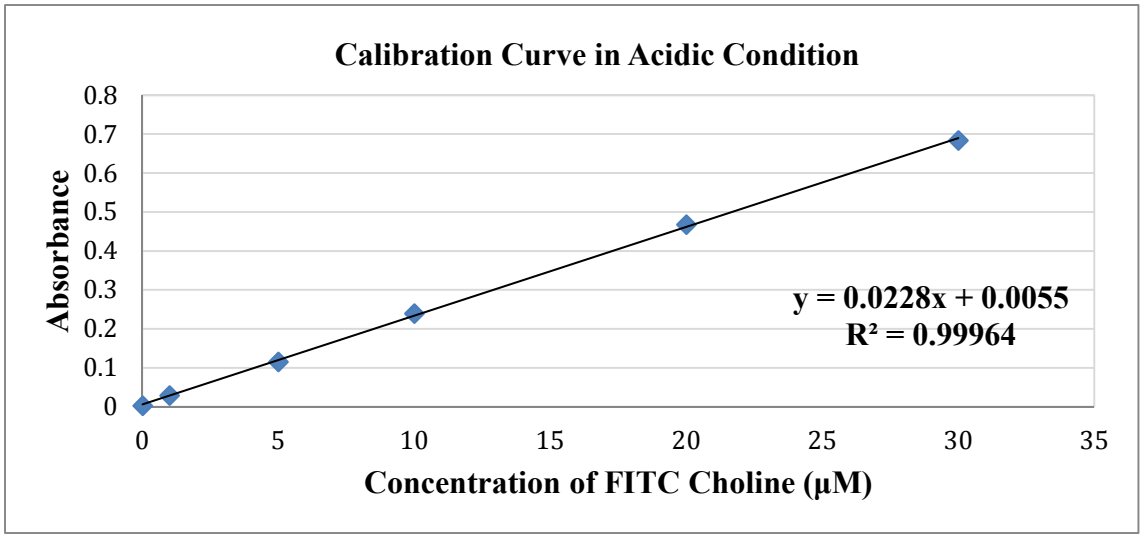

FIGURE 19. Calibration curve of FITC-choline in acidic condition.

Concentration of the substrate (µM)	UV-Vis Absorbance
30	0.684
20	0.468
10	0.239
5	0.115
1	0.029
0.1	0.003

Transport flux calculation of FITC-choline **26**:

Receptor: Calix[5]CH_2COOH
Receiving Phase: Neutral

Dilution factor of the Initial solution	25
Dilution factor of the source phases	25
Dilution factor of the receiving phases	3

TABLE 7. Transport Flux Calculations of FITC-Choline in Neutral Condition

	Initial guest solution	Control	1st Trial	2nd Trial	3rd Trial	Mean of Trials	STDEV
Source phase absorbance	0.757	0.757	0.57	0.622	0.65		
Receiving phase absorbance		0	0.126	0.176	0.055		
Source phase concentration	22.4646	22.4646	16.9157	18.45875	19.2896		
Receiving phase concentration		0.0017	3.74065	5.2243	1.6338		
Source phase's actual concentration	561.6172	561.6172	422.8931	461.4688	482.2403		
Receiving phase's actual concentration		0.0053	11.2219	15.6729	4.9014		
% Transported from source phase		0	24.7008	17.8321	14.1336	18.8888	5.3622
% Appeared in receiving phase		0.0009	1.9981	2.7906	0.8727	1.8871	0.9637
Mass Transported		2.1365E-05	0.0448	0.0626	0.0196	0.0423	0.0216
Transport Flux ($\mu molcm^{-2}min^{-1}$)		4.37664E-09	9.1953E-06	1.2842E-05	4.0162E-06	8.684E-06	4.4352E-06

Transport flux calculation of FITC-choline **26**:

Receptor: Calix[5]CH_2COOH
Receiving Phase: Acidic (0.1M HCl)

Dilution factor of the Initial solution	25
Dilution factor of the source phases	25
Dilution factor of the receiving phases	3

TABLE 8. Transport Flux Calculations of FITC-Choline in Acidic Condition

	Initial guest solution	Control	1st Trial	2nd Trial	3rd Trial	Mean of Trials	STDEV
Source phase absorbance	0.465	0.465	0.292	0.321	0.302		
Receiving phase absorbance		0	0.071	0.063	0.076		
Source phase concentration	20.1535	20.1535	12.5657	13.8377	13.0043		
Receiving phase concentration		-0.2412	2.8728	2.5219	3.0921		
Source phase's actual concentration	503.8377	503.8377	314.1447	345.9429	325.1096		
Receiving phase's actual concentration		-0.7236	8.6184	7.5657	9.2763		
% Transported from source phase		0	37.6496	31.3384	35.4733	34.8204	3.2058
% Appeared in receiving phase		-0.1436	1.7105	1.5016	1.8411	1.6844	0.1712
Mass Transported		-0.0028	0.034473684	0.0302	0.0371	0.0339	0.0034
Transport Flux ($\mu molcm^{-2}min^{-1}$)		-5.9298E-07	7.06196E-06	6.1994E-06	7.6010E-06	6.9541E-06	7.0699E-07

Transport results of NBD-choline **27**:

Experimental conditions:

Receptor's concentration: 0.5 mM

Receptor's volume: 10 mL

Substrate's concentration: 0.5 mM

Stirring speed: 400 rpm

λmax in neutral and acidic conditions: 464 nm

Stirring time: 72 Hours

Volume of source and receiving phases: 4 mL

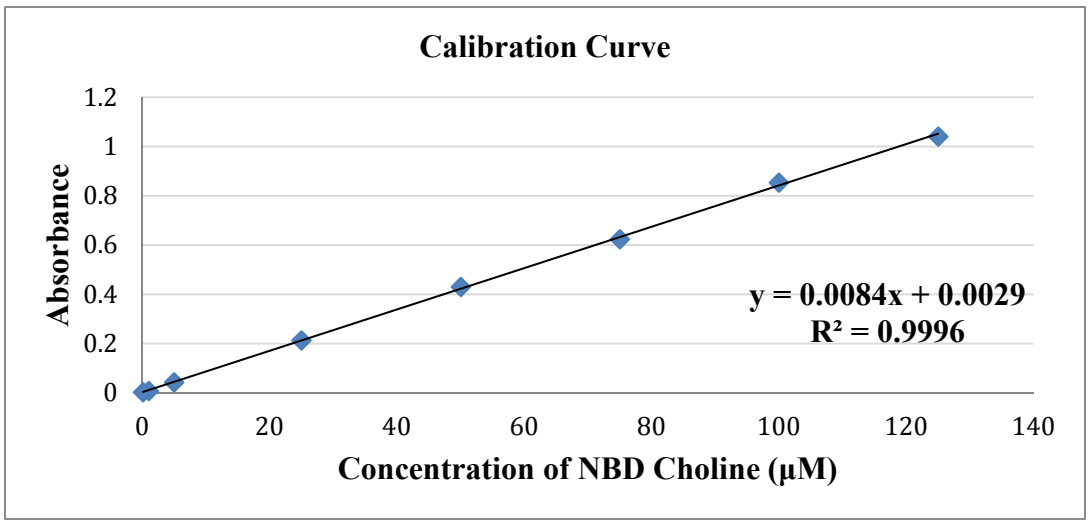

FIGURE 20. Calibration curve of NBD-choline.

Concentration of the substrate (µM)	UV-Vis Absorbance
125	1.042
100	0.855
75	0.624
50	0.431
25	0.214
5	0.043
1	0.008
0.1	0.003

Transport flux calculation of NBD-choline **27**:

Receptor: Calix[5]CH_2COOH
Receiving Phase: Neutral

Dilution factor of the Initial solution	25
Dilution factor of the source phases	25
Dilution factor of the receiving phases	3

TABLE 9. Transport Flux Calculations of NBD-Choline in Neutral Condition

	Initial guest solution	Control	1st Trial	2nd Trial	3rd Trial	Mean of Trials	STDEV
Source phase absorbance	0.177	0.177	0.121	0.125	0.136		
Receiving phase absorbance		0	0.005	0.007	0.006		
Source phase concentration	20.7261	20.7261	14.0595	14.5357	15.8452		
Receiving phase concentration		-0.3452	0.25	0.4880	0.3690		
Source phase's actual concentration	518.1547	518.1547	351.4880	363.3928	396.1309		
Receiving phase's actual concentration		-1.0357	0.75	1.4642	1.1071		
% Transported from source phase		0	32.1654	29.8678	23.5496	28.5276	4.4614
% Appeared in receiving phase		-0.1998	0.1447	0.2825	0.2136	0.2136	0.0689
Mass Transported		-0.0041	0.003	0.0058	0.0044	0.0044	0.0014
Transport Flux ($\mu molcm^{-2}min^{-1}$)		-8.4866E-07	6.1455E-07	1.1998E-06	9.0719E-07	9.0719E-07	2.9264E-07

Transport flux calculation of NBD-choline **27**:

Receptor: Calix[5]CH_2COOH
Receiving Phase: Acidic (0.1M HCl)

Dilution factor of the Initial solution	25
Dilution factor of the source phases	25
Dilution factor of the receiving phases	3

TABLE 10. Transport Flux Calculations of NBD-Choline in Acidic Condition

	Initial guest solution	Control	1st Trial	2nd Trial	3rd Trial	Mean of Trials	STDEV
Source phase absorbance	0.177	0.177	0.11	0.131	0.142		
Receiving phase absorbance		0	0.243	0.167	0.163		
Source phase concentration	20.7261	20.7261	12.75	15.25	16.56		
Receiving phase concentration		-0.3452	28.58	19.53	19.06		
Source phase's actual concentration	518.1547	518.1547	381.75	381.25	413.99		
Receiving phase's actual concentration		-1.0357	85.75	58.61	57.18		
% Transported from source phase		0	38.4836	26.42	20.10	28.34	9.34
% Appeared in receiving phase		-0.1998	16.549	11.31	11.03	12.96	3.10
Mass Transported		-0.0041	0.343	0.2344	0.2287	0.2687	0.0644
Transport Flux ($\mu molcm^{-2}min^{-1}$)		-8.4866E-07	7.0264E-05	4.8023E-05	4.6852E-05	5.5046E-05	1.3192E-05

Transport results of tryptophan-choline **28**:

Experimental conditions:

Receptor's concentration: 0.5 mM

Receptor's volume: 10 mL

Substrate's concentration: 5 mM

Stirring speed: 400 rpm

λmax in neutral and acidic Conditions: 280 nm

Stirring time: 72 Hours

Volume of source and receiving Phases: 4 mL

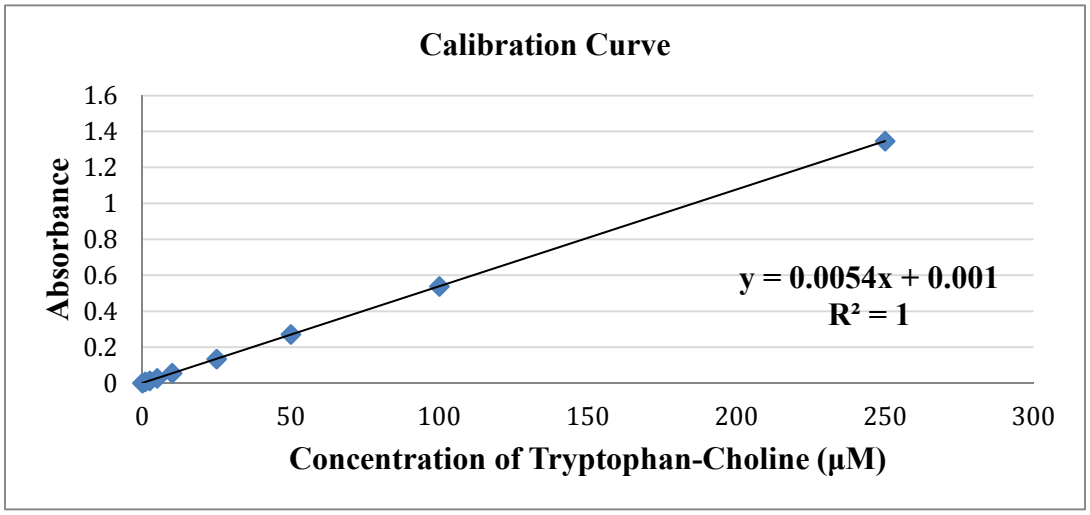

FIGURE 21. Calibration curve of tryptophan-choline.

Concentration of the substrate (µM)	UV-Vis Absorbance
250	1.347
100	0.539
50	0.271
25	0.135
10	0.055
5	0.028
2.5	0.014
1	0.008

Transport flux calculation of tryptophan-choline **28**:

Receptor: Calix[5]CH_2COOH
Receiving Phase: Neutral

Dilution factor of the Initial solution	5
Dilution factor of the source phases	5
Dilution factor of the receiving phases	2

TABLE 11. Transport Flux Calculations of Tryptophan-Choline in Neutral Condition

	Initial guest solution	Control	1st Trial	2nd Trial	Mean of Trials
Source phase absorbance	0.536	0.492	0.319	0.278	
Receiving phase absorbance		0.043	0.012	0.01	
Source phase concentration	99.07407407	90.92592593	58.88888889	51.2962963	
Receiving phase concentration		7.777777778	2.037037037	1.666666667	
Source phase's actual concentration	495.3703704	454.6296296	294.4444444	256.4814815	
Receiving phase's actual concentration		15.55555556	4.074074074	3.333333333	
% Transported from source phase		8.224299065	40.56074766	48.22429907	44.39252336
% Appeared in receiving phase		3.140186916	0.822429907	0.672897196	0.747663551
Mass Transported		0.062222222	0.016296296	0.013333333	0.014814815
Transport Flux (μmolcm-2min-1)		1.27463E-05	3.33831E-06	2.73134E-06	3.03483E-06

Transport flux calculation of tryptophan-choline **28**:

Receptor: Calix[5]CH_2COOH
Receiving Phase: Acidic (0.1 M HCl)

Dilution factor of the Initial solution	5
Dilution factor of the source phases	5
Dilution factor of the receiving phases	2

TABLE 12. Transport Flux Calculations of Tryptophan-Choline in Acidic Condition

	Initial guest solution	Control	1st Trial	2nd Trial	Mean of Trials
Source phase absorbance	0.536	0.516	0.235	0.301	
Receiving phase absorbance		0.06	0.626	0.506	
Source phase concentration	99.07407407	95.37037037	43.33333333	55.55555556	
Receiving phase concentration		10.92592593	115.7407407	93.51851852	
Source phase's actual concentration	495.3703704	476.8518519	216.6666667	277.7777778	
Receiving phase's actual concentration		21.85185185	231.4814815	187.037037	
% Transported from source phase		3.738317757	56.26168224	43.92523364	50.09345794
% Appeared in receiving phase		4.411214953	46.72897196	37.75700935	42.24299065
Mass Transported		0.087407407	0.925925926	0.748148148	0.837037037
Transport Flux (μmolcm-2min-1)		1.79055E-05	0.000189677	0.000153259	0.000171468

Transport results of acetaminophen-choline **29**:

Experimental conditions:

Receptor's concentration: 0.5 mM

Receptor's volume: 10 mL

Substrate's concentration: 0.5 mM

Stirring speed: 400 rpm

λmax in neutral and acidic conditions: 254 nm

Stirring time: 72 Hours

Volume of source and receiving phases: 4 mL

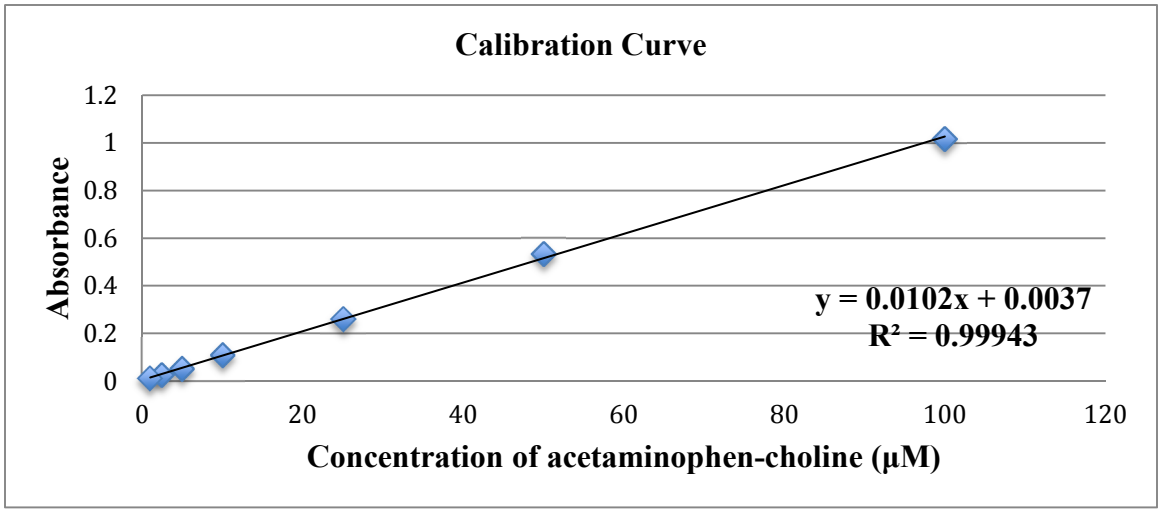

FIGURE 22. Calibration curve of acetaminophen-choline.

Concentration of the substrate (µM)	UV-Vis Absorbance
100	1.017
50	0.534
25	0.260
10	0.108
5	0.052
2.5	0.026
1	0.012

Transport flux calculation of acetaminophen-choline **29**:

Receptor: Calix[4]CH_2COOH
Receiving Phase: Neutral

Dilution factor of the Initial solution	5
Dilution factor of the source phases	5
Dilution factor of the receiving phases	2

TABLE 13. Transport Flux Calculations of Acetaminophen-Choline in Neutral Condition

	Initial guest solution	Control	1st Trial	2nd Trial	Mean of Trials
Source phase absorbance	0.93	0.905	0.509	0.891	
Receiving phase absorbance		0.01	0.036	0.042	
Source phase concentration	90.81372549	88.3627451	49.53921569	86.99019608	
Receiving phase concentration		0.617647059	3.166666667	3.754901961	
Source phase's actual concentration	454.0686275	441.8137255	247.6960784	434.9509804	
Receiving phase's actual concentration		3.088235294	6.333333333	7.509803922	
% Transported from source phase		2.698909641	45.44963835	4.210299039	24.82996869
% Appeared in receiving phase		0.680125229	1.394796502	1.653891828	1.524344165
Mass Transported		0.012352941	0.025333333	0.030039216	0.027686275
Transport Flux (μmolcm-2min-1)		1.89788E-06	3.89217E-06	4.61517E-06	4.25367E-06

Transport flux calculation of acetaminophen-choline **29**:

Receptor: Calix[4]CH_2COOH
Receiving Phase: Acidic (0.1 M HCl)

Dilution factor of the Initial solution	5
Dilution factor of the source phases	5
Dilution factor of the receiving phases	2

TABLE 14. Transport Flux Calculations of Acetaminophen-Choline in Acidic Condition

	Initial guest solution	Control	1st Trial	2nd Trial	Mean of Trials
Source phase absorbance	0.93	0.914	0.798	0.886	
Receiving phase absorbance		0.02	0.114	0.089	
Source phase concentration	90.81372549	89.24509804	77.87254902	86.5	
Receiving phase concentration		1.598039216	10.81372549	8.362745098	
Source phase's actual concentration	454.0686275	446.2254902	389.3627451	432.5	
Receiving phase's actual concentration		3.196078431	21.62745098	16.7254902	
% Transported from source phase		1.72730217	14.2502429	4.750080967	9.500161935
% Appeared in receiving phase		0.703875634	4.763035734	3.683471877	4.223253805
Mass Transported		0.012784314	0.086509804	0.066901961	0.076705882
Transport Flux (μmolcm-2min-1)		1.96416E-06	1.32912E-05	1.02787E-05	1.17849E-05

Transport results of ibuprofen-choline **30**:

Experimental conditions:

Receptor's concentration: 0.5 mM

Receptor's volume: 10 mL

Substrate's concentration: 0.5 mM

Stirring speed: 400 rpm

λmax in neutral and acidic conditions: 263 nm

Stirring time: 72 Hours

Volume of source and receiving phases: 4 mL

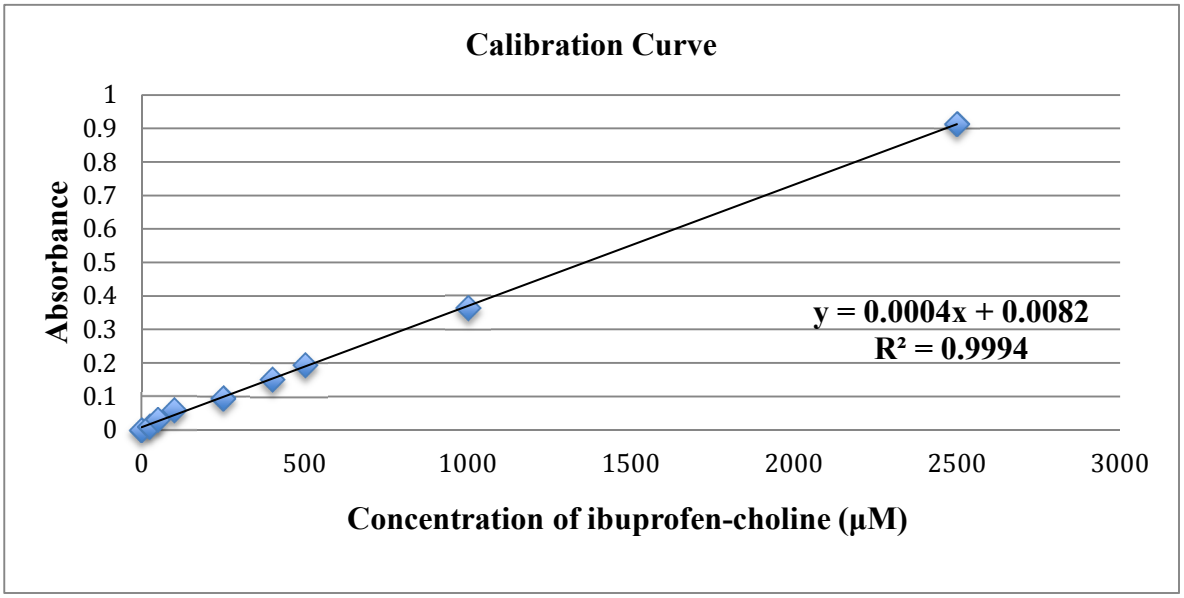

FIGURE 23. Calibration curve of ibuprofen-choline.

Concentration of the substrate (µM)	UV-Vis Absorbance
2500	0.914
1000	0.363
500	0.194
400	0.152
250	0.095
100	0.059
50	0.031
25	0.011

Transport flux calculation of ibuprofen-choline **30**:

Receptor: Calix[4]CH_2COOH
Receiving Phase: Neutral

Dilution factor of the Initial solution	5
Dilution factor of the source phases	5
Dilution factor of the receiving phases	2

TABLE 15. Transport Flux Calculations of Ibuprofen-Choline in Neutral Condition

	Initial guest solution	Control	1st Trial	2nd Trial	Mean of Trials
Source phase absorbance	0.051	0.037	0.021	0.019	
Receiving phase absorbance		0.014	0.005	0.006	
Source phase concentration	107	72	32	27	
Receiving phase concentration		14.5	-8	-5.5	
Source phase's actual concentration	535	360	160	135	
Receiving phase's actual concentration		29	-16	-11	
% Transported from source phase		32.71028037	70.09345794	74.76635514	72.42990654
% Appeared in receiving phase		5.420560748	-2.990654206	-2.056074766	-2.523364486
Mass Transported		0.116	-0.064	-0.044	-0.054
Transport Flux (μmolcm-2min-1)		2.37627E-05	-1.31105E-05	-9.01344E-06	-1.10619E-05

Transport flux calculation of ibuprofen-choline **30**:

Receptor: Calix[4]CH_2COOH
Receiving Phase: Acidic (0.1 M HCl)

Dilution factor of the Initial solution	5
Dilution factor of the source phases	5
Dilution factor of the receiving phases	2

TABLE 16. Transport Flux Calculations of Ibuprofen-Choline in Acidic Condition

	Initial guest solution	Control	1st Trial	2nd Trial	Mean of Trials
Source phase absorbance	0.048	0.038	0.037	0.035	
Receiving phase absorbance		0.014	0.025	0.026	
Source phase concentration	99.5	74.5	72	67	
Receiving phase concentration		14.5	42	44.5	
Source phase's actual concentration	497.5	372.5	360	335	
Receiving phase's actual concentration		29	84	89	
% Transported from source phase		25.12562814	27.63819095	32.66331658	30.15075377
% Appeared in receiving phase		5.829145729	16.88442211	17.88944724	17.38693467
Mass Transported		0.116	0.336	0.356	0.346
Transport Flux (μmolcm-2min-1)		2.37627E-05	6.88299E-05	7.29269E-05	7.08784E-05

Transport results of dopamine **31**:

Experimental conditions:

Receptor's concentration: 0.5 mM

Receptor's volume: 10 mL

Substrate's concentration: 5 mM

Stirring speed: 400 rpm

λmax in neutral and acidic condition: 281 nm

Stirring time: 72 Hours

λmax in HEPES buffer: 279.6 nm

Volume of source and receiving

phases: 4 mL

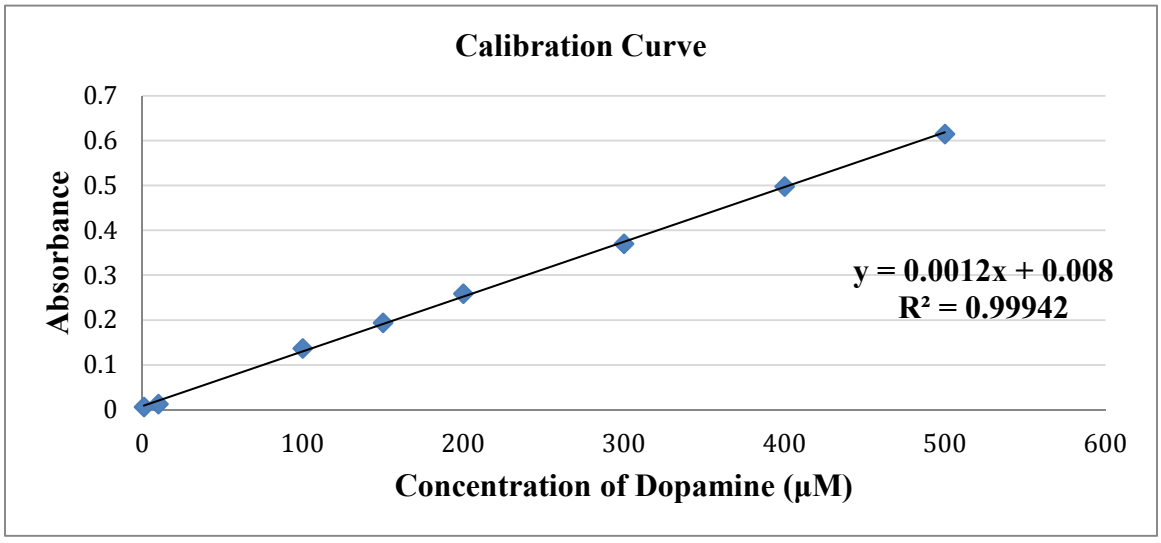

FIGURE 24. Calibration curve of dopamine in neutral and acidic condition.

Concentration of the substrate (µM)	UV-Vis Absorbance
500	0.615
400	0.498
300	0.370
200	0.259
150	0.194
100	0.137
10	0.013
1	0.006

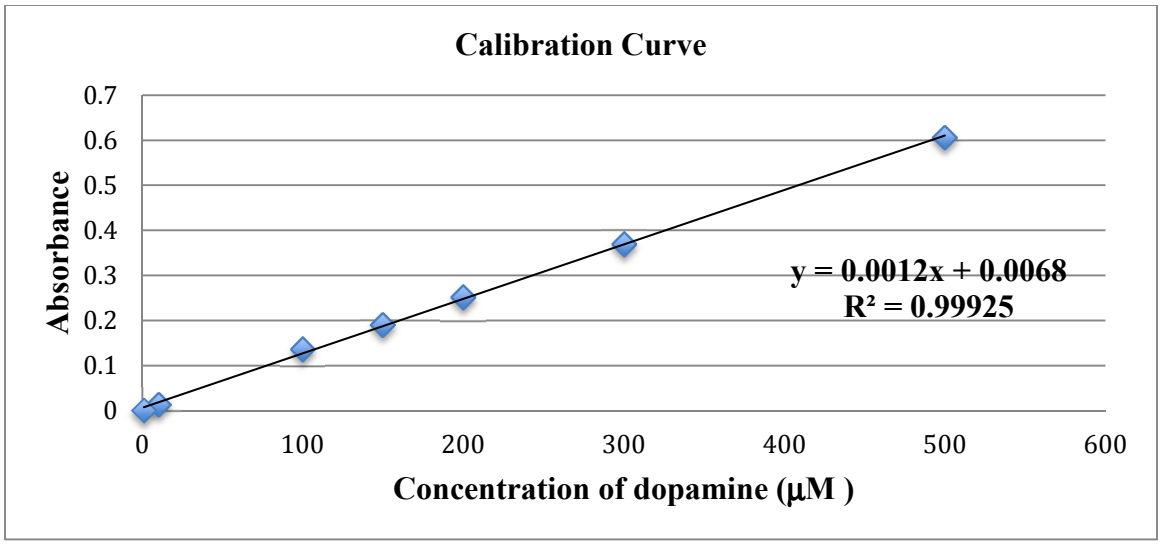

FIGURE 25. Calibration curve of dopamine in HEPES buffer.

Concentration of the substrate (µM)	UV-Vis Absorbance
500	0.606
300	0.370
200	0.252
150	0.190
100	0.137
10	0.014
1	0.001

Transport flux calculation of dopamine **31**:

Receptor: Calix[5]CH_2COOH
Receiving Phase: MQ Water

Dilution factor of the Initial solution	10
Dilution factor of the source phases	10
Dilution factor of the receiving phases	2

TABLE 17. Transport Flux Calculations of Dopamine in Neutral Condition

	Initial guest solution	Control	1st Trial	2nd Trial	Mean of Trials
Source phase absorbance	1.363	1.286	1.312	1.306	
Receiving phase absorbance		0.005	0.085	0.074	
Source phase concentration	504.7037037	476.1851852	485.8148148	483.5925926	
Receiving phase concentration		1.740740741	31.37037037	27.2962963	
Source phase's actual concentration	5047.037037	4761.851852	4858.148148	4835.925926	
Receiving phase's actual concentration		3.481481481	62.74074074	54.59259259	
% Transported from source phase		5.650546709	3.742569898	4.182872239	3.962721068
% Appeared in receiving phase		0.0689807	1.243120276	1.081676084	1.16239818
Mass Transported		0.013925926	0.250962963	0.21837037	0.234666667
Transport Flux (μmolcm-2min-1)		2.85274E-06	5.141E-05	4.47334E-05	4.80717E-05

Transport flux calculation of dopamine **31**:

Receptor: Calix[5]CH_2COOH
Receiving Phase: Acidic (0.1M HCl)

Dilution factor of the Initial solution	10
Dilution factor of the source phases	10
Dilution factor of the receiving phases	2

TABLE 18. Transport Flux Calculations of Dopamine in Acidic Condition

	Initial guest solution	Control	1st Trial	2nd Trial	Mean of Trials
Source phase absorbance	1.357	1.321	1.217	1.211	
Receiving phase absorbance		0.009	0.027	0.018	
Source phase concentration	502.4814815	489.1481481	450.6296296	448.4074074	
Receiving phase concentration		3.222222222	9.888888889	6.555555556	
Source phase's actual concentration	5024.814815	4891.481481	4506.296296	4484.074074	
Receiving phase's actual concentration		6.444444444	19.77777778	13.11111111	
% Transported from source phase		2.653497457	10.31915678	10.76140635	10.54028157
% Appeared in receiving phase		0.128252377	0.393602123	0.26092725	0.327264686
Mass Transported		0.025777778	0.079111111	0.052444444	0.065777778
Transport Flux (μmolcm-2min-1)		5.2806E-06	1.6206E-05	1.07433E-05	1.34746E-05

Transport flux calculation of dopamine **31**:

Receptor: Calix[4]PO_3H
Receiving Phase: HEPES buffer

Dilution factor of the Initial solution	10
Dilution factor of the source phases	10
Dilution factor of the receiving phases	1

TABLE 19. Transport Flux Calculations of Dopamine in HEPES Buffer

	Initial guest solutions	Control #1	Control #2	1st Trial	2nd Trial	Mean of Controls	Mean of Trials
Source phase absorbance	0.467	0.527	0.472	0.391	0.492		
Receiving phase absorbance		0.022	0.02	0.126	0.074		
Source phase concentration	465.1	525.1	470.1	389.1	490.1		
Receiving phase concentration		20.1	18.1	124.1	72.1		
Source phase's actual concentration	4651	5251	4701	3891	4901		
Receiving phase's actual concentration		20.1	18.1	124.1	72.1		
% Transported from source phase		-12.9004	-1.0750	16.3405	-5.3751	-6.9877	5.4826
% Appeared in receiving phase		0.4321	0.3891	2.6682	1.5502	0.4106	2.1092
Mass Transported		0.0804	0.0724	0.4964	0.2884	0.0764	0.3924
Transport Flux ($\mu molcm^{-2}min^{-1}$)		1.647E-05	1.48312E-05	0.0001016	5.9079E-05	1.56506E-05	8.03835E-05

Transport results of serotonin **32**:

Experimental conditions:

Receptor's concentration: 0.5 mM

Receptor's volume: 10 mL

Substrate's concentration: 5 mM

Stirring speed: 400 rpm

λmax in neutral and acidic Conditions: 277 nm

Stirring time: 72 Hours

λmax in HEPES buffer: 275 nm

Volume of source and receiving phases: 4 mL

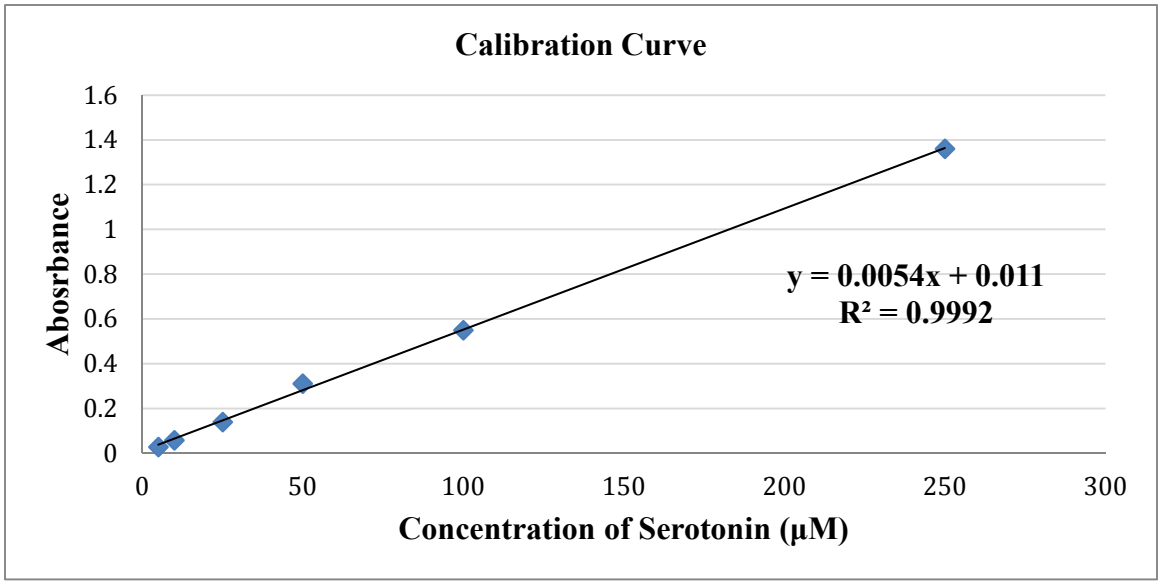

FIGURE 26. Calibration curve of serotonin in HEPES buffer, neutral condition and acidic condition.

Concentration of the substrate (µM)	UV-Vis Absorbance
250	1.360
100	0.550
50	0.311
25	0.140
10	0.058
5	0.028

Transport flux calculation of serotonin **32**:

Receptor: Calix[5]CH_2COOH
Receiving Phase: MQ Water

Dilution factor of the Initial solution	20
Dilution factor of the source phases	20
Dilution factor of the receiving phases	2

TABLE 20. Transport Flux Calculations of Serotonin in Neutral Condition

	Initial guest solution	Control	1st Trial	2nd Trial	Mean of Trials
Source phase absorbance	1.471	1.315	1.377	1.349	
Receiving phase absorbance		0.01	0.096	0.101	
Source phase concentration	270.3703704	241.4814815	252.962963	247.7777778	
Receiving phase concentration		-0.185185185	15.74074074	16.66666667	
Source phase's actual concentration	5407.407407	4829.62963	5059.259259	4955.555556	
Receiving phase's actual concentration		-0.37037037	31.48148148	33.33333333	
% Transported from source phase		10.68493151	6.438356164	8.356164384	7.397260274
% Appeared in receiving phase		-0.006849315	0.582191781	0.616438356	0.599315068
Mass Transported		0	0.125925926	0.133333333	0.12962963
Transport Flux (μmolcm-2min-1)		0	2.5796E-05	2.73134E-05	2.65547E-05

Transport flux calculation of serotonin **32**:

Receptor: Calix[5]CH_2COOH
Receiving Phase: Acidic (0.1M HCl)

Dilution factor of the Initial solution	20
Dilution factor of the source phases	20
Dilution factor of the receiving phases	2

TABLE 21. Transport Flux Calculations of Serotonin in Acidic Condition

	Initial guest solution	Control	1st Trial	2nd Trial	Mean of Trials
Source phase absorbance	1.461	1.434	1.377	1.38	
Receiving phase absorbance		0	0.17	0.205	
Source phase concentration	268.5185185	263.5185185	252.962963	253.5185185	
Receiving phase concentration		-2.037037037	29.44444444	35.92592593	
Source phase's actual concentration	5370.37037	5270.37037	5059.259259	5070.37037	
Receiving phase's actual concentration		-4.074074074	58.88888889	71.85185185	
% Transported from source phase		1.862068966	5.793103448	5.586206897	5.689655172
% Appeared in receiving phase		-0.075862069	1.096551724	1.337931034	1.217241379
Mass Transported		0	0.235555556	0.287407407	0.261481481
Transport Flux (μmolcm-2min-1)		0	4.82538E-05	5.88757E-05	5.35647E-05

Transport flux calculation of serotonin **32**:

Receptor: Calix[4]PO_3H
Receiving Phase: HEPES buffer

Dilution factor of the Initial solution	20
Dilution factor of the source phases	20
Dilution factor of the receiving phases	1

TABLE 22. Transport Flux Calculations of Serotonin in HEPES Buffer

	Initial guest solutions	Control #1	Control #2	1st Trial	2nd Trial	Mean of Controls	Mean of Trials
Source phase absorbance	0.56	0.542	0.565	0.508	0.546		
Receiving phase absorbance		0.136	0.133	1.068	0.392		
Source phase concentration	101.6666667	98.33333333	102.5925926	92.03703704	99.07407407		
Receiving phase concentration		23.14814815	22.59259259	195.7407407	70.55555556		
Source phase's actual concentration	2033.333333	1966.666667	2051.851852	1840.740741	1981.481481		
Receiving phase's actual concentration		23.14814815	22.59259259	195.7407407	70.55555556		
% Transported from source phase		3.278688525	-0.910746812	9.471766849	2.550091075	1.183970856	6.010928962
% Appeared in receiving phase		1.138433515	1.111111111	9.626593807	3.469945355	1.124772313	6.548269581
Mass Transported		0.092592593	0.09037037	0.782962963	0.282222222	0.091481481	0.532592593
Transport Flux (μmolcm-2min-1)		1.89677E-05	1.85124E-05	0.000160391	5.78135E-05	1.87401E-05	0.000109102

Transport results of bentiromide-choline **33**:

Experimental conditions:

Receptor's concentration: 0.5 mM

Receptor's volume: 10 mL

Substrate's concentration: 0.5 mM

Stirring speed: 400 rpm

λmax in neutral and acidic conditions: 267 nm

Stirring time: 72 Hours

Volume of source and receiving phases: 4 mL

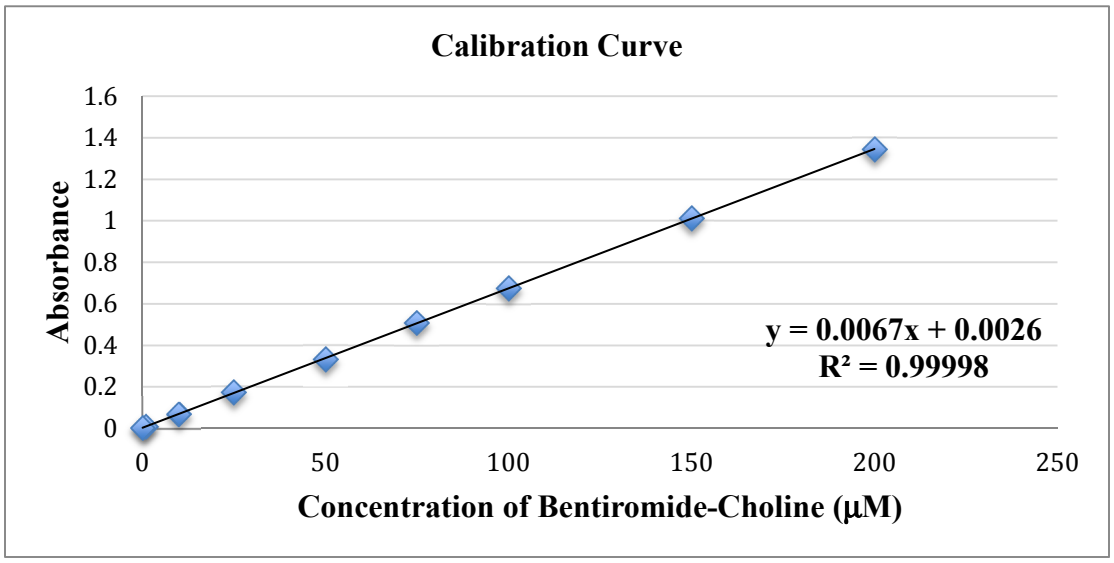

FIGURE 27. Calibration curve of dopamine in neutral and acidic condition.

Concentration of the substrate (µM)	UV-Vis Absorbance
200	1.345
150	1.011
100	0.676
75	0.508
50	0.333
25	0.172
10	0.069
1	0.010

Transport flux calculation of bentiromide-choline **33**:

Receptor: Calix[4]CH_2COOH
Receiving Phase: MQ Water

Dilution factor of the Initial solution	3
Dilution factor of the source phases	3
Dilution factor of the receiving phases	1

TABLE 23. Transport Flux Calculations of Bentiromide-Choline in Neutral Condition Using Calix[4]CH_2COOH as Receptor

	Initial guest solution	Control #1	Control #2	1st Trial	2nd Trial	Mean of Controls	Mean of Trials
Source phase absorbance	1.126	1.098	1.125	1.013	1.032		
Receiving phase absorbance		0.033	0.016	0.299	0.206		
Source phase concentration	167.6716	163.4925	167.5223	150.8059	153.6417		
Receiving phase concentration		4.5373	2	44.2388	30.3582		
Source phase's actual concentration	503.0149	490.4776	502.5671	452.4179	460.9253		
Receiving phase's actual concentration		4.5373	2	44.2388	30.3582		
% Transported from source phase		2.4924	0.0890	10.0587	8.3674	2.5814	9.2131
% Appeared in receiving phase		0.9020	0.3976	8.7947	6.0352	1.2996	7.4149
Mass Transported		0.0181	0.008	0.1769	0.1214	0.0261	0.1491
Transport Flux ($\mu molcm^{-2}min^{-1}$)		3.7178E-06	1.6388E-06	3.6249E-05	2.4875E-05	5.356E-06	3.0562E-05

Transport flux calculation bentiromide-choline **33**:

Receptor: Calix[4]PO_3H
Receiving Phase: MQ Water

Dilution factor of the Initial solution	3
Dilution factor of the source phases	3
Dilution factor of the receiving phases	1

TABLE 24. Transport Flux Calculations of Bentiromide-Choline in Neutral Condition Using Calix[4]PO_3H as Receptor

	Initial guest solution	Control	1st Trial	2nd Trial	3rd Trial	Mean of Trials	STDEV
Source phase absorbance	1.122	1.094	1.002	1.014	0.995		
Receiving phase absorbance		0.029	0.226	0.141	0.197		
Source phase concentration	167.0746	162.8955	149.1641	150.9552	148.1194		
Receiving phase concentration		3.9402	33.3432	20.6567	29.0149		
Source phase's actual concentration	501.2238	488.6865	447.4925	452.8656	444.3582		
Receiving phase's actual concentration		3.9402	33.3432	20.6567	29.0149		
% Transported from source phase		2.5013	10.7200	9.6480	11.3453	10.5711	0.8584
% Appeared in receiving phase		0.7861	6.6523	4.1212	5.7888	5.5208	1.2866
Mass Transported		0.0157	0.1333	0.08262	0.1160	0.1106	0.0257
Transport Flux ($\mu molcm^{-2}min^{-1}$)		3.2286E-06	2.7321E-05	1.6926E-05	2.3774E-05	2.2674E-05	5.2843E-6

Transport flux calculation bentiromide-choline **33**:

Receptor: Calix[4]PO_3H
Receiving Phase: Acidic (0.1M HCl)

Dilution factor of the Initial solution	3
Dilution factor of the source phases	3
Dilution factor of the receiving phases	1

TABLE 25. Transport Flux Calculations of Bentiromide-Choline in Acidic Condition Using Calix[4]PO_3H as Receptor

	Initial guest solution	Control	1st Trial	2nd Trial	Mean
Source phase absorbance	1.0910	1.07	0.98	1.009	
Receiving phase absorbance		0.037	0.198	0.161	
Source phase concentration	162.4477	159.3134	145.8805	150.2089	
Receiving phase concentration		5.1343	29.1641	23.6417	
Source phase's actual concentration	487.3432	477.9402	437.6417	450.6268	
Receiving phase's actual concentration		5.1343	29.1641	23.6417	
% Transported from source phase		1.9294	10.1984	7.5339	8.8662
% Appeared in receiving phase		1.0535	5.9843	4.8511	5.4177
Mass Transported		0.0205	0.1166	0.0945	0.1056
Transport Flux ($\mu molcm^{-2}min^{-1}$)		4.2070E-06	2.3897E-05	1.9372E-05	2.1634E-05

Transport results of bentiromide:

Experimental conditions:

Receptor's concentration: 0.5 mM

Receptor's volume: 10 mL

Substrate's concentration: 0.5 mM

Stirring speed: 400 rpm

λmax in neutral condition: 262 nm

Stirring time: 72 Hours

Volume of source and receiving phases: 4 mL

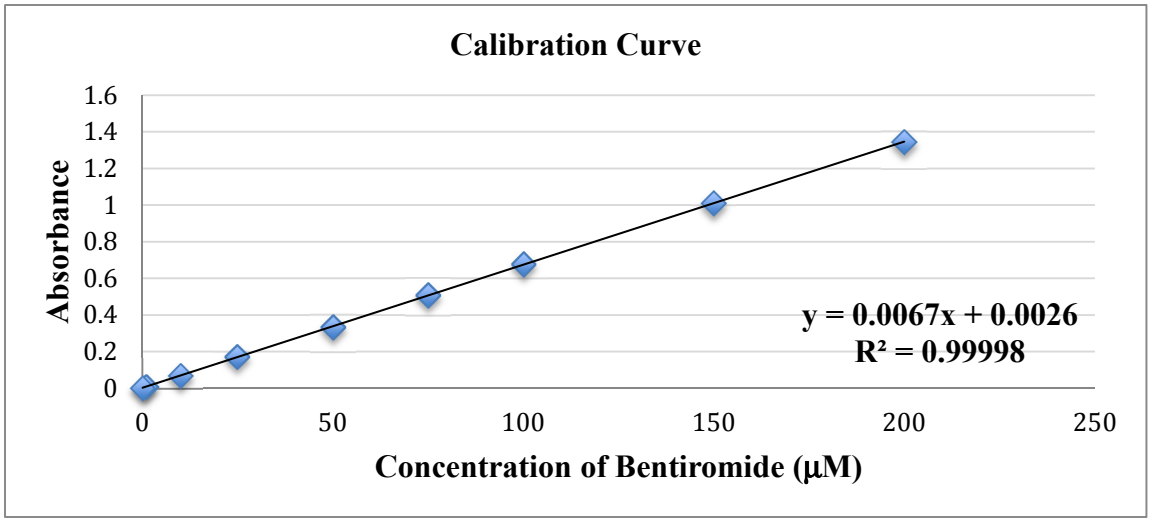

FIGURE 28. Calibration curve of bentiromide in neutral condition.

Concentration of the substrate (µM)	UV-Vis Absorbance
200	1.345
150	1.011
100	0.676
75	0.508
50	0.333
25	0.172
10	0.069
1	0.010

Transport flux calculation of bentiromide:

Receptor: Calix[4]PO_3H
Receiving Phase: MQ Water

Dilution factor of the Initial solution	3
Dilution factor of the source phases	3
Dilution factor of the receiving phases	1

TABLE 26. Transport Flux Calculations of Bentiromide in Neutral Condition

	Initial guest solution	Control #1	Control # 2	1st Trial	2nd Trial	Mean of Controls	Mean of Trials
Source phase absorbance	1.19	0.482	0.502	0.555	0.636		
Receiving phase absorbance		0.229	0.303	0.34	0.434		
Source phase concentration	177.2238	71.5522	74.5373	82.4477	94.5373		
Receiving phase concentration		33.7910	44.8358	50.3582	64.3880		
Source phase's actual concentration	531.6716	214.6567	223.6119	247.3432	283.6119		
Receiving phase's actual concentration		33.7910	44.8358	50.3582	64.3880		
% Transported from source phase		59.626	57.9417	53.4781	46.6565	58.7838	50.0673
% Appeared in receiving phase		6.3556	8.4329	9.4716	12.1104	7.3943	10.7910
Mass Transported		0.1351	0.1793	0.2014	0.2575	0.1572	0.2294
Transport Flux ($\mu molcm^{-2}min^{-1}$)		2.7688E-05	3.6738E-05	4.1263E-05	5.2759E-05	3.2213E-05	4.7011E-05

APPENDIX B

NMR SPECTRA OF THE SYNTHESIZED COMPOUNDS

^{1}H NMR of **6**

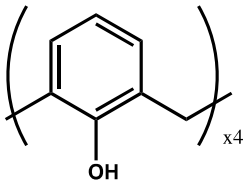

6

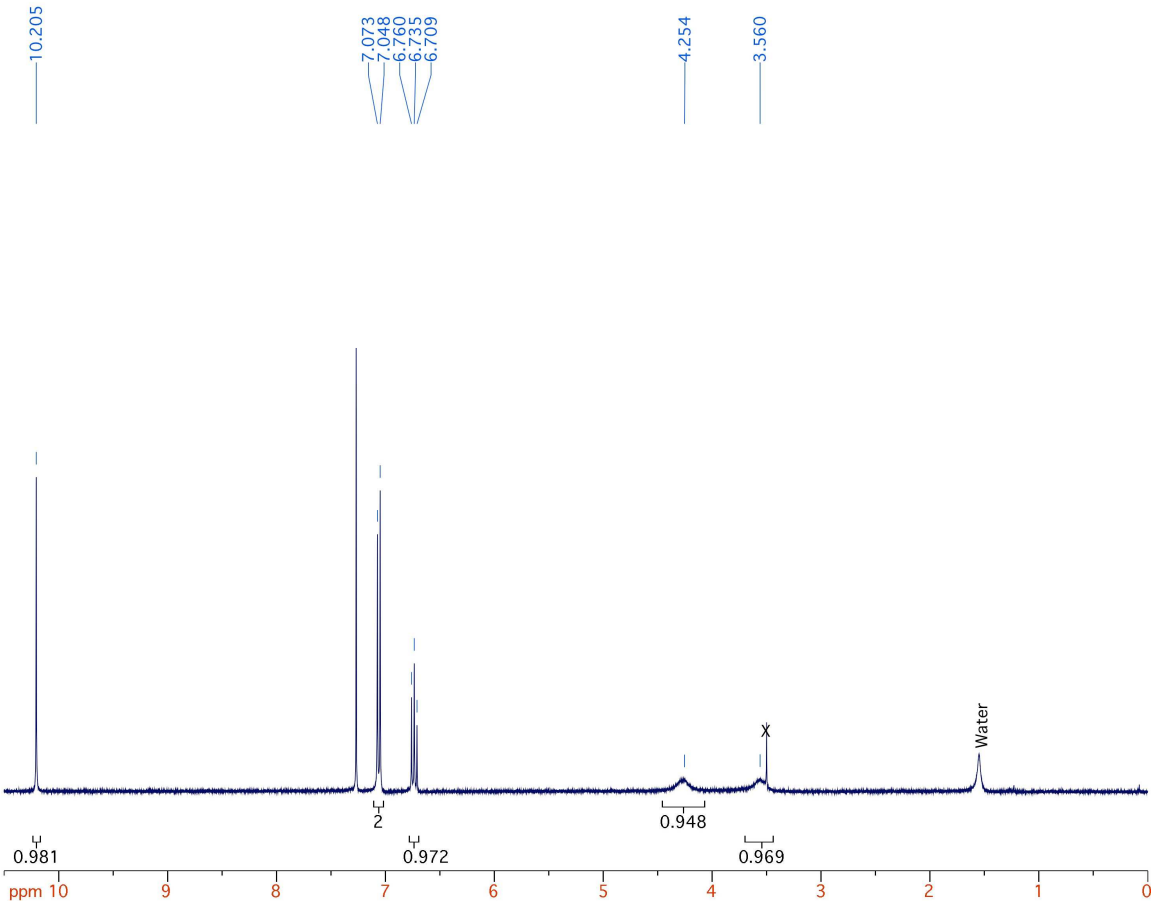

FIGURE 29. ^{1}H NMR of 6.

^{1}H NMR of **7**

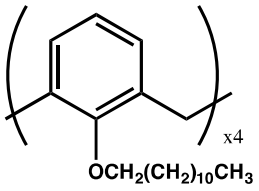

7

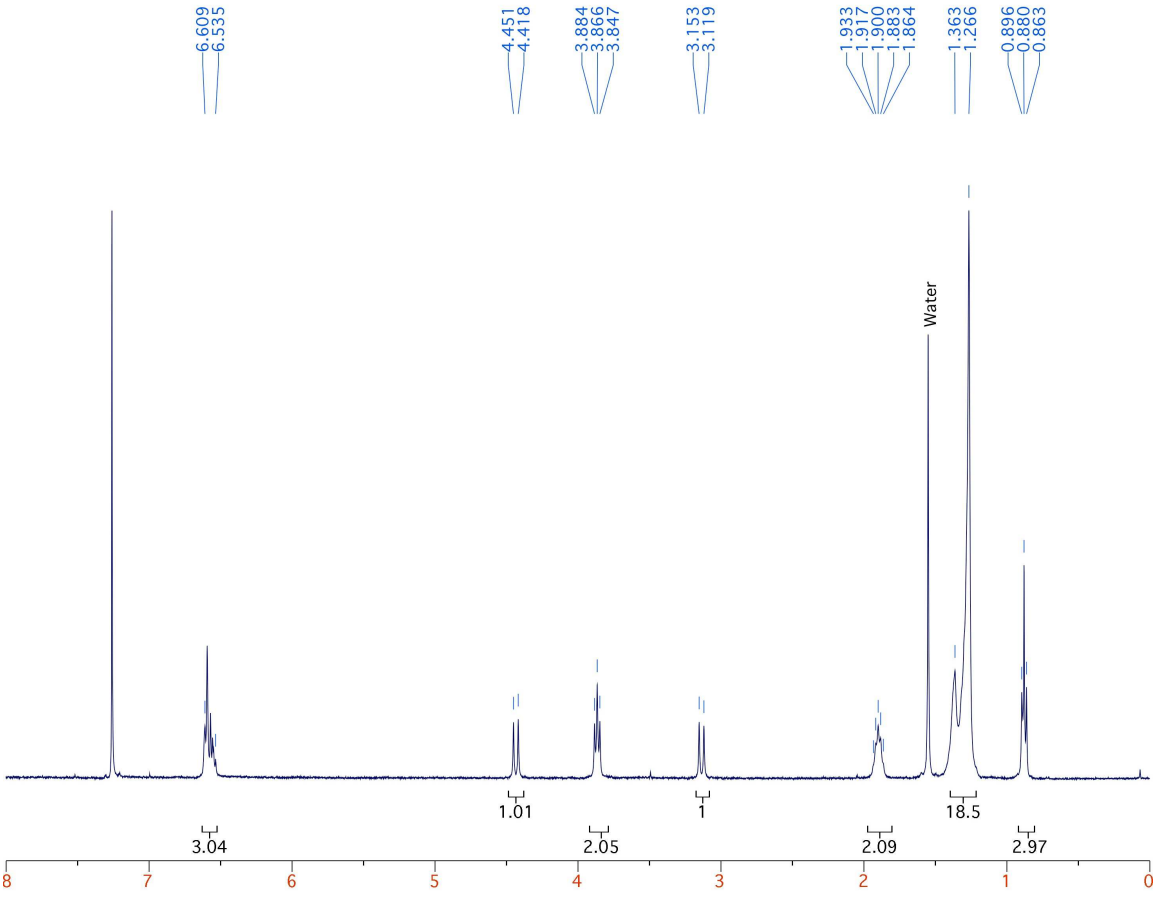

FIGURE 30. ^{1}H NMR of 7.

^{1}H NMR of **8**

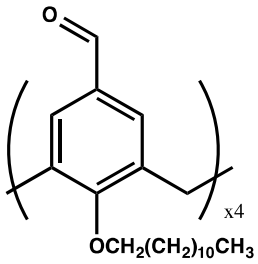

8

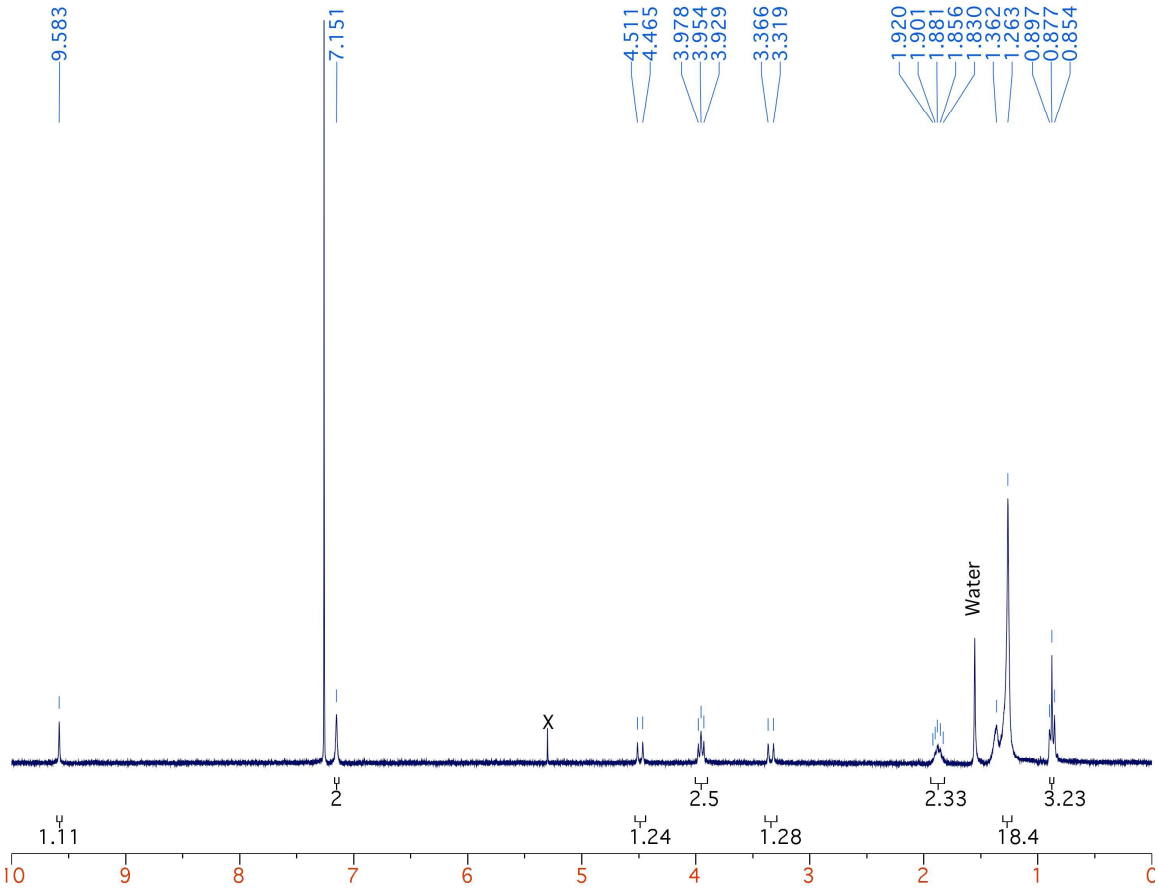

FIGURE 31. ^{1}H NMR of 8.

^{1}H NMR of **12**

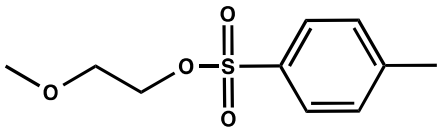

12

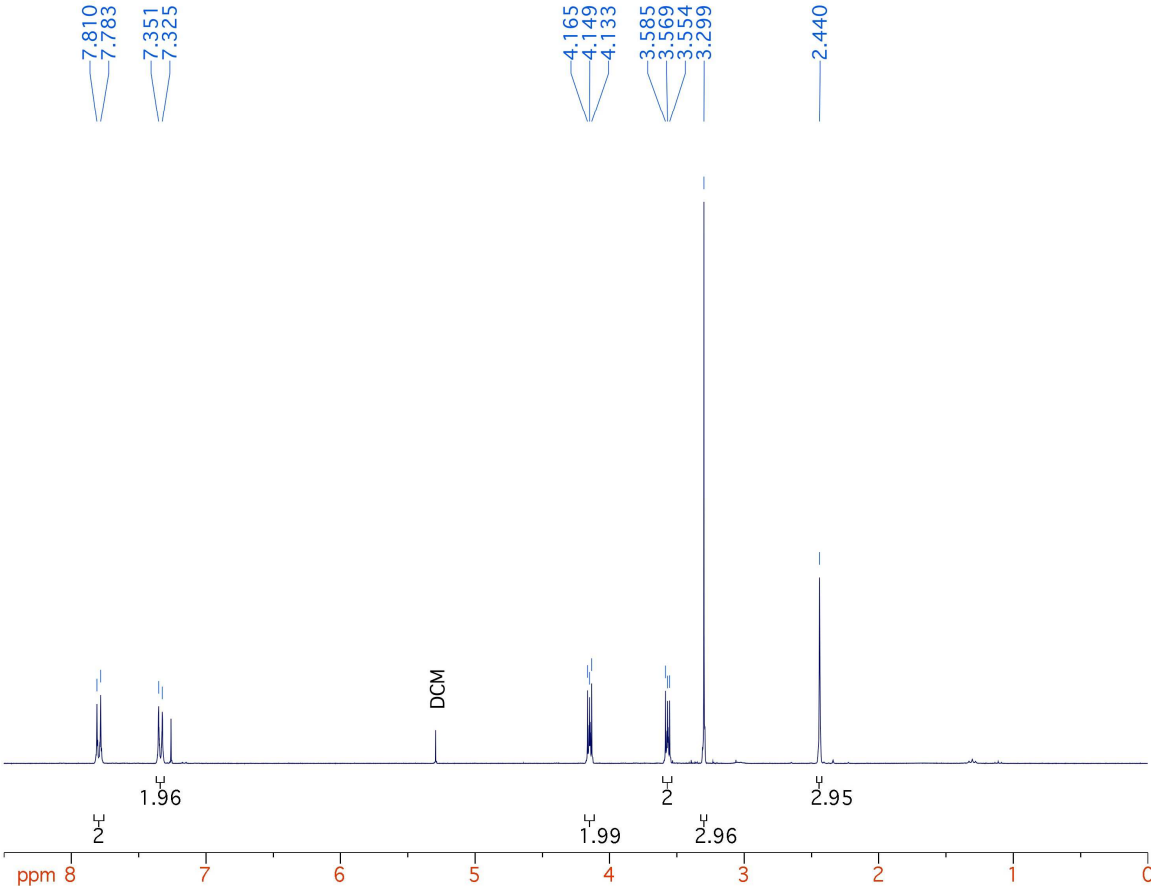

FIGURE 32. ^{1}H NMR of 12.

^{1}H NMR of **13**

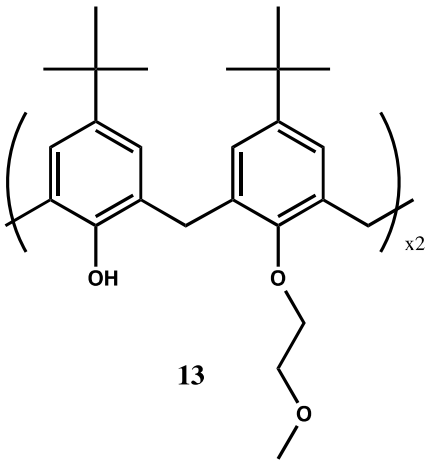

13

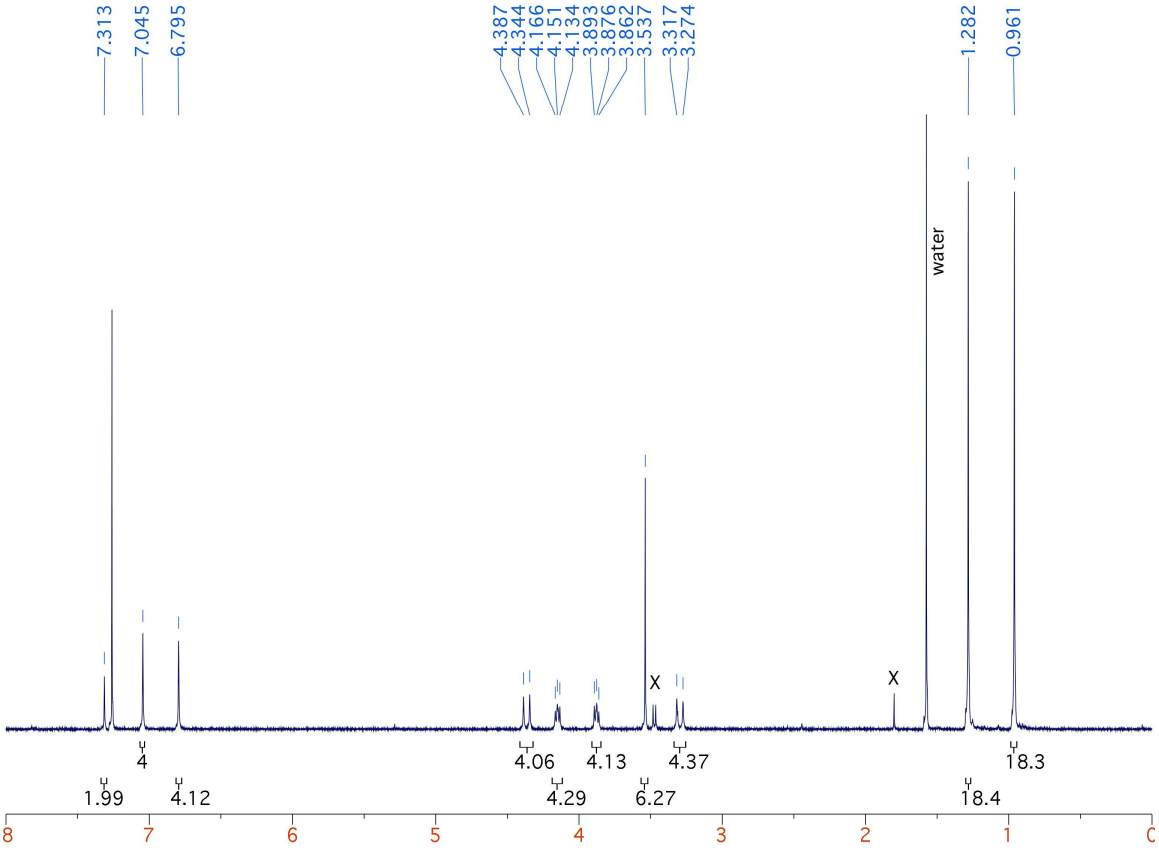

FIGURE 33. ^{1}H NMR of 13.

^{1}H NMR of **14**

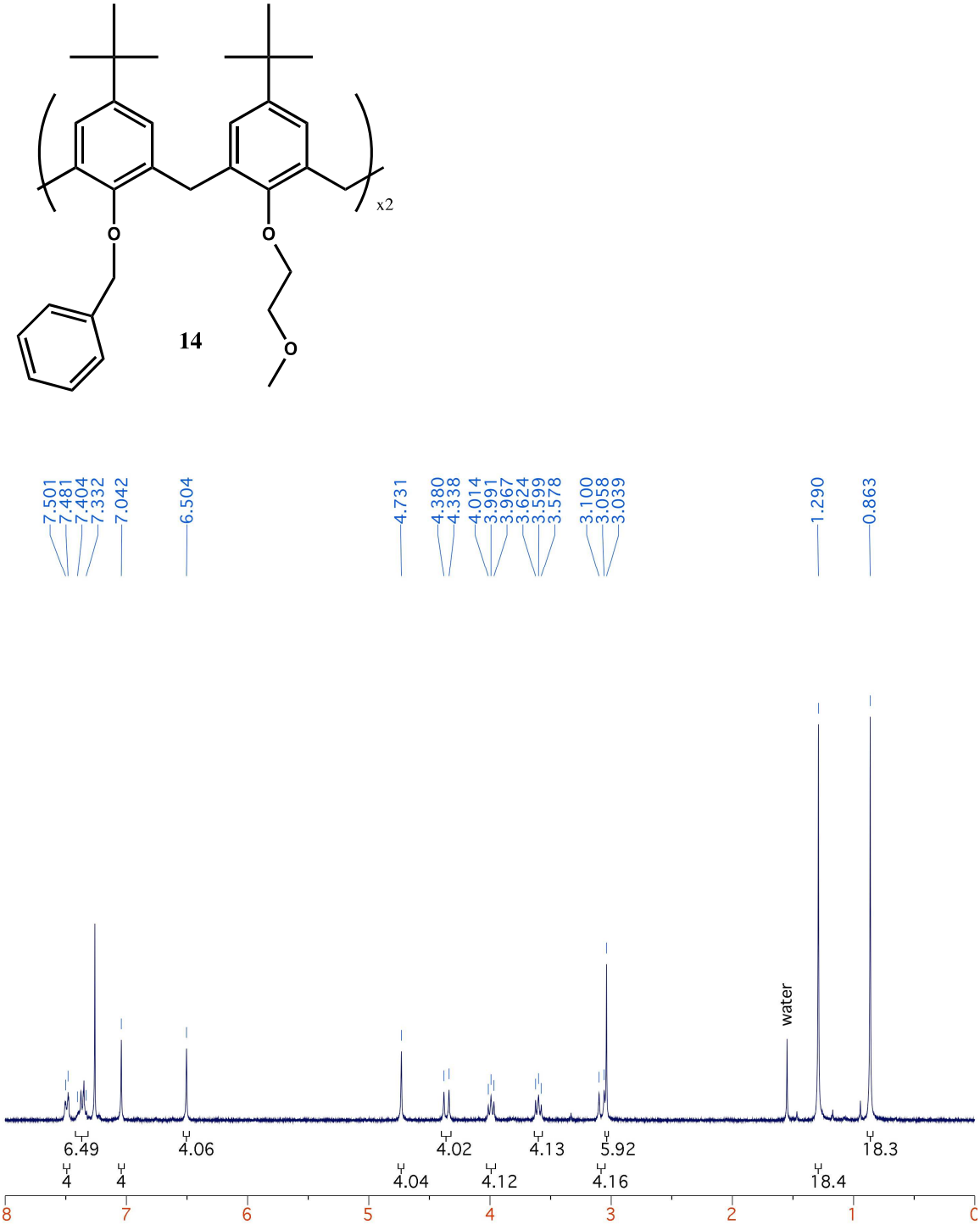

FIGURE 34. ^{1}H NMR of 14.

^{1}H NMR of **15**

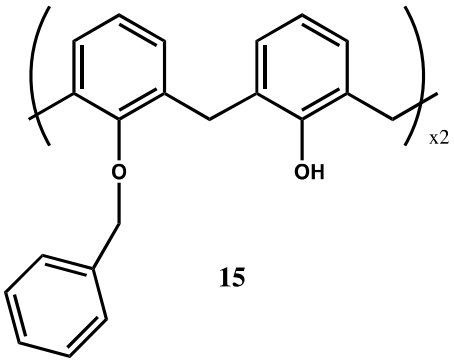

15

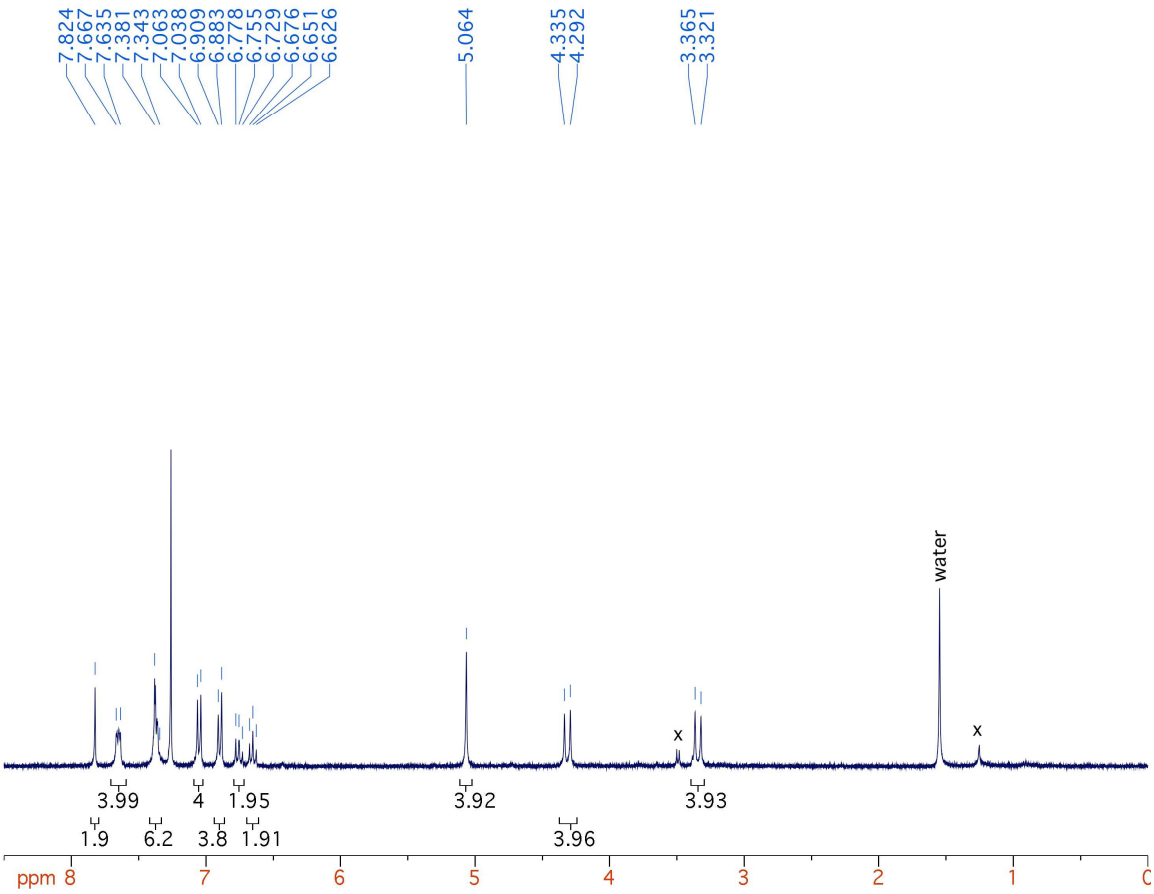

FIGURE 35. ^{1}H NMR of 15.

^{1}H NMR of **16**

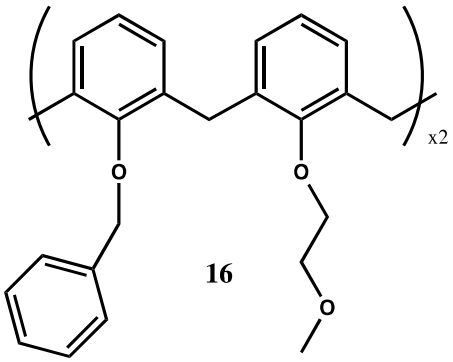

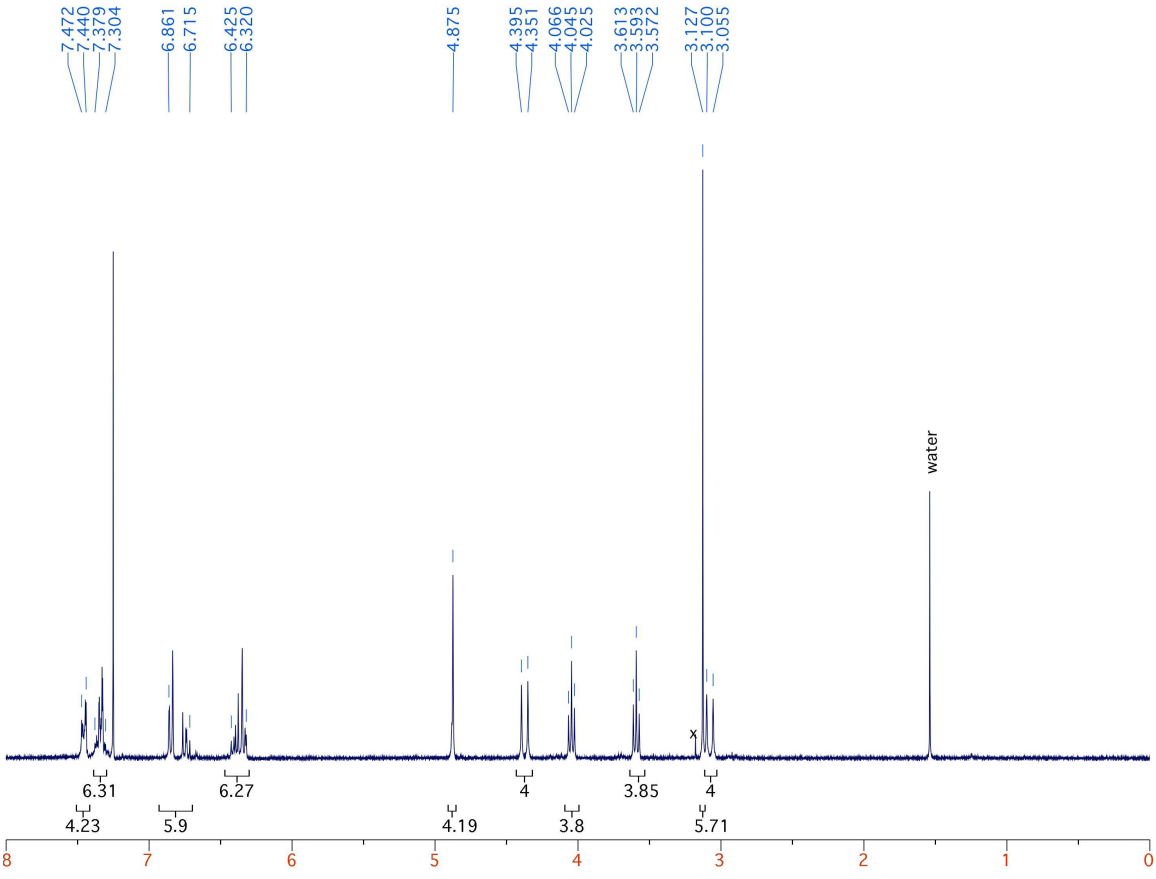

FIGURE 36. ^{1}H NMR of 16.

^{1}H NMR of **17**

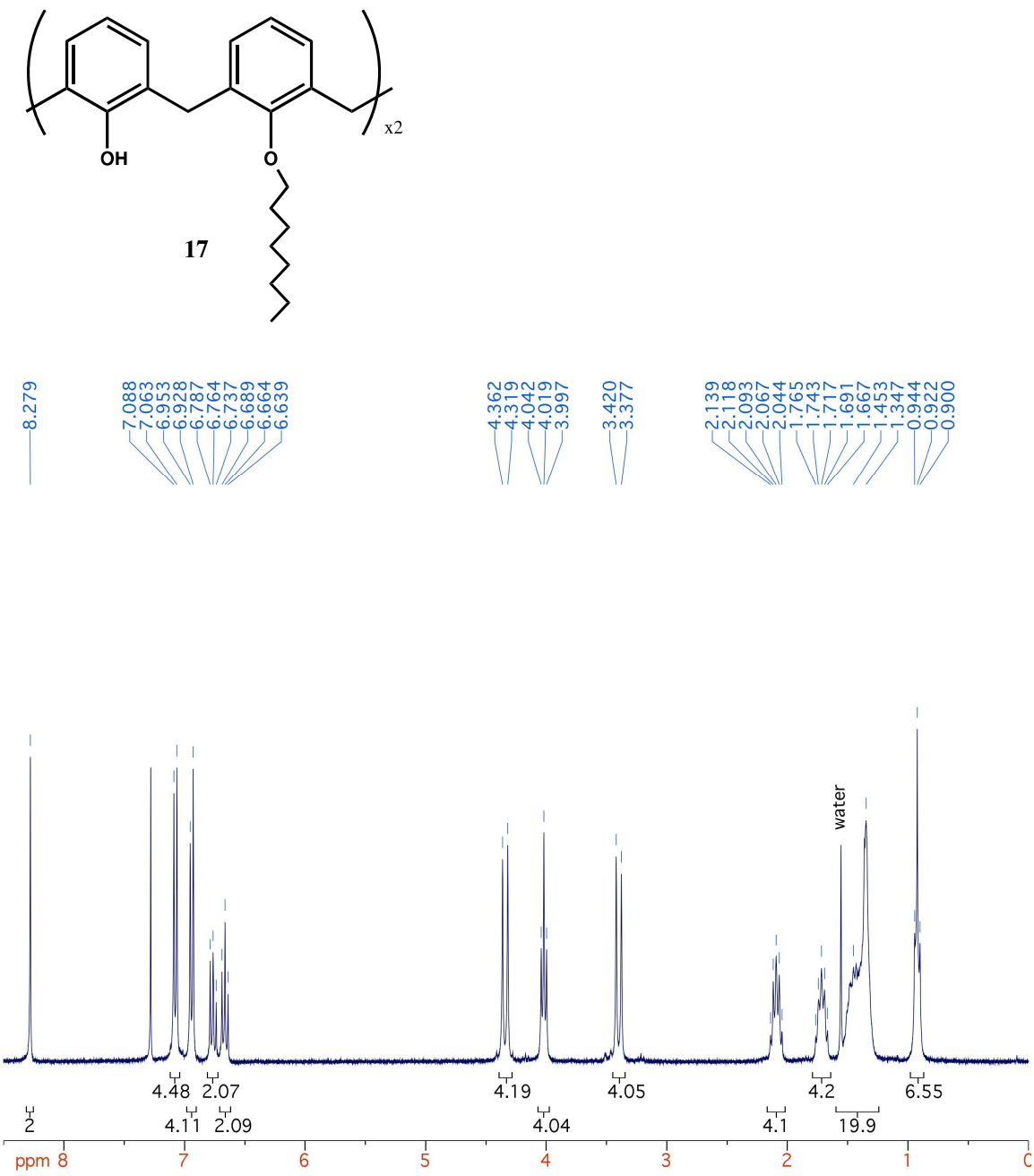

FIGURE 37. ^{1}H NMR of 17.

^{1}H NMR of **19**

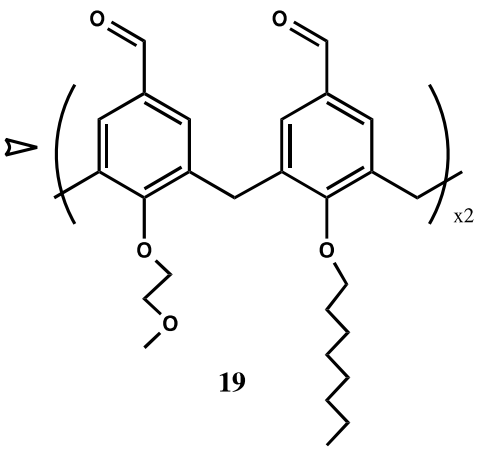

19

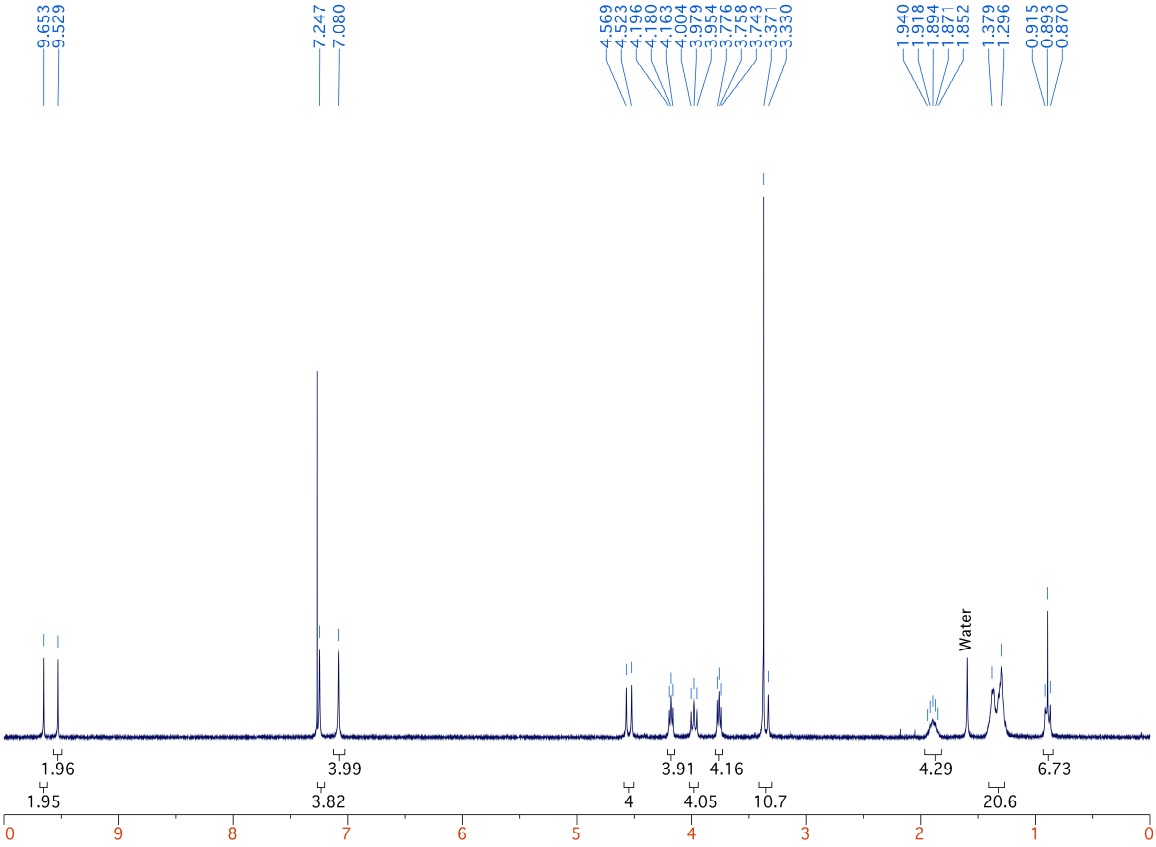

FIGURE 38. ^{1}H NMR of 19.

^{1}H NMR of **25**

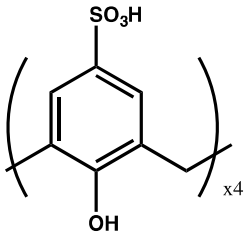

25

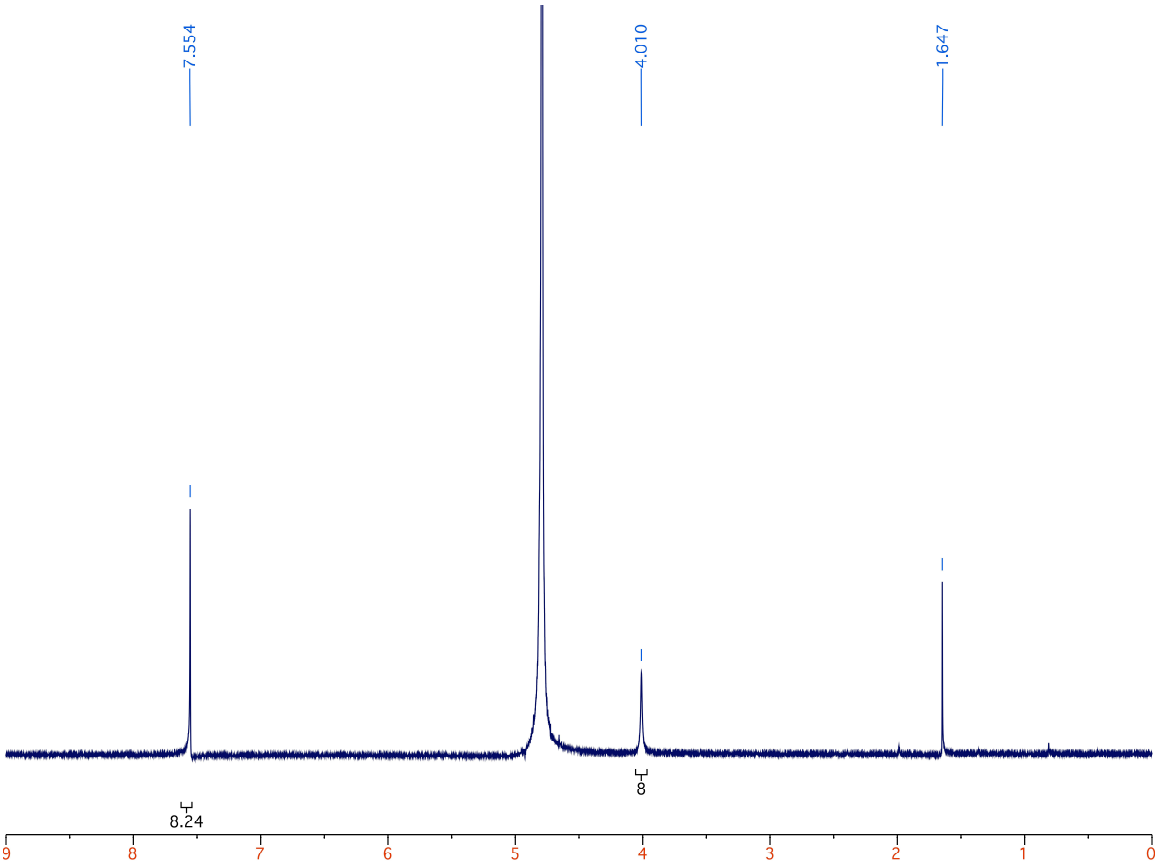

FIGURE 39. ^{1}H NMR of 25.

^{1}H NMR of **B**

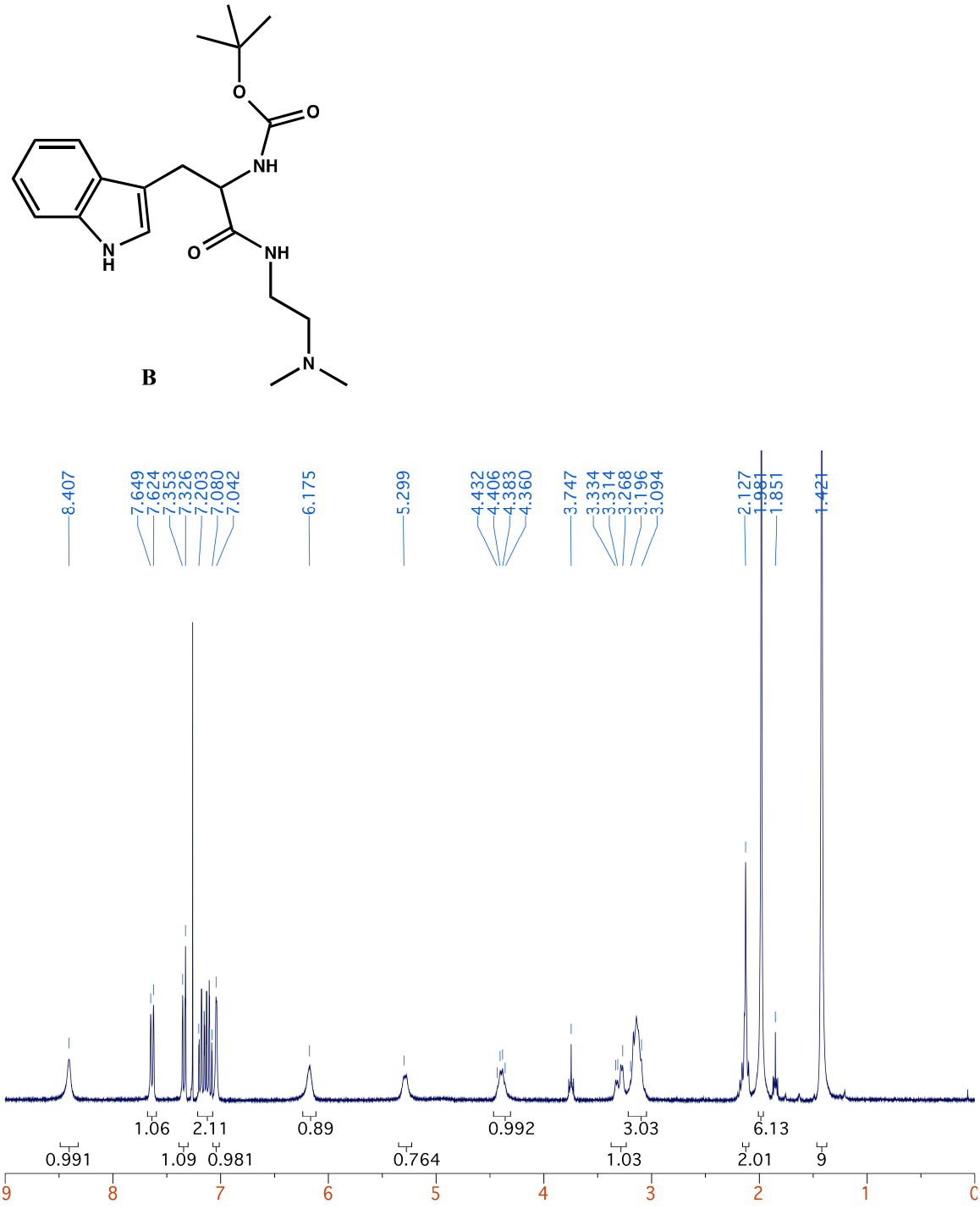

FIGURE 40. ^{1}H NMR of B.

^{1}H NMR of **28**

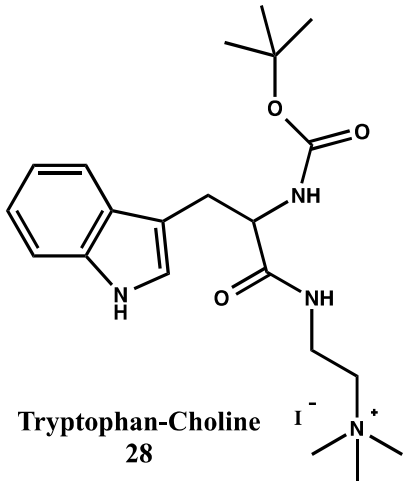

Tryptophan-Choline
28

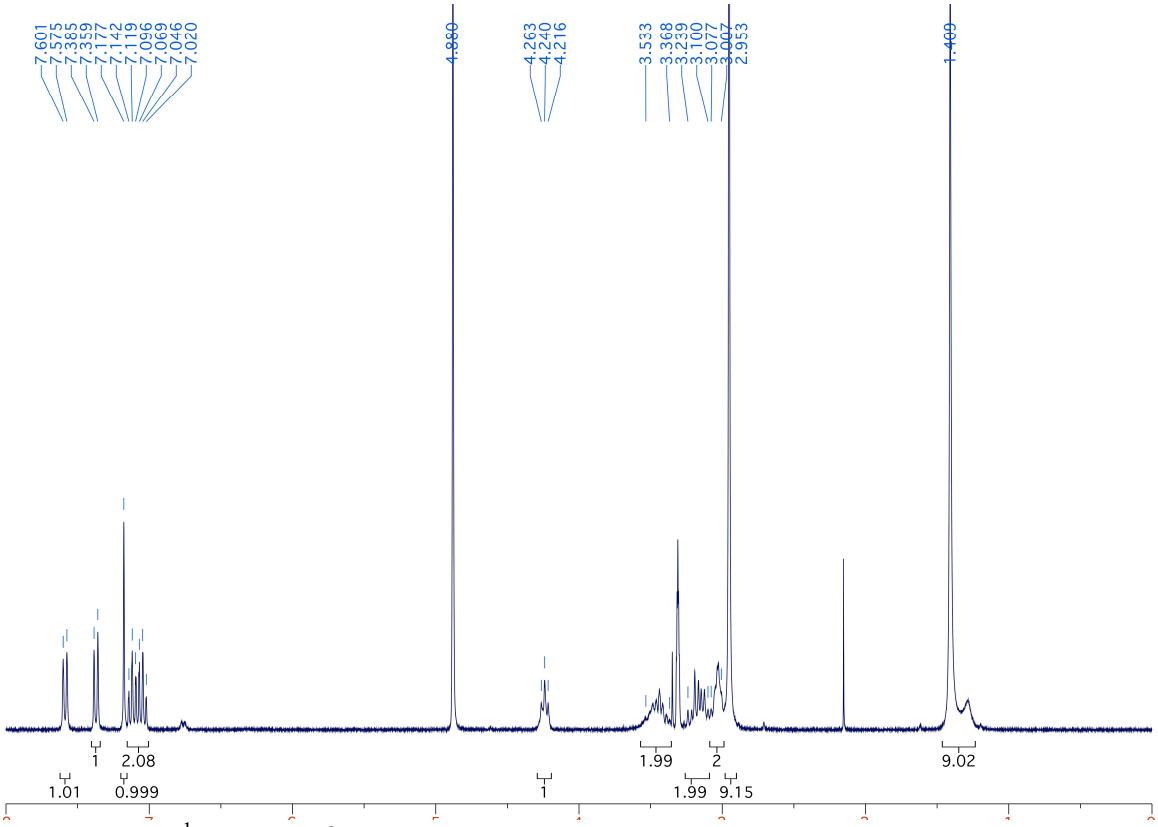

FIGURE 41. ^{1}H NMR of 28.

^{1}H NMR of **29**

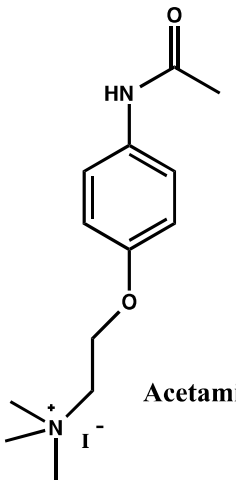

Acetaminophen-Choline
29

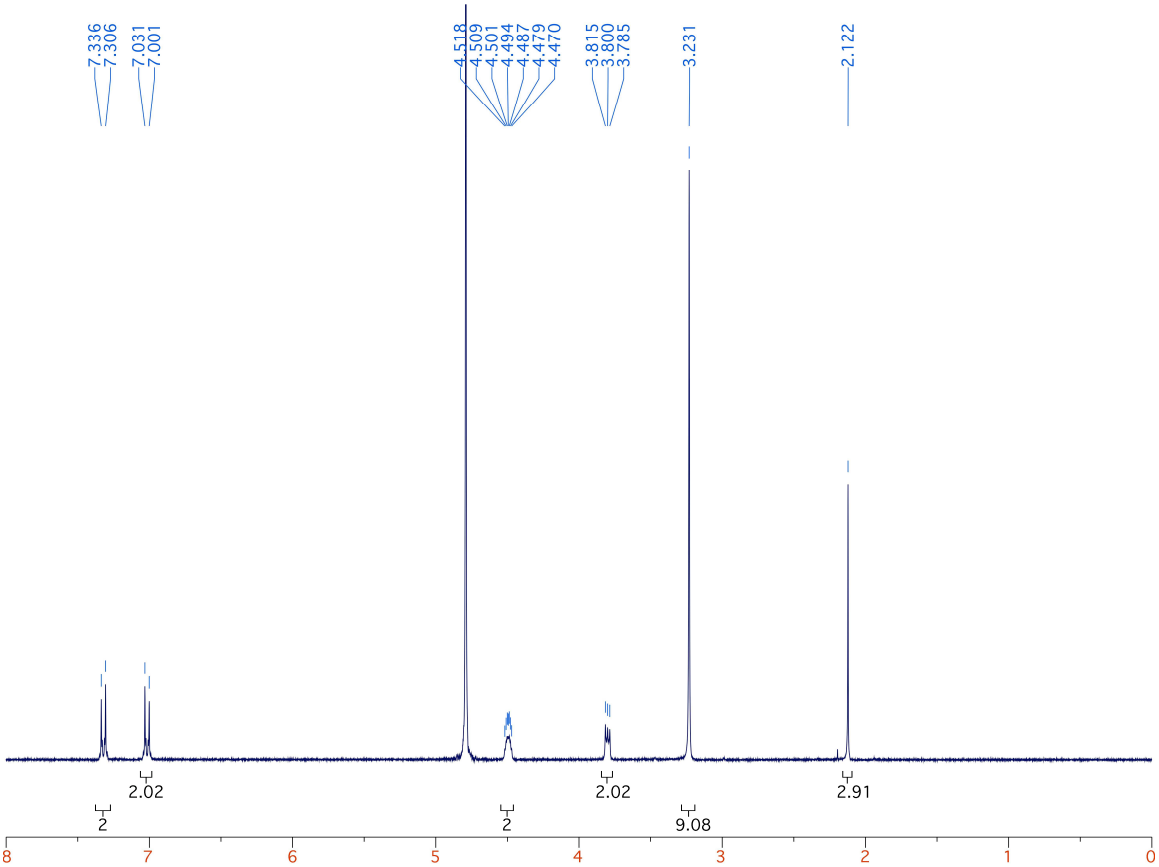

FIGURE 42. ^{1}H NMR of 29.

^{1}H NMR of **30**

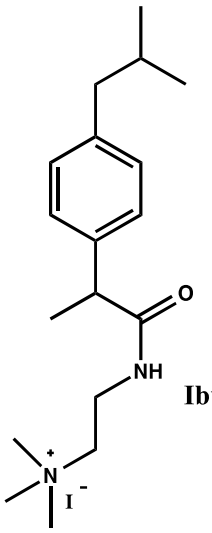

Ibuprofen-Choline
30

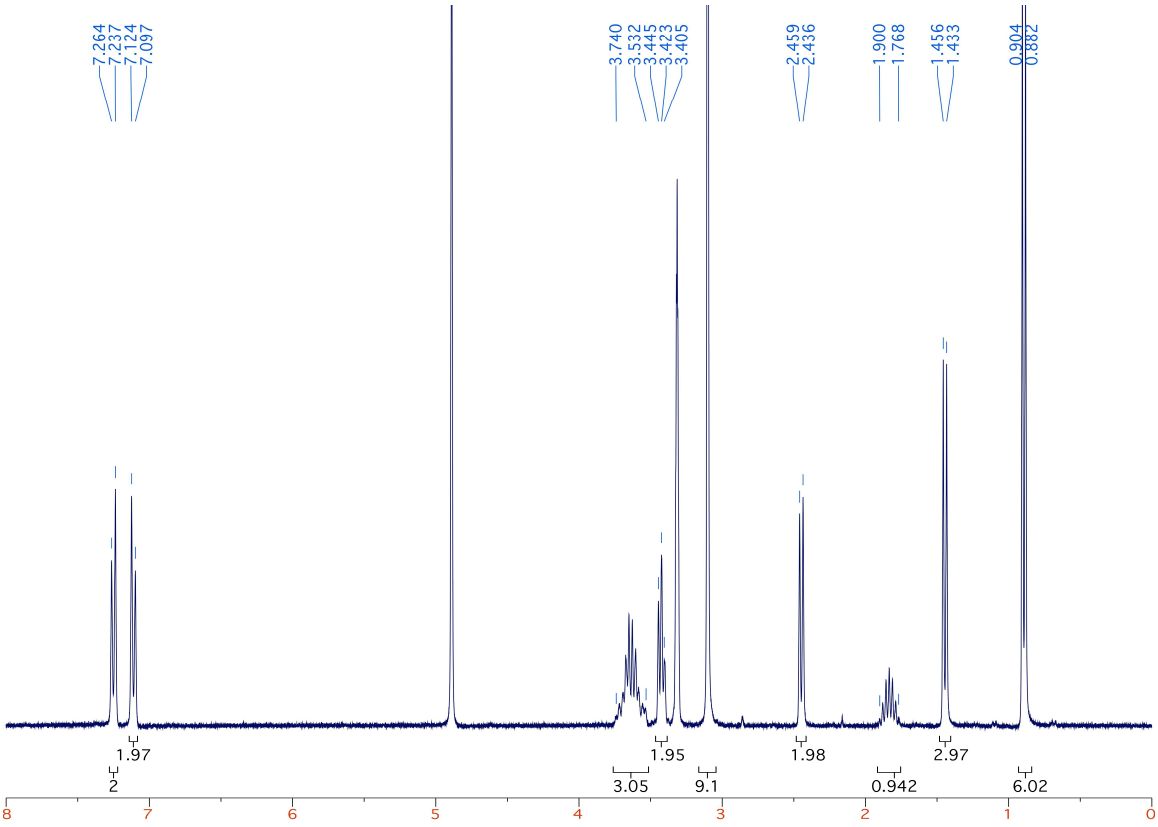

FIGURE 43. ^{1}H NMR of 30.

^{1}H NMR of **33**

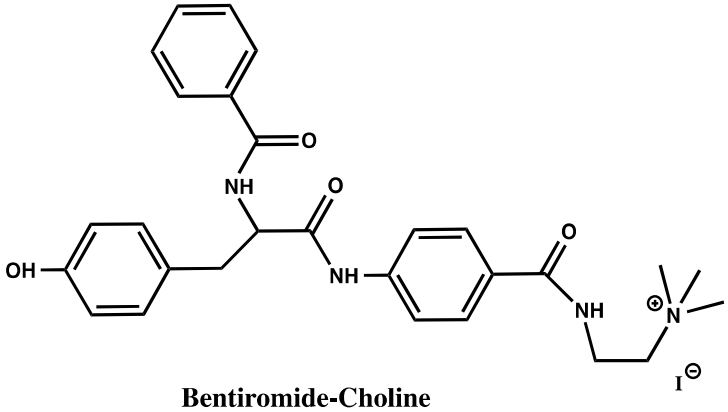

Bentiromide-Choline
33

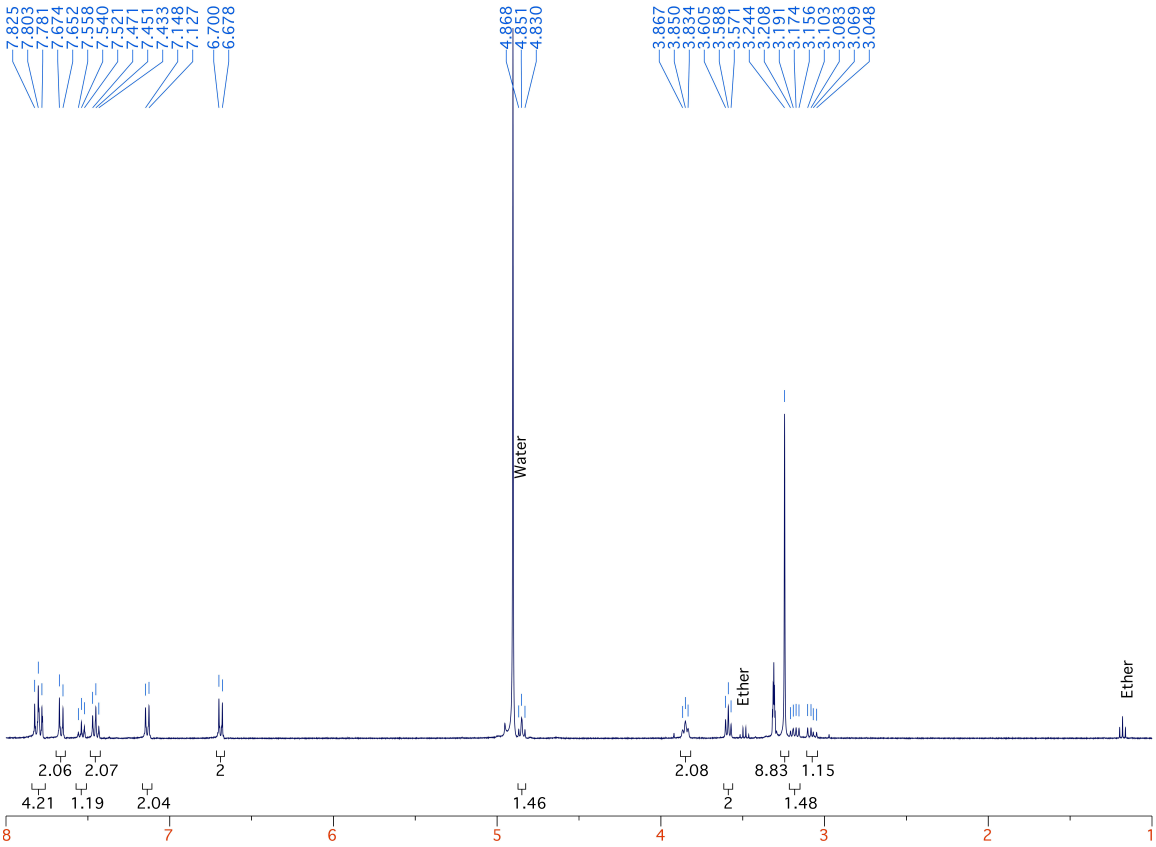

FIGURE 44. ^{1}H NMR of 33.

^{1}H NMR of **34**

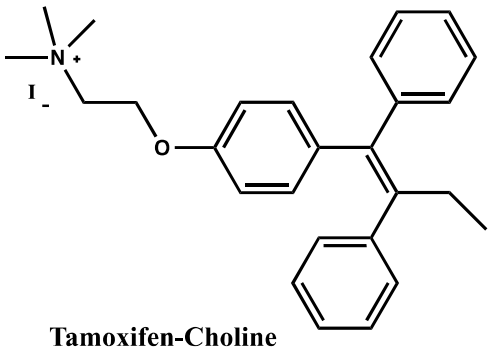

Tamoxifen-Choline
34

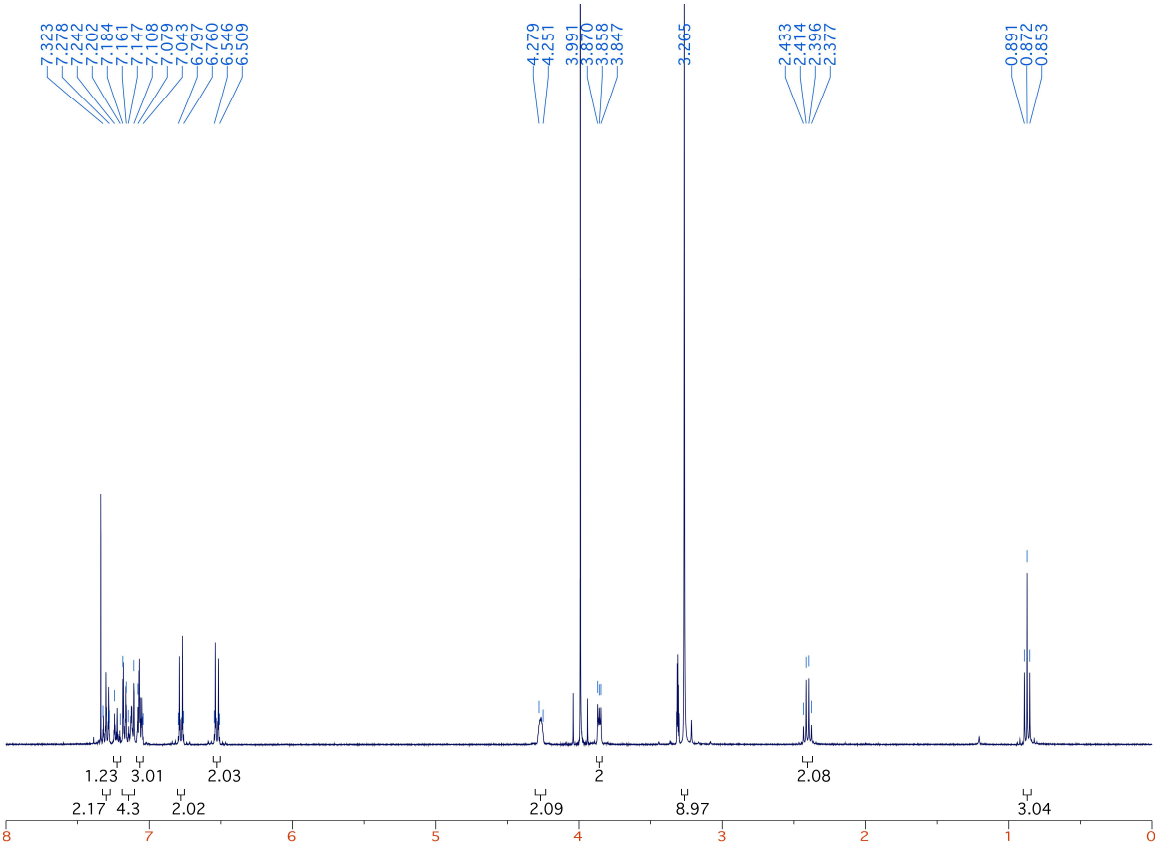

FIGURE 45. ^{1}H NMR of 34.

REFERENCES

REFERENCES

1. Steed, J. W.; Atwood, J. L. *Supramolecular chemistry*, 2nd ed.; Wiley: Chichester, UK, 2009.

2. Mandolini, L., Ungaro, R., Eds. *Calixarenes in Action*; World Scientific Publishing Company: River Edge, NJ, 2000.

3. Moran, J. R.; Karbach, S.; Cram, D. J. *J. Am. Chem. Soc.* **1982**, *104* (21), 5826–5828.

4. Rudkevich, D. M.; Hilmersson, G.; Rebek, *J. J. Am. Chem. Soc.* **1998**, *120* (47), 12216–12225.

5. Wyler, R.; de Mendoza, J.; Rebek, *J. Angew. Chem. Int. Ed. Engl.* **1993**, *32* (12), 1699–1701.

6. Branda, N.; Wyler, R.; Rebek, J. *Science* **1994**, *263* (5151), 1267–1268.

7. Heinz, T.; Rudkevich, D. M.; Rebek Jr., J. *Nature* **1998**, *394*, 764–766.

8. Scarso, A.; Trembleau, L.; Rebek, J. *J. Am. Chem. Soc.* **2004**, *126* (41), 13512–13518.

9. Ajami, D.; Rebek, J. *J. Am. Chem. Soc.* **2006**, *128* (16), 5314–5315.

10. Ajami, D.; Rebek, *J. Angew. Chem. Int. Ed.* **2007**, *46* (48), 9283–9286.

11. Rebek, J. *Acc. Chem. Res.* **2009**, *42* (10), 1660–1668.

12. Ajami, D.; Rebek, J. *Acc. Chem. Res.* **2012**, *46* (4), 990–999.

13. Langer, R. *Science* **1990**, *249* (4976), 1527–1533.

14. Haag, R.; Kratz, F. *Angew. Chem. Int. Ed.* **2006**, *45* (8), 1198–1215.

15. Vries, H. E. de; Kuiper, J.; Boer, A. G. de; Berkel, T. J. C. V.; Breimer, D. D. *Pharmacol. Rev.* **1997**, *49* (2), 143–156.

16. Pardridge, W. M. *Drug Discov. Today.* **2007**, *12* (1–2), 54–61.

17. Schramm, M. P.; Hooley, R. J.; Rebek, J. *J. Am. Chem. Soc.* **2007**, *129* (31), 9773–9779.

18. Purse, B. W.; Gissot, A.; Rebek, J. *J. Am. Chem. Soc.* **2005**, *127* (32), 11222–11223.

19. Hooley, R. J.; Rebek, J. *J. Am. Chem. Soc.* **2005**, *127* (34), 11904–11905.

20. Zelder, F. H.; Jr, J. R. *Chem. Commun.* **2006**, *No. 7*, 753–754.

21. Adhikari, B. B.; Fujii, A.; Schramm, M. P. *Eur. J. Org. Chem.* **2014**, *14*, 2972–2979.

22. Neupert-Laves, K.; Dobler, M. *Helv. Chim. Acta* **1975**, *58* (2), 432–442.

23. Späth, A.; König, B. *Beilstein J. Org. Chem.* **2010**, *6*, No.32.

24. Ludwig, R. Fresenius *J. Anal. Chem.* **2000**, *367* (2), 103–128.

25. Cadogan, A.; Gao, Z.; Lewenstam, A.; Ivaska, A.; Diamond, D. *Anal. Chem.* **1992**, *64* (21), 2496–2501.

26. Diamond, D.; Nolan, K. *Anal. Chem.* **2001**, *73* (1), 22 A–29 A.

27. Métivier, R.; Leray, I.; Valeur, B. *Chem. – Eur. J.* **2004**, *10* (18), 4480–4490.

28. Schrader, T. *Nat. Chem.* **2012**, *4* (7), 519–520.

29. Colston, M. J.; Hailes, H. C.; Stavropoulos, E.; Hervé, A. C.; Hervé, G.; Goodworth, K. J.; Hill, A. M.; Jenner, P.; Hart, P. D.; Tascon, R. E. *Infect. Immun.* **2004**, *72* (11), 6318–6323.

30. Kim, S. I.; Shin, T. J.; Ree, M.; Hwang, G. T.; Kim, B. H.; Han, H.; Seo, J. *J. Polym. Sci. Part Polym. Chem.* **1999**, *37* (13), 2013–2026.

31. Dudic, M.; Colombo, A.; Sansone, F.; Casnati, A.; Donofrio, G.; Ungaro, R. *Tetrahedron* **2004**, *60* (50), 11613–11618.

32. Vreekamp, R. H.; Verboom, W.; Reinhoudt, D. N. *J. Org. Chem.* **1996**, *61* (13), 4282–4288.

33. Abidi, R.; Harrowfield, J. M.; Skelton, B. W.; White, A. H.; Asfari, Z.; Vicens, J. *J. Incl. Phenom. Mol. Recognit. Chem.* **1997**, *27* (4), 291–302.

34. Abidi, R.; Oueslati, I.; Amri, H.; Thuéry, P.; Nierlich, M.; Asfari, Z.; Vicens, J. *Tetrahedron Lett.* **2001**, *42* (9), 1685–1689.

35. Dondoni, A.; Marra, A.; Scherrmann, M.-C.; Casnati, A.; Sansone, F.; Ungaro, R. *Chem. – Eur. J.* **1997**, *3* (11), 1774–1782.

36. Kim, Y. J.; Lek, M. T.; Schramm, M. P. *Chem. Commun.* **2011**, *47* (34), 9636–9638.

37. Feher, K. M.; Hoang, H.; Schramm, M. P. *New J. Chem.* **2012**, *36* (4), 874–876.

38. Adhikari, B. B.; Roshandel, S.; Fujii, A.; Schramm, M. P. *Eur. J. Org. Chem.* **2015**, *12*, 2683–2690.

39. Tao, H.; Cao, D.; Liu, L.; Kou, Y.; Wang, L.; Meier, H. *Sci. China Chem.* **2012**, *55* (2), 223–228.

40. Daze, K. D.; Pinter, T.; Beshara, C. S.; Ibraheem, A.; Minaker, S. A.; Ma, M. C. F.; Courtemanche, R. J. M.; Campbell, R. E.; Hof, F. *Chem. Sci.* **2012**, *3* (9), 2695–2699.

41. Ogoshi, T.; Kanai, S.; Fujinami, S.; Yamagishi, T.; Nakamoto, Y. *J. Am. Chem. Soc.* **2008**, *130* (15), 5022–5023.

42. Zadmard, R.; Schrader, T. *J. Am. Chem. Soc.* **2004**, *127* (3), 904–915.

43. Koh, K. N.; Araki, K.; Ikeda, A.; Otsuka, H.; Shinkai, S. *J. Am. Chem. Soc.* **1996**, *118* (4), 755–758.

44. Shinkai, S.; Araki, K.; Manabe, O. *J. Am. Chem. Soc.* **1988**, *110* (21), 7214–7215.

45. Bird, R. B.; Stewart, W. E.; Lightfoot, E. N. *Transport phenomena*; Wiley: New York, 1960.

46. Ohto, K.; Yamasaki, T.; Inoue, K. *Ars Separatoria Acta* **2006**, *No. 4*, 96–106.

47. Arduini, A.; Pochini, A.; Raverberi, S.; Ungaro, R. *J. Chem. Soc. Chem. Commun.* **1984**, *No. 15*, 981–982.

48. Adhikari, B. B.; Gurung, M.; Kawakita, H.; Ohto, K. *Analyst* **2011**, *136* (18), 3758–3769.

49. Tauran, Y.; Brioude, A.; Shahgaldian, P.; Cumbo, A.; Kim, B.; Perret, F.; Coleman, A. W.; Montasser, *I. Chem. Commun.* **2012**, *48* (76), 9483–9485.

50. Liu, Y.; Liao, P.; Cheng, Q.; Hooley, R. J. *J. Am. Chem. Soc.* **2010**, *132* (30), 10383–10390.

51. Bednarczyk, D.; Mash, E. A.; Aavula, B. R.; Wright, S. H. *Pflüg. Arch. Eur. J. Physiol.* **2000**, *440* (1), 184–192.

52. Späth, A.; König, B. *Beilstein J. Org. Chem.* **2010**, *6*, No. 32.

53. Arnaud-Neu, F.; Fuangswasdi, S.; Notti, A.; Pappalardo, S.; Parisi, M. F. *Angew. Chem. Int. Ed.* **1998**, *37* (1-2), 112–114.

54. Pappalardo, S.; Parisi, M. F. *J. Org. Chem.* **1996**, *61* (25), 8724–8725.

55. Han, S.-Y.; Kang, M.-H.; Jung, Y.; Chang, S.-K. *J. Chem. Soc. Perkin Trans. 2* **1994**, *No. 4*, 835–839.

56. Breccia, P.; Van Gool, M.; Pérez-Fernández, R.; Martín-Santamaría, S.; Gago, F.; Prados, P.; de Mendoza, J. *J. Am. Chem. Soc.* **2003**, *125* (27), 8270–8284.

57. Newcomb, M.; Toner, J. L.; Helgeson, R. C.; Cram, D. J. *J. Am. Chem. Soc.* **1979**, *101* (17), 4941–4947.

58. Yilmaz, M. *Turk. J. Chem.* **2013**, *37*, 558-585.

59. Paugam, M.-F.; Smith, B. D. *Tetrahedron Lett.* **1993**, *34* (23), 3723–3726.

60. Arena, G.; Casnati, A.; Contino, A.; Lombardo, G. G.; Sciotto, D.; Ungaro, R. *Chem. – Eur. J.* **1999**, *5* (2), 738–744.

61. Tammler, U.; Mark Quillan, J.; Lehmann, J.; Sadée, W.; Kassack, M. U. *Eur. J. Med. Chem.* **2003**, *38* (5), 481–493.